1990

Formation and Destruction of Nitric Oxide in Fuel-Rich Combustion: Reburning.

Thomas Emmett Burch
Louisiana State University and Agricultural & Mechanical College

Order Number 9104117

Formation and destruction of nitric oxide in fuel rich combustion: Reburning

Burch, Thomas Emmett, Ph.D.

The Louisiana State University and Agricultural and Mechanical Col., 1990

U·M·I
300 N. Zeeb Rd.
Ann Arbor, MI 48106

FORMATION AND DESTRUCTION OF NITRIC OXIDE IN FUEL RICH COMBUSTION: REBURNING

A Dissertation

submitted to the Graduate Faculty of the
Louisiana State University and
Agricultural and Mechanical College
in partial fulfillment of the
requirements for the degree of
Doctor of Philosophy

in

The Department of Mechanical Engineering

by

Thomas Emmett Burch
B.S.M.E., Auburn University, 1979
M.S.M.E., Auburn University, 1982
May 1990

Preface

This dissertation is composed of five chapters and three appendices. The first chapter is an introduction to the subject matter and gives the motivation for the research effort. The second chapter is a literature survey on the fundamentals of coal combustion and NO_x formation and destruction mechanisms.

The third chapter is a preface to the experimental work. It contains an overview of the objectives for the research and the experimental methods employed. It also contains a paper that describes an important portion of the experimental facility.

The fourth chapter is composed of two papers readied for publication. They contain pertinent experimental details, experimental results, and relevant discussion.

Chapter five is a summary of the work containing conclusions drawn from this study and recommendations for future research. This is followed by a list of references used for text other than the three papers in Chapters 3 and 4, where references are given at the end of the papers in a form required by the particular journal. The references are followed by the three appendices. Appendix I describes the development of the GC/MS procedure used. Appendix II describes the procedure used to determine the reactor wall and gas temperature profiles. Appendix III explains the data reduction techniques utilized in the experimental work.

The figures and tables for the three journal articles are presented at the end of each paper as required by the journal's publication guidelines. All other figures and tables are incorporated into the text of the dissertation.

Acknowledgements

The author would like to thank his major professors, Dr. Arthur M. Sterling and Dr. Wei Yin Chen, for accepting responsibility for his guidance in this research. The author also would like to express his appreciation to his coworkers Franz Tillman, Bill Burleigh and Rodger Conway for their technical and emotional support. The technical contributions of Bill Hayes (Hayes Separations) and Dr. Fred Merklin (Kansas State University) are also appreciated.

Financial support for the author was provided by the Louisiana State University Alumni Federation, the Mineral Institute and the Mechanical Engineering Department. The research was funded by the U.S. Department of Energy, Pittsburgh Energy Technology Center Contract DE-AC22-88PC88859.

The author offers special thanks to his wife, Patti, for her undying faith and devotion throughout their stay at LSU. Without her strength and understanding this work would not have been possible.

Finally, the author thanks God for the opportunities provided to learn and the abilities and persistence he instilled.

Table of Contents

List of Figures

Figures from Coal Feeder Paper:

Figures from Research Paper 1:

Figures from Research Paper 2:

List of Tables

Tables from Research Paper 1:

Table from Research Paper 2:

Abstract

The effect of fuel type on reburning of a simulated flue gas containing 1000 ppm of NO is studied. Stable nitrogen species concentrations are provided for reburning experiments with five fuels in a premixed, laminar flow reactor. The reactor was operated at atmospheric pressure and gave a maximum gas temperature of approximately 1100 °C for a residence time near 0.2 seconds. The experimental facility used to collect this data is described including a novel coal feeding device. A new gas chromatographic method used to analyze fixed-nitrogen species is described.

For each of the five fuels, the fixed-nitrogen speciation as a function of stoichiometry is studied. The first three fuels, methane, hexane, and benzene, demonstrate the influence of fuel type on homogeneous gas-phase nitrogen chemistry. The last two fuels, lignite coal and bituminous coal, introduce heterogeneous and catalytic effects as well as fuel-bound nitrogen. For lignite coal, the heterogeneous reduction of NO on char and the catalytic conversion of HCN to NH_3 are shown to be important contributors to N_2 formation.

For lignite coal and bituminous coal the gas-phase nitrogen speciation is separated by origin using isotopically labelled $N^{15}O$ and GC/MS for isotope separation. Probability analysis is used to show that significant NO reduction occurs through non-NO mechanisms. Nitrogen evolution for both coals is observed to be delayed beyond the onset of NO conversion to N_2.

CHAPTER I

Introduction

Historically, coal has played a significant role in the energy picture for the United States as well as the world. During the early 1900's coal provided the major portion of energy needs for the industrial sector and was heavily utilized even for home heating applications. With time, oil and gas reserves were developed and became more competitive in price. Gradually, because of their convenience, oil and gas replaced coal as energy sources, so that by 1970 coal provided only about 20% of our energy needs, and it's use was limited primarily to electric power generation and large industrial energy consumers.[1]

The oil embargo of the early 1970's focused world attention on the fact that oil and gas reserves were limited and were being rapidly depleted. Also, the once-promising nuclear industry came under pressure because of growing concerns over safety and long term storage of radioactive wastes. At the present, growth in nuclear power has essentially been halted. These developments, coupled with the fact that coal accounts for approximately 88% of the world's known fossil energy reserves, have led to a revived interest in expanding the use of coal.

Although attractive in price and certainty of long term supply, the use of coal does have environmental drawbacks. The last two decades have seen increasing importance placed on reducing atmospheric pollutants associated with fossil fuel

combustion. Sulfur oxides (SO_x), nitrogen oxides (NO_x), and particulate emissions, all of which are generally more acute with coal than other fossil fuels, have been targeted as particular concerns.

Air pollution from coal combustion is not a new issue. The burning of "Sea Coale" was protested in England even in the 13th century.[2] However, concerted efforts to control emissions are rather recent and major advances in pollution control have come only in the last 20 years.

With coal, the major problem lies in the nature of the fuel itself. Inherent in the coal structure are sulfur and nitrogen compounds that are chemically bound to the coal molecule. During combustion, the sulfur is oxidized as:

$$S \rightarrow SO_2, SO_3$$

and the fuel nitrogen is converted during combustion to:

$$N \rightarrow NO, NO_2, N_2$$

Mineral matter is also trapped within the coal matrix and comprises the combustion residue known as ash, which contributes to particulate emissions.

Several control techniques have been developed for SO_x control. These include: prewashing of the coal to reduce the sulfur content before combustion, wet scrubbers to wash the sulfur oxides from the exhaust gases after combustion, and limestone capture of the sulfur during combustion. Although expensive, these techniques have

been shown to be effective measures and are now commonly used in coal burning operations.

Efforts to control particulate emissions have also met with a great deal of success. Baghouses (large fabric filters) and electrostatic precipitators have both been shown to be viable alternatives that all but eliminate particulate emissions from coal combustors.

Less success has been achieved with oxides of nitrogen. Although fuel nitrogen is not oxidized with a high efficiency compared to fuel sulfur, acceptable concentrations of NO_x are much lower than for SO_x. NO contributes to acid rain and photochemical smog, and is hazardous to health. Some measure of success has been achieved through control of NO_x formation by combustion modifications but the kinetic pathways in the process are not well understood and the effectiveness of the modifications varies. Efforts to produce a post combustion cleanup technique so far have failed to yield a cost effective method of removal.

Improvements in fuel NO_x control hinge on our developing insight into the formation and destruction of NO_x in flame and post flame conditions.[3] This insight can only be gained through fundamental combustion experiments which help identify kinetic pathways. The focus of this work is to investigate the destruction of NO_x in hydrocarbon environments with the ultimate goal of maximizing this destruction through manipulation of the combustion environment.

CHAPTER II

Review of the Literature

In order to understand and interpret the detailed literature on NO_x formation from coal, a fundamental understanding of the nature of coal and coal combustion is necessary. Thus, the following review will begin by providing some limited background information before discussing the current theories of NO_x formation and destruction. It should be understood that this review is not exhaustive. But it does represent the current understanding and views of researchers studying these topics.

Coal Structure and Classification

Coal is a brownish-black material produced by the natural slow pyrolysis of prehistoric vegetable matter. Differences in coal properties are the result of varying degrees of coalification as well as the type of plants included and even the type of soil they grew in. Thus, it is not surprising to find radical variations in coal composition and structure. Coal samples taken from the same mine or even different particles within a single sample can have significantly different characteristics.

Coals have traditionally been classified according to gross parameters that are relatively easy to measure and provide some degree of success in predicting overall combustion characteristics. The American Society of Testing and Materials (ASTM) proximate analysis[4] and ultimate analysis have long provided the primary basis of this classification.

The proximate analysis provides some qualitative information about how the coal behaves when heated. The results are reported as the weight % of moisture, volatile matter, fixed carbon, and ash. Prior to testing, the sample is air-dried under specified conditions and then ground. The sample is then oven dried, and the weight loss reported as moisture content. Next, the sample is heated in a carefully controlled sequence to determine the weight of gases and vapors driven off as volatile matter. The remaining portion is then oxidized, so that only ash remains, to determine the fixed carbon and ash content. The heating value is also included as part of the proximate analysis. Additional information is provided by the elemental or ultimate analysis which gives the weight percent of carbon, hydrogen, sulfur, nitrogen and oxygen in the sample.

Based on information provided by the proximate and ultimate analyses, coals are typically classified by rank or degree of coalification[5], progressing from lignite (youngest coal) through subbituminous and bituminous to anthracite (oldest coal). In general, increasing rank is accompanied by decreasing volatile content (50-5%) and increasing fixed carbon (10-85%). Moisture (12-70%) and oxygen (1-25%) are also usually less for higher ranked coals, but sulfur (1-10%), nitrogen (1-2%), and ash (4-50%) follow no specific pattern.

These tests and classification methods have been demonstrated to be useful for design of furnaces, heat transfer surfaces and fuel handling equipment, but they do not provide any insight into how the coal particle is bound together or how it decomposes during combustion.

The shortcomings of these tests with respect to NO_x formation are obvious in that coals of similar composition (including nitrogen content) and rank, fired under identical laboratory conditions, may produce variations in NO_x emissions of 3 or 4 fold.

Indeed, more detailed analysis of "similar" coal samples shows substantial variations in particle structures. Scanning electron microscope (SEM) photographs of pulverized coal particles show drastic differences in surface area and roughness for particles of different coals.[6] Also, porosity measured by absorption has been shown to be an important variable in reactivity[7], and researchers have further classified coals as large pore and small pore coals. Ash compositions have been studied to determine if some ash constituents may act as a catalyst for NO_x formation or reduction[8]. Finally, the complex molecular structures of coals have been found to contain significant variations in basic structures as well as functional groups.[7,9]

In short, there are many variables that have been identified as important for a complete understanding of coal combustion and in particular pollutant formation. Due to the complex and variable nature of coal, a simplified and yet comprehensive description of NO_x formation is unlikely.

Coal Combustion

The division of combustible constituents of coal into volatile matter and fixed carbon by the proximate analysis alludes to the traditional view of how a coal particle burns. In this view the two-stage process begins with the devolatilization of the coal

particle upon introduction into the heated environment. The pyrolysate then ignites homogeneously and burns in suspension as a diffusion flame surrounding the coal char (fixed carbon). After the volatile matter is depleted, the heated char burns in the solid phase by diffusion of oxygen to the char surface and diffusion of products away from the surface.

For many years, this theory provided an acceptable and easily-grasped explanation of many observed phenomena in coal combustion. Although this simplistic view is still thought to be qualitatively correct, time and research have illuminated many complicating factors. In combustion of smaller particles, such as in pulverized coal flames, these two seemingly distinct processes overlap strongly. Some researchers now suggest that the ignition mode may be heterogeneous instead of homogeneous[7]. The division between volatile matter and fixed carbon has been found to be ill-defined, so that variations in parameters such as heating rate and maximum temperature can affect not only volatile yield and composition but the structure (and thus reactivity) of the remaining char. In some coals with larger pores, the pyrolysate may even partially react inside the particle with oxygen that has diffused to the interior. Also, the nonhomogeneous nature of coal prevents a uniform volatile flux at the surface, so that the combustion environment varies from point to point on the particle surface and in the surrounding atmosphere.

In spite of the complexity of adequately describing coal combustion, many of the standard combustion parameters remain important with pulverized coal combustion. The stoichiometric ratio (defined as the air-to-fuel ratio divided by the air-to-fuel ratio

for stoichiometric conditions) has been shown to be important in determining both reaction rate and particle burnout. Flame temperature, turbulent mixing, and particle size are also primary factors. The degree of premixing is important but, at the same time, somewhat misleading in that local conditions surrounding a coal particle are almost certainly fuel-rich even though the overall stoichiometry is lean.

The complex interactions observed in the physical description of how coal burns are multiplied when the kinetic pathways of combustion (e.g., char oxidation mechanisms) are considered, and only limited pieces of the kinetic puzzle are available. The intimate relationship between NO_x formation and combustion has only begun to be explored and much basic research remains to be done, particularly on the early stages of pyrolysis and combustion.

NO_x Formation and Reduction Mechanisms

Combustion generated NO_x, known to be produced by three basic mechanisms, are termed thermal NO_x, prompt NO_x, and fuel NO_x respectively. Depending on the fuel and/or the combustion environment, any combination of these mechanisms may be at work.

Thermal NO_x, as the name implies, is a temperature related phenomenon. When any fuel is burned in air, the heat of reaction increases the degree of dissociation of molecular nitrogen and oxygen. These dissociated products produce NO by the well known Zeldovich mechanism, which is a two-step sequence.

$$N + O_2 \rightarrow NO + O \qquad (1)$$

$$O + N_2 \rightarrow NO + N \qquad (2)$$

This mechanism was first identified by Yakov B. Zeldovich in 1946. The first step is rate limiting and, due to its high activation energy (about 75 kcal per mol), requires high temperatures to be effective. Thermal NO_x is most pronounced in lean, high-temperature flames with long residence times. As flame conditions move closer to stoichiometric (i.e., depleting the oxygen pool), the second step may be replaced by

$$N + OH \rightarrow NO + H \qquad (3)$$

This trio of steps is often called the extended Zeldovich mechanism.[10]

While studying thermal NO_x formation in rich hydrocarbon flames in 1971, Charles Fenimore of General Electric noticed that NO profiles did not extrapolate to zero at the burner surface. These results were at variance with other experiments with hydrogen and carbon monoxide flames, which exhibited a zero intercept. Following a detailed experimental investigation, Fenimore concluded that this phenomenon resulted from the attack of hydrocarbon fragments on molecular nitrogen.[11]

He proposed the reaction

$$CH + N_2 \rightarrow HCN + N \qquad (4)$$

followed by other reactions with these products to form NO. Alternative reactions have been suggested, such as

$$CH_2 + N_2 \rightarrow HCN + NH \qquad (5)$$

but the idea and even the specific reaction proposed by Fenimore for prompt NO formation have been verified by other researchers. At short residence times and fuel-rich conditions (i.e., stoichiometric ratios less than 0.85), the Fenimore mechanism accounts for virtually all of the fixed nitrogen (the sum of all nitrogenous species except N_2).[10]

The third principal source of NO_x in combustion systems is nitrogen that is chemically bound in the fuel. Fuel NO_x formation is particularly important in combustion of coal which typically contains from 1 to 2% nitrogen. Although the total quantity of nitrogen present in coal is small compared to the molecular nitrogen in the combustion air, the high conversion efficiency of fuel nitrogen to NO_x (typically 15-40 percent) makes fuel NO_x an important and often dominant NO_x producing mechanism. For coal, as much as 80% of the NO_x formed can be from fuel NO_x.

Neither the structure of the fuel nitrogen species in coal nor the mechanisms by which nitrogen is released from the fuel are well defined. However, since pyrolysis studies (discussed later) have indicated a delayed nitrogen release, the nitrogen is thought to be tightly bound in the aromatic rings that constitute the basic building

blocks of the coal structure. During pyrolysis the nitrogen is divided between the volatile matter and the char. The volatile nitrogen components are then thought to fragment and rapidly form cyanic and amine species, which are precursors to NO_x[11] (the proposed pathways will be discussed later). Oxidation of char nitrogen is then presumed to take place heterogeneously with a somewhat lower conversion efficiency. This scenario is fairly well documented, but the variability of fuel nitrogen conversion remains largely unexplained. This emphasizes our lack of understanding regarding nitrogen bonding in the coal and its subsequent release.

Homogeneous Reactions

The chemical mechanisms by which gas-phase nitrogen compounds are interconverted have been the subject of numerous investigations[12-20], but they are still not completely understood. There is also no universal agreement on which reactions dominate. In most flames of practical interest (i.e., flames with an overall lean stoichiometry), the end products of fuel nitrogen compounds are predominantly N_2 and NO with relatively minute quantities of NO_2, HCN, NH_3, and other nitrogen compounds. In very fuel-lean flames, however, NO_2 concentrations can be significant.[3] It is generally agreed that the reactions producing NO are dependent on the production of N, O, and OH in the flame.[21,10,3]

Most researchers also agree that a common intermediate in the early stages of combustion is HCN. In hydrocarbon flames the gas-phase nitrogen compounds are very rapidly converted to HCN, which is subsequently converted to a variety of other

intermediates depending on flame conditions.[14,15,19,22] Sung et al.[21] make the statement "The conversion of nitrogen in the fuel to NO_x appears to be insensitive to the form in which the nitrogen was originally bound in the fuel." Basing his approach on this primary proposition, DeSoete[19] studied overall rate constants obtained from measurements carried out on flat, premixed hydrocarbon/oxygen/argon (or helium) flames doped with small amounts of ammonia or cyanogen. He concluded that the importance of HCN as an intermediate did vary with the form of the primary nitrogen compound. He found the sequence of increasing HCN importance to be ammonia, cyanogen, and molecular nitrogen.

Haynes et al.[18] concluded that HCN formation is related to the decay of hydrocarbons. In his studies of a number of hydrocarbon flames with and without the addition of pyridine, he found that HCN formation extended well into the post-flame gases. In very fuel-rich flames, in the absence of hydrocarbons, he found the cyano-pool decayed via the CN radical:

$$CN + CO_2 \rightarrow NCO + CO \qquad (6)$$

The reaction steps leading from HCN to NO are much more controversial, but amine species (NH_i, i = 0,1,2,3) are likely candidates for intermediates between HCN and NO. Miller et al.[23], in a theoretical investigation of a variety of NH_3/O_2 and $NH_3/H_2/O_2$ flames, identified important NO and N_2 forming reactions. They found that in lean flames NO is produced primarily through the nitroxyl (HNO) intermediate,

formed by the reaction of NH_2 with oxygen atoms or NH with hydroxyl and oxygen molecules. In rich flames, NH_2 and NH were found to convert to nitrogen atoms, with the extended Zeldovich mechanism controlling the formation of NO and N_2.

Other intermediates determined to be of importance in fuel-bound nitrogen conversion are NCO, HNCO, and HOCN.[14,16,24-26] The decay of HCN is thought to be linked through these intermediates by the reactions:

$$HCN + OH \rightarrow HOCN + H \qquad (7)$$

$$HCN + O \rightarrow NCO + H \qquad (8)$$

and the sequence

$$\begin{aligned} HCN + OH &\rightarrow CN + H_2O \\ CN + OH &\rightarrow NCO + H \end{aligned} \qquad (9)$$

Haynes[14] and Morley[16] studied the decay of HCN in fuel-rich hydrocarbon flames and identified reactions 7 and 9 as rate-controlling steps. They also proposed the reactions

$$HOCN \rightarrow HNCO + H \rightarrow NH_2 + CO \qquad (10)$$

$$NCO + H \rightarrow NH + CO \qquad (11)$$

as mechanisms that could give rise to the amine species that are the measured products of HCN decay. Louge and Hanson[26] studied NCO consuming reactions, using laser absorption for NCO in shock heated gases, and obtained rate constants for

$$NCO + O \rightarrow CO + NO \qquad (12)$$

$$NCO + M \rightarrow N + CO + M \qquad (13)$$

$$NCO + H_2 \rightarrow HNCO + H \qquad (14)$$

as well as reaction 11 at 1490 K. Reaction (14) was also studied by Perry[24] at somewhat lower temperatures (592-913 K), using excimer laser photolysis - laser induced fluorescence.

In addition to the reaction pathways leading to the production of NO, it is widely recognized that there are a number of reaction paths by which NO is reduced. The most effective of the NO reduction pathways discovered thus far are; reduction by hydrocarbon fragments, reduction by amine species (NH_i i = 0, 1, 2, 3), and reduction via HNCO. These three reduction mechanisms have been studied extensively in an effort to produce a viable NO reduction scheme.

Myerson[27] studied the gas-phase reduction of NO by hydrocarbons and found that an overall fuel-rich environment is required for effective NO reduction. However, he found that, in the absence of oxygen, the reaction between hydrocarbons and NO was too slow and produced too much HCN. He identified temperature, HC/NO ratio, and O_2/HC ratio as key parameters. He concluded that the addition of carefully

controlled amounts of oxygen accelerated the production of effective, reducing free radicals such as CH and CH_2. He proposed that the process was a competition between

$$CH + NO \rightarrow HCO + N + 52\ kcal(est.) \qquad (15)$$

and

$$CH + NO \rightarrow HCN + O + 73\ kcal \qquad (16)$$

The N atom produced from reaction (15) could quickly react with another NO molecule by

$$N + NO \rightarrow N_2 + O + 73\ kcal \qquad (17)$$

Myerson's observations were verified by Muzio et al.[28] in a study of the homogeneous decomposition of NO by H_2, CH_4, C_2H_6, CO, and amines by mixing these reducing agents with the primary combustion products from a natural gas flame. Their data showed that H_2, CH_4, C_2H_6, and CO reacted preferentially with the excess oxygen. Significant reductions of NO occurred only after enough reductant was injected to make the overall stoichiometry fuel rich. The work of DeSoete[29] corroborates Myerson's findings on the sensitivity of the NO yield to oxygen concentration.

From this fundamental foundation, the process of air-staged combustion was

developed as a practical tool for NO_x reduction. Air-staged combustion is the term given to the multiple (usually 2) step introduction of combustion air to the combustion zone, which results in a fuel-rich (stage 1) combustion followed by a fuel-lean (stage 2) burnout. The merits of air-staged combustion were recognized by several early investigators.[30-32] Takagi et al.[33] studied the effect of staged combustion on NO formation from fuel nitrogen (ammonia) in hydrocarbon (C_3H_8) and nonhydrocarbon ($CO + H_2$) flames. They found that the NO yield from the overall process was a strong function of the stage 1 stoichiometric ratio (SR_1). As shown in Figure 1, in hydrocarbon flames, the NO yield vs $1/SR_1$ exhibited a characteristic dip, or minimum, typically around $1/SR_1 = 1.4$, whereas in nonhydrocarbon flames the NO yield was a monotonically decreasing function of $1/SR_1$. This fundamental difference was explained by observing that substantial HCN was formed in the hydrocarbon flames, but not in the $CO + H_2$ flames. The conclusion was that the conversion of HCN to NO was greater than for NH_3 in the second stage.

The selective gas-phase reduction of NO by ammonia (NH_3) proposed by Lyon[34] has stimulated considerable interest and research in recent years (e.g., references 28, 35-38). Although the overall reaction can be written as

$$4NO + 4NH_3 + O_2 \rightarrow 4N_2 + 6H_2O \qquad (18)$$

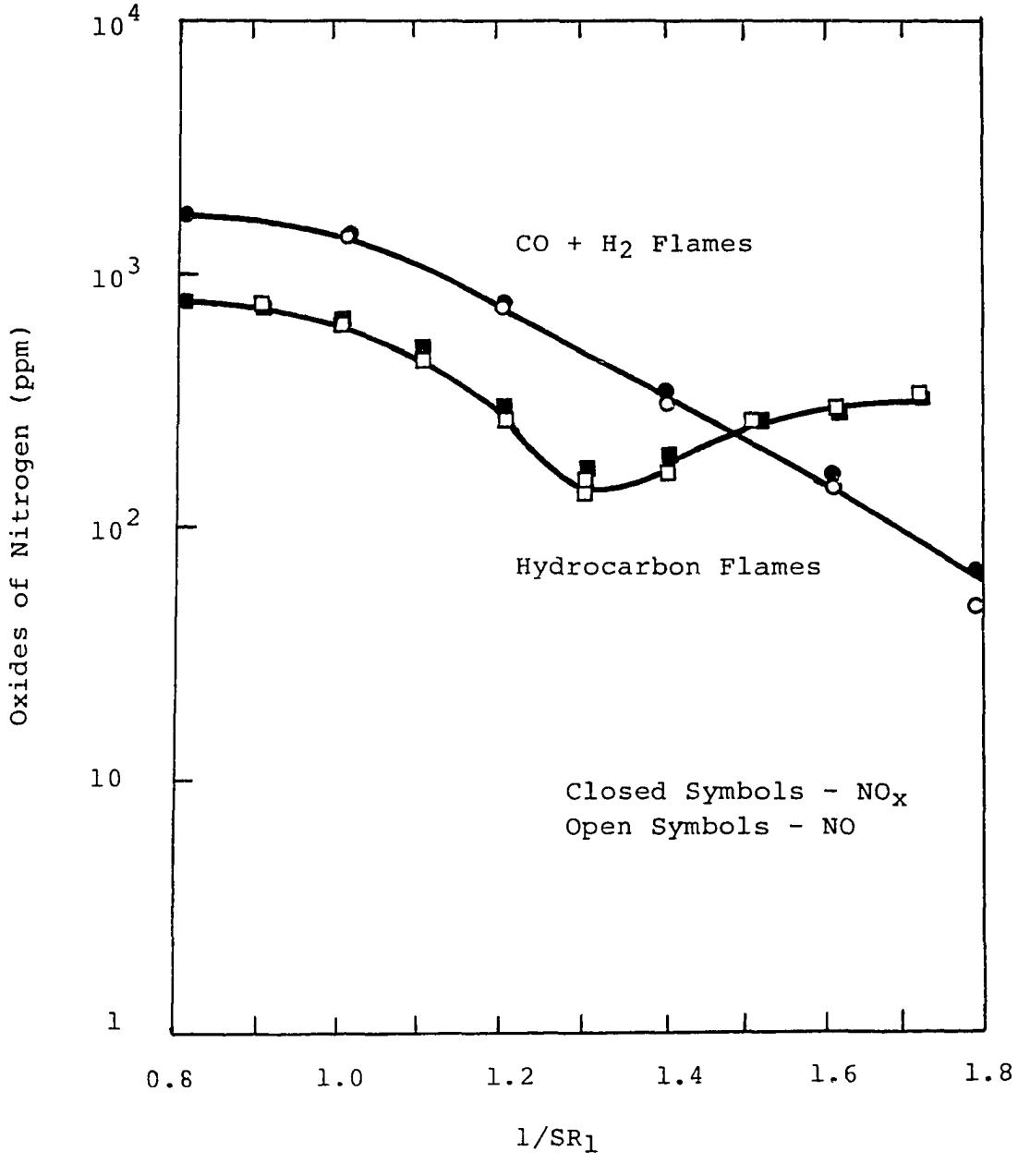

Figure 1. Influence of hydrocarbons on staged combustion. (Takagi et al., Ref. 33)

The actual process involves many elementary reactions, with ultimate NO reduction probably occurring via NH_2 or NH.

Seery and Zabilski[37] studied oxygen-rich $CO/NH_3/O_2$ flames and found that, for relatively large amounts of NH_3 added (ca. 3%), the yield of NO was reduced while the N_2 yield increased. By studying the composition profiles, they found that the NH_3 disappears at a rate that is faster than the overall reaction and that NO and N_2 formation also takes place rapidly. The study was not conclusive, but based on estimates of rate constants for various reactions, the authors argued in favor of the NH radical for NO reduction by the reaction

$$NH + NO \rightarrow N_2 + OH \qquad (19)$$

In the previously mentioned work by Muzio et al.[28], ammonia and other amines were found to react preferentially with NO in the presence of excess oxygen. However, they discovered that effective reduction occurred in a narrow temperature window centered about 1240 K and was almost nonexistent outside the temperature range of 1000 K to 1500 K. They also found that NH_3 and NO reacted in a one to one correspondence and, between the temperatures of 1145 K and 1240 K, any excess ammonia passed through the test section unreacted.

Miller et al.[38] examined the NO-NH_3 system, using a chemical kinetic model involving eighty-two elementary reactions, and successfully predicted the important features of this system observed in experiments. At temperatures below 1000 K, the

hydrogen abstraction reaction between ammonia and hydroxyl is too slow, and insufficient NH_2 is produced for significant NO reduction. Also, at these low temperatures, the chain terminating steps dominate over the chain branching steps and hydroxyl concentrations are reduced. At temperatures above 1500 K, the chain branching steps dominate and the process becomes counter productive producing additional NO. In between 1000 K and 1500 K the mix between the chain branching and chain terminating steps is balanced so that sufficient NH_2 is produced for effective NO conversion, but the temperature is low enough to allow chain termination steps resulting in the conversion of NO to N_2.

In the same work the effect of hydrogen addition was examined and found to produce a shift of the temperature window to somewhat lower temperatures without changing the width of the window. This finding was explained by noting that the addition of H_2 resulted in an increase in the hydroxyl pool, which is the limiting factor for low temperature reduction.

The NH_3/NO chemistry has been developed into control techniques via Exxon's Thermal DeNO$_x$ process and the Selective Catalytic Reduction (SCR) process. The Thermal DeNO$_x$ process is simply an injection of ammonia into the combustion gases at temperatures between 1170 K and 1280 K. Generally, 40 to 60 percent reduction of NO_x is achievable with NH_3/NO_x molar ratios of 1:1 to 2:1. SCR requires passing the combustion products,and NH_3, through a catalyst (usually a formula consisting of vanadium and titanium oxides) at temperatures between 570 K and 670 K. NO_x emissions from boilers using SCR processes are generally reduced by 80 percent.[39]

A relatively new NO reduction scheme has been proposed by Perry and Siebers[40] using HNCO. In his studies of the chemical kinetics of NCO, Perry[24] found that the radical reacted very rapidly with NO and suggested that HNCO might be involved in a series of reactions that would remove NO_x from combustion gases. In subsequent flow-reactor experiments, Perry and Siebers found that at temperatures of 700 K or higher HNCO and NO were removed simultaneously and rapidly in 1:1 correlation. The products of this reaction were found to be CO, CO_2 and H_2O with N_2 inferred as a product. There was no evidence of objectionable species, such as HCN or NH_3. They proposed the following mechanism as consistent with their data.

$$HNCO \rightarrow NH + CO \qquad (20)$$

$$NH + NO \rightarrow H + N_2O \qquad (21)$$

$$H + HNCO \rightarrow NH_2 + CO \qquad (22)$$

$$NH_2 + NO \rightarrow N_2H + OH \qquad (23)$$

$$NH_2 + NO \rightarrow N_2 + H_2O \qquad (24)$$

$$N_2H \rightarrow N_2 + H \qquad (25)$$

$$OH + CO \rightarrow H + CO_2 \qquad (26)$$

The process now called RAPRENO$_x$ (Rapid Reduction of NO$_x$) was further tested by treating the exhaust gases from a diesel engine running at an equivalence ratio of 0.5. In the diesel experiments, Perry verified the insensitivity of the process to oxygen concentration, which makes this process substantially different than other exhaust gas treatments. Also, he found that similar to earlier experiments more than

99% of the NO_x was removed without the production of objectionable effluents.

This process shows promise in that it appears to be highly effective as an NO reducing scheme at relatively low temperatures. Also, isocyanic acid is easily and cleanly produced by heating cyanuric acid above approximately 600 K. Cyanuric acid is a nontoxic, commercially available compound that is a solid at room temperature and therefore poses no significant handling hazards.

Heterogeneous Reactions

In addition to the homogeneous mechanisms discussed above, the fate of nitrogen species also depends on heterogeneous mechanisms. This is especially true for combustion of coal where the combustion effluents have relatively high loadings of solid particles. The heterogeneous reduction of NO can come about from gas-solid and solid catalyzed gas-gas relations.[29]

NO has been observed to be reduced to molecular N_2 at temperatures as low as 870 K when fed over coal or char particles.[41] The primary products of this reaction were found to be N_2, CO, and CO_2 which accounted quantitatively for the nitrogen and oxygen in the NO consumed. Similar NO reduction has been observed by other carbonaceous materials such as graphite and activated carbon[42-44] and soot generated by flames[43]. The overall reaction for direct NO reduction by carbon is

$$NO + C \rightarrow CO + 0.5N_2 \qquad (27)$$

$$2NO + C \rightarrow CO_2 + N_2 \qquad (28)$$

Levy et al.[45] found that these reactions proceed rapidly at temperatures between 1250 and 1750 K. In the absence of oxygen, their experiments showed that the reaction is enhanced by CO and retarded by water vapor. The amount of enhancement or retardation was decreased as the temperature increased. Merryman et al.[46] in studying NO reduction on carbon-containing ash in the presence of oxygen found no significant enhancement by CO but did find enhancement by oxygen. Oxygen enhancement has also been observed by Furasawa and Kunii[47]. Understanding of heterogeneous NO reduction by carbon is complicated by the fact that accurate estimates of active surface area (which may be poisoned by chemisorbed oxygen) are difficult to obtain.

Reduction of NO on fly ash has been the subject of several investigations including those by Merryman et al.[46] and DeSoete[7]. Merryman et al. found the carbon content of the fly ash to be of major importance in the NO conversion rate. Significant reduction of NO in the free board of a fluidized bed coal combustor was measured by Walsh et al.[48] and attributed to reaction with entrained char.

Solid catalyzed gas-gas reactions may also be significant. The SCR NO_x control technique described earlier is an example of this type of reaction. Also, the characteristically low NO_x emissions from fluidized bed coal combustors is thought to be partially a result of a $CaSO_4$ catalyzed reduction of NO[49]. Solid catalyzed gas-gas reactions may involve numerous solid catalysts as well as gas-phase reductants including NH_3, H_2, and CO.[7]

Fuel NO_x from Pulverized Coal

The importance of the fuel nitrogen contribution to NO_x emissions from coal combustion has been known for some time.[50,51] In fact, by using argon/oxygen/carbon dioxide mixtures as an oxidant, fuel NO has been isolated and shown to contribute over 75% of the total NO emissions from pulverized coal.[52] However, other studies have inferred a much lower contribution of fuel nitrogen.[53] In subsequent research, several parameters thought to be important in determining the contribution of fuel nitrogen to NO_x have been examined, and our understanding of NO_x formation during coal combustion has been enhanced considerably. The following discussion addresses some of the more important findings thus far.

Perhaps the most obvious variable to explore in determining fuel NO_x emissions is coal nitrogen content. In general the percent conversion of coal nitrogen to NO decreases with increasing nitrogen content.[52,54] However, Pershing and Wendt[52] showed in their investigations of four different coals and one coal char that fuel NO could not be correlated with nitrogen content alone, even though flow conditions were kept constant.

A further division of the coal nitrogen into volatile nitrogen and char nitrogen components has been helpful. Pershing and Wendt found the char nitrogen conversion to be only 12-16% versus 28% for a pulverized coal of the same nitrogen content and concluded that a better knowledge of the process of nitrogen devolatilization was required. These results were verified in separate experiments by Chen et al.[55] and Song et al.[56]. In the latter of these, the contribution of volatile nitrogen to total NO_x

was found to range from highs of 80% to as low as 5% depending on flame conditions. But in general, volatilized nitrogen accounted for a major fraction of the fuel NO_x.

In addition to the distinction between char and volatile nitrogen, there is also evidence that the form of the nitrogen-bearing volatiles can vary and thus affect the conversion of volatile nitrogen to NO. Chen et al.[55], in their examination of fifty coals under air-staged combustion conditions, found that total fixed nitrogen (NH_3 + NO + HCN) leaving the first stage generally increased with coal nitrogen content, but the species distribution was dependent on the coal rank. In their experiments, HCN was generally greater than NH_3 with bituminous coals, but less than NH_3 with subbituminous and lignite coals. Also, first-stage NO was found to generally decrease with decreasing coal rank. The TFN speciation leaving the first stage was found to be important in determining the ultimate NO yield. The conversion of first-stage nitrogen species to second-stage NO decreases in the order NO,HCN, and NH_3. Peck et al.[57], in studying subbituminous coal flames found TFN speciation to be a function of flame conditions with HCN appearing only in richer flames.

The effects of stoichiometric ratio and mixing have also been examined and found to have a significant impact on NO_x emissions. Fuel NO_x emissions have been demonstrated to monotonically increase with increasing stoichiometric ratio for a variety of coals and in various flame conditions.[52,56,58] However, the importance of stoichiometric ratio appears to be a strong function of the coal type as shown in Figure 2. Increased mixing rate also appears to enhance the formation of fuel NO_x.[52,58] Both

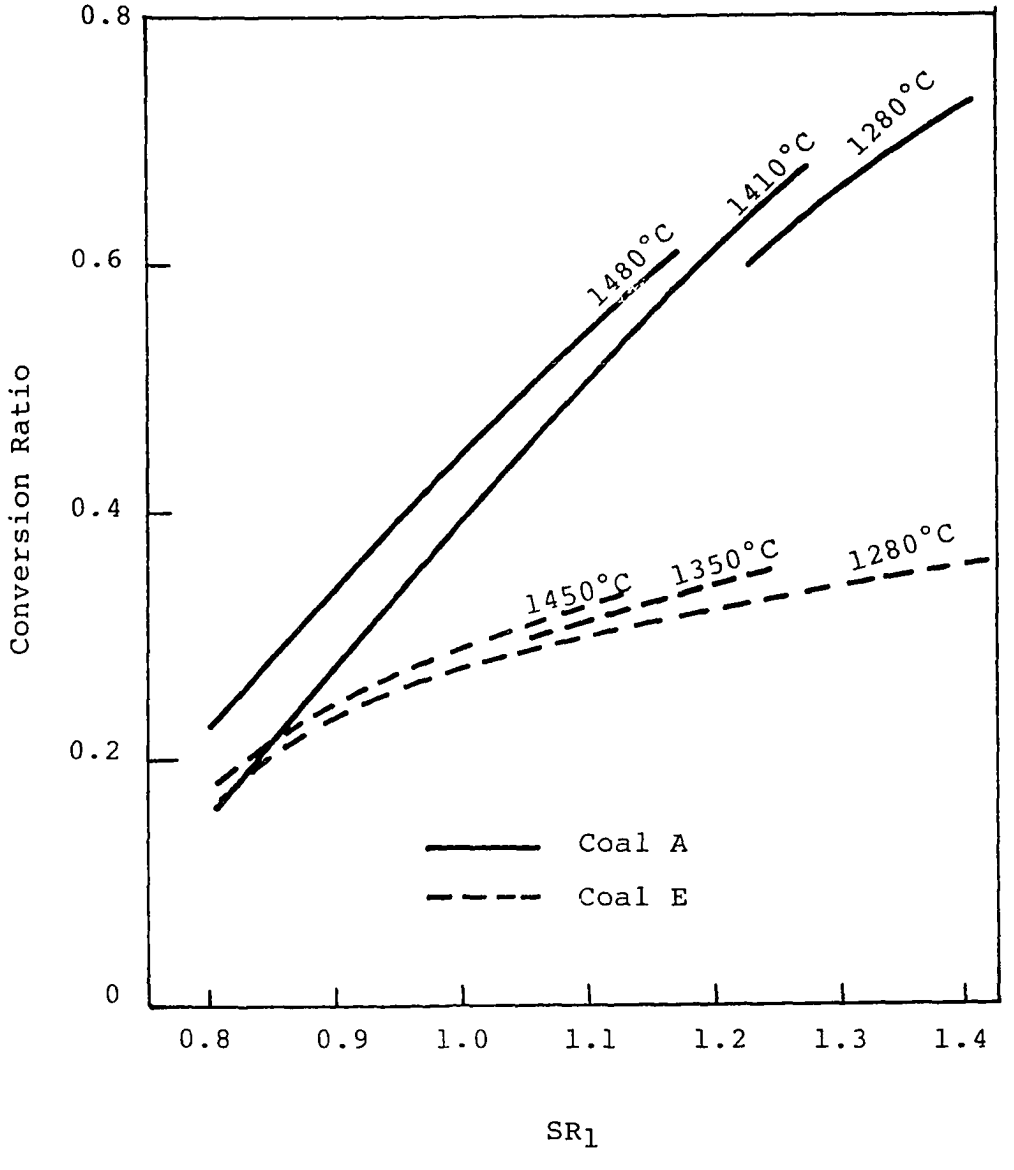

Figure 2. Influence of fuel type on fuel NO_x. The conversion ratio is the fuel NO_x formed divided by the maximum possible.
(Okazaki et al., Ref. 54)

of these phenomena are attributed to increased availability of oxygen during early stages of combustion. One interesting observation is that mixing rate appears to have little effect on the conversion rate of char nitrogen which indicates that this process may be kinetically controlled.

Another, perhaps related, parameter is coal particle size. Seeker et al.[59] note that NO formation is greater from small (40 μm) coal particles than from larger (80 μm) particles. This has been explained by observing that mixing behind the small particles is more rapid and thus less time is spent in a locally fuel-rich environment. This reasoning appears logical, but other results seem to contradict the conclusion. Experiments conducted in a test furnace by Morris at Babcock and Wilcox[60] (Figure 3) show that NO_x emissions from a course micronized coal with a mass mean diameter of 9.4 μm were significantly lower than from pulverized coal with a mass mean diameter of 31 μm. In addition, the course micronized coal showed a decrease in NO_x emissions with increasing stoichiometric ratio. There is also some evidence that as particle sizes decrease further (Figure 3, fine micronized coal), the NO_x production will again rise.[54,60,61] Similar indications of an inversion of fuel NO_x production as the particle size decreases were reported by Briceland et al.[61]. Whether this phenomenon is real or an artifact of the experiment is not known.

Temperature is another parameter that would logically seem to be important. Since devolatilization and nitrogen partitioning between the volatiles and char are known to be functions of the temperature and particle heating rate[57], an increase in temperature should produce more gas-phase nitrogen compounds and thus affect the

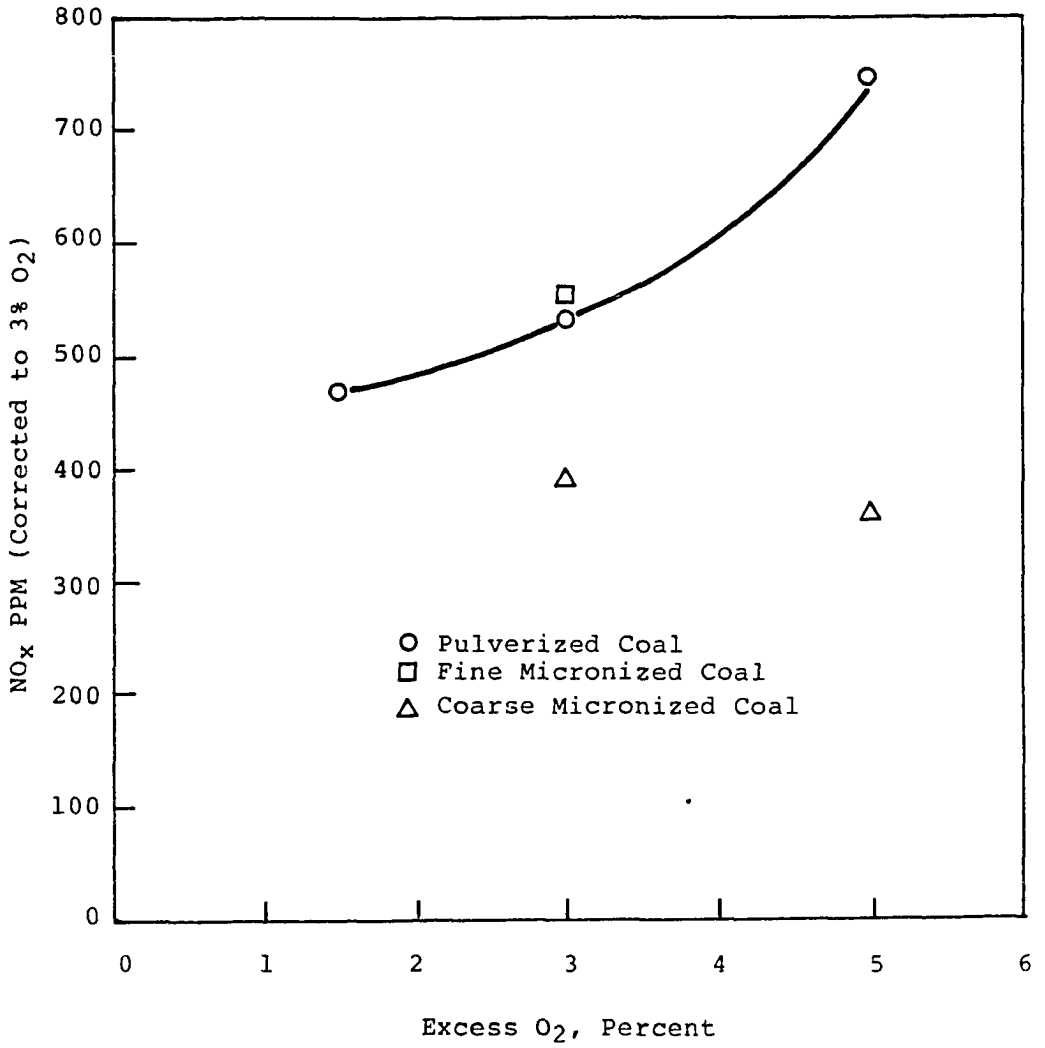

Figure 3. Influence of particle size on NO_x. (Morris, Ref. 60)

NO_x yield. In lab-scale tests performed by Pershing et al.[52], using four coals in a turbulent diffusion flame, temperature was found to have no appreciable effect on fuel nitrogen conversion for temperatures below approximately 2500 K. Above approximately 2550 K, however, fuel NO exhibited a sudden increase. This effect was observed to occur at slightly different temperatures for each coal tested. Song et al.[56] reported a slight decrease in fuel NO with increasing temperature. For a Montana sub-bituminous coal, the NO_x yields were essentially the same for furnace temperatures of 1200 K and 1500 K but decreased by 20 to 25 percent when the furnace temperature was raised to 1750 K.

Chen et al.[55], while studying air-staged combustion of pulverized coals, examined the effects of decreasing the first-stage exit temperature ca. 200 K by heat extraction from the first stage. Their data showed that cooling had little effect on the amount and speciation of the TFN or char nitrogen exiting the first stage, but caused a significant decrease in NO yield from the second stage. Further investigation showed that cooling had little effect on oxidation of char nitrogen in the second-stage flame but could affect TFN conversion. Further, they discussed that the effect of temperature on TFN conversion was dependent on TFN speciation. The thermal environment was found to have essentially no effect on NO retention in the second stage but had a profound effect on NH_3 conversion to NO.

Thus, in general, the effect of temperature is dependent on the TFN speciations which in turn depends on coal type. In lower rank coals, the TFN speciation tends to shift in favor of NH_3 and thus temperature would be expected to have a greater impact

on nitrogen conversion. The results of Okazaki[54] are consistent with this reasoning.

The emergence of air-staged combustion as a viable fuel NO_x control technique sparked considerable research which has aided our understanding of fuel nitrogen conversion in coal. The most striking feature of staged coal combustion is the characteristic dip in ultimate NO_x emissions versus stage 1 stoichiometric ratio (usually between SR_1 = .6 and .7) as shown in Figure 4. Rees et al.[62] noted that the TFN exiting the first stage is minimized at the same stoichiometric ratio. This feature is consistent with experiments using gas-phase nitrogen compounds discussed previously.

At high SR_1, the reactions produce too much NO which has a high retention in the second-stage flame. As SR_1 is decreased below 0.6, the production of HCN begins to dominate and conversion to NO in the second stage is high. However, in the range of SR_1 = 0.6 to 0.7, molecular nitrogen is the dominant nitrogen product and thus overall NO_x emissions are minimized.

In coal combustion, this understanding is complicated somewhat by coal properties. In lean Stage 1 flames the temperatures and consequently the volatilized nitrogen are higher. This may increase the TFN exiting the first stage but decreases the char nitrogen available for conversion in Stage 2. As discussed previously, the coal properties strongly affect the gas-phase speciation of fuel nitrogen compounds. In spite of these complications, the optimum value for SR_1 seems to be fairly consistent for all coals. But the ultimate success of staged combustion depends heavily on coal properties.

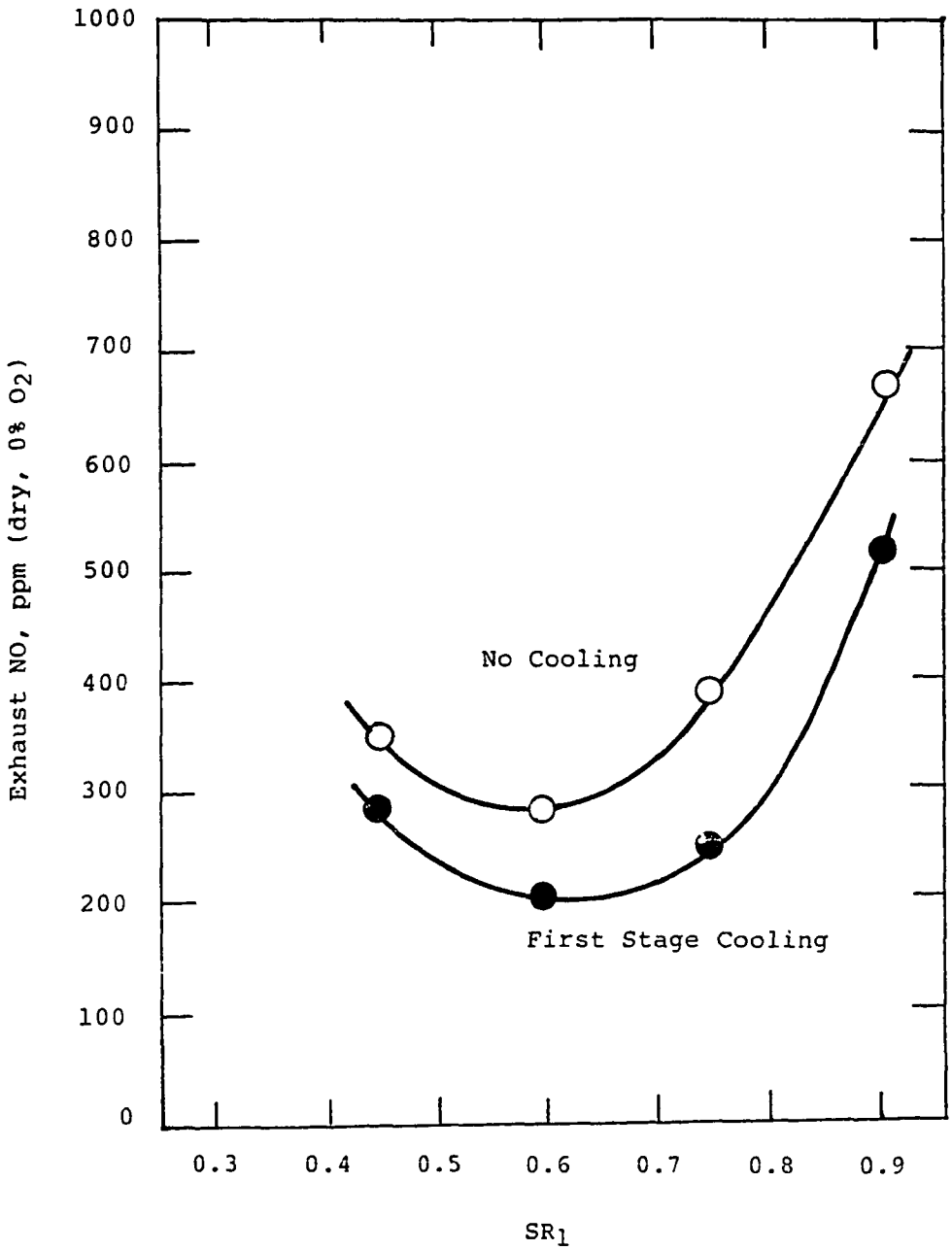

Figure 4. NO_x emissions from staged combustion of coal. (Chen et al., Ref. 55)

Pyrolysis

Coal pyrolysis is the thermally induced decomposition of the basic structure of coal. The associated volatile production and char formation processes are an integral part of coal combustion. The instantaneous release rate as well as the instantaneous heating value of the volatiles produced determine whether volatile combustion occurs in a detached diffusion flame, on the particle surface, or even within the particle. Also, due to the plastic behavior of bituminous coal during pyrolysis, the density and pore structure of the char can be influenced by volatiles production and release patterns. This in turn affects the active surface area available for char combustion and char-catalyzed gas-phase reactions.

The pyrolysis process also impacts the form and fate of fuel nitrogen compounds. Of primary interest is the effect of pyrolysis rate on the division of fuel nitrogen between the volatiles and char. The change in gas-phase speciation of nitrogen-bearing volatiles that occurs with changes in pyrolysis conditions also influences the NO_x formation processes.

Insight into the pyrolysis process is obviously important in understanding coal combustion and pollutant formation. Unfortunately, detailed and accurate pyrolysis data during the combustion process are difficult to obtain because of the strong interaction between pyrolysis and combustion.[63] Thus, conclusions drawn from inert pyrolysis data (i.e., virtually all available data) may not be totally accurate, but they do provide a fundamental basis on which to build.

Coal pyrolysis has been characterized as the release of products or groups of

products in sequential but overlapping temperature intervals.[63] Four general phases of pyrolysis are noted: (i) removal of surface moisture at low temperature; (ii) evolution of pyrolytically formed water; (iii) a broad phase encompassing softening of the coal and evolution of tar and heavy hydrocarbons; and (iv) evolution of light hydrocarbons, CO, and H_2.

The temperature ranges in which these phases occur and the degree of phase overlap are determined by the stability and chemical environment of the parent structures within the coal particle. The temperature of the maximum rates of evolution of some products have been found to vary by up to 100 °C for different coals, but in general, the temperature dependent rates for particular species are remarkably similar for a variety of coals.[64] Thus, the rate of evolution for a given species appears to depend on the nature of the functional group that serves as its source but not on the coal rank. The pyrolysis process proceeds rapidly, particularly at high temperatures (i.e., T > 1000 °C) where it is virtually complete in a fraction of a second.[65,66]

Influence of Coal Properties

The gas-phase speciation of pyrolysis volatiles is a strong function of the structure and composition of the parent coal. Even though the evolution rate and the temperature of maximum evolution rate for a particular product are relatively constant, the quantity of the product produced is determined by the amount of the source functional group present in the coal.[64]

Lignites typically contain high concentrations of oxygen primarily in carboxyl,

carbonyl, and hydroxyl groups. Consequently, lignite volatiles are dominated by oxygenated species such as CO, CO_2, and H_2O. Bituminous coals, on the other hand, contain a higher percentage of heterocyclic rings, and the pyrolysis volatiles are dominated by tar. Also, pyrolytic water is formed at lower temperatures for bituminous coals than for lignites because the hydroxyl groups are not as stable in bituminous coals.[63]

Tar production is largely a function of the aromaticity of the parent coal. Lignites typically produce less than 20 weight percent tar in the volatiles, while bituminous volatiles may contain more than 80 weight percent tar. Eastern bituminous coals contain a greater fraction of carbon in condensed aromatic ring structures and thus produce more tar than Western bituminous coals.[67]

Nitrogen Evolution

The evolution of nitrogen-bearing species from coal is not well described by a single first order kinetic rate. Thus, some investigators, including Solomon and Colket[68] and Freihaut et al.[67] have suggested that coal nitrogen may be contained in two types of structures of different thermal stability. However, the predominance of evidence indicates that organic nitrogen occurs mainly as a heteroatom in aromatic rings which are fairly stable. Consequently, little nitrogen is released in the very early stages of pyrolysis.

Delayed nitrogen evolution has been observed for a variety of very different coals under diverse experimental conditions. Pohl and Sarofim[69], in pyrolysis studies

of a lignite and a bituminous coal, found that little nitrogen was evolved until 10 to 15 percent of the coal had been devolatilized. Blair et al.[70] also observed delayed nitrogen evolution but found that at temperatures above 900 °C, the volatiles contained a higher concentration of nitrogen than the parent coal. This is shown in Figure 5 (evolution rates correspond to the slope dm/dT). In all cases for temperatures above 1600 °C, the mass fraction of nitrogen evolved exceeded the mass fraction of coal evolved. These authors observed the delay in nitrogen evolution and suggested that the escape velocity of nitrogen-bearing compounds would be low. This could indicate that oxidation of nitrogen-bearing compounds would occur at or near the particle surface affecting the ultimate fate of fuel nitrogen.

Song et al.[71] found that for coal char, oxidation of carbon and nitrogen is non-selective but at higher temperatures (i.e., above 1250 K), nitrogen devolatilization can occur even without further carbon loss from the char. Thus, removal of char nitrogen can occur by either oxidation or further devolatilization. The relative proportion depends primarily on temperature. There is also some evidence indicating that the difficulty of nitrogen pyrolysis from char increases with increasing coal rank.[64]

Oxygen Evolution

The basic structural unit of the coal macromolecule has been shown to contain oxygen even for coals of relatively low oxygen content.[72] Thus, the content and form of organically bound oxygen is an important factor in the thermal decomposition of

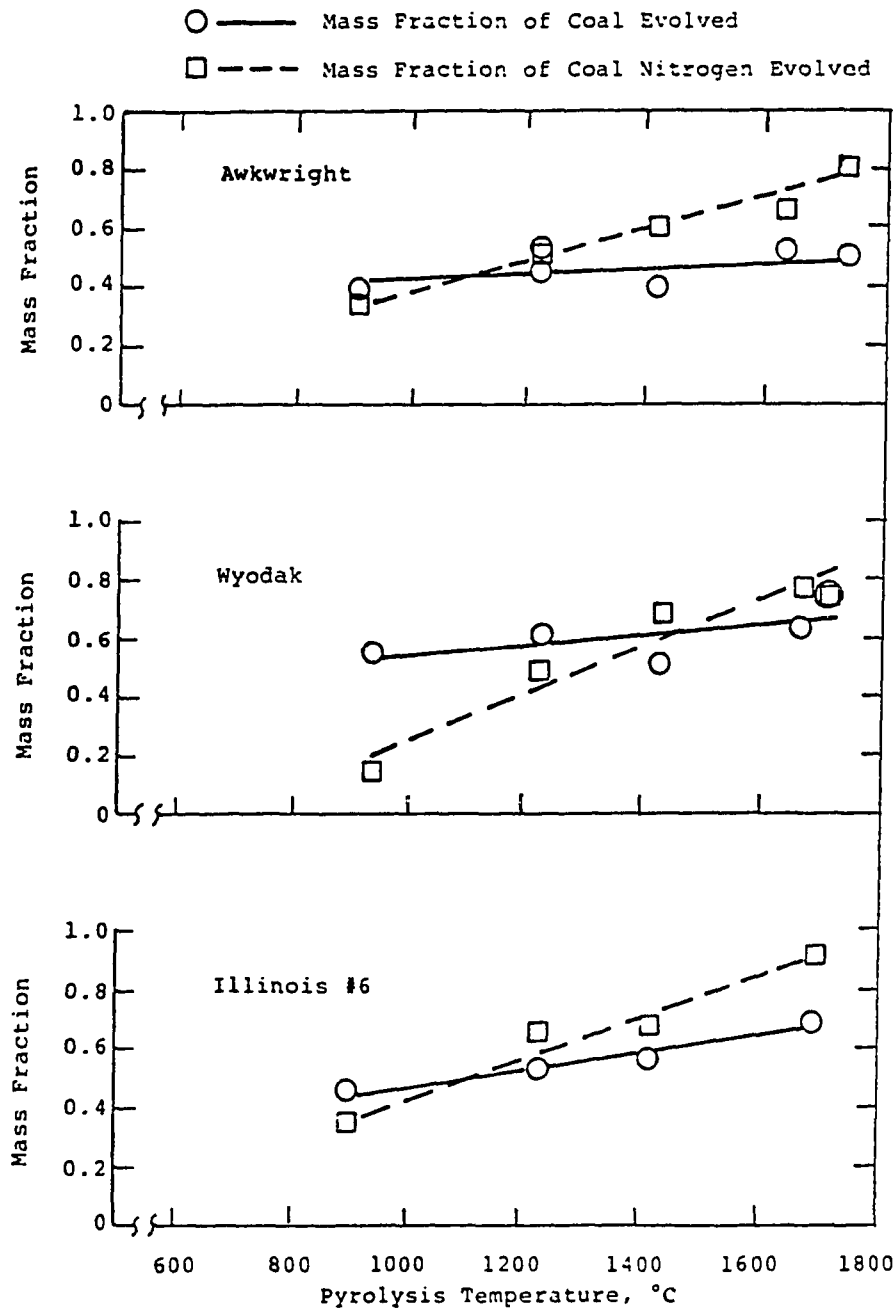

Figure 5. Delayed nitrogen devolatilization. (Blair et al., Ref. 70)

coal. This is particularly evident in low rank coals where oxygenated fragments dominate volatiles production.

In contrast to nitrogen, oxygen appears in volatiles from the very beginning of pyrolysis. Char concentration profiles taken at various stages of pyrolysis show oxygen mass fraction in the char decreases as pyrolysis proceeds.[68] This indicates that a substantial portion of coal oxygen is contained in functional groups that are somewhat loosely bound to the coal. Solomon and Colket[68] proposed that H_2O and CO_2, the dominant oxygenated products, are formed from reactions such as

$$\Phi\text{-}COOH \rightarrow \Phi\text{-}H + CO_2 \qquad (29)$$

$$\Phi\text{-}OH + \Phi'\text{-}H \rightarrow \Phi\text{-}\Phi' + H_2O \qquad (30)$$

$$\Phi\text{-}OH + \Phi'\text{-}OH \rightarrow \Phi\text{-}O\text{-}\Phi' + H_2O \qquad (31)$$

where Φ is an aromatic cluster.

Some organic oxygen remains in the char and is fairly stable. Mrazikova et al.[72] found that substantial quantities of hydroxyl groups persisted even after pyrolysis for 1 second at a temperature of 850 °C. Further, they found that the number of OH groups actually increased between the temperatures of 500 and 600 °C for some coals. Thus, it would seem that shifting among functional groups during pyrolysis is possible.

Tar Evolution

The tar component of coal volatiles is particularly interesting and may constitute a good model for the parent coal. Tar represents the parent coal not only as a major

mass fraction of coal volatiles but also in elemental composition and infrared absorption characteristics.[64,67]

Suuberg et al.[63] developed an empirical formula for the tar of a Pittsburgh Seam (No 8) bituminous coal and found the mass fractions of carbon, nitrogen and oxygen to be almost identical to the parent coal. However, the hydrogen content of the tar was approximately 50 percent higher. Solomon and Colket[68] studied twelve bituminous coals and one lignite and also found relatively high hydrogen content especially for tars of the bituminous coals. They explained this phenomenon as a result of hydrogen abstraction by the coal "monomers" (tars) to stabilize the free radical sites produced when the "monomer" was freed from the coal "polymer". The overall similarity of coal tars to parent coals suggests that tar is a primary decomposition product.

Freihaut et al.[67] studied coal tar formation in a heated grid reactor with monitoring thermocouples and noted a short-term temperature drop at the onset of the formation indicating that tar formation is endothermic. They, along with other investigators, have also noted that tar evolution occurs predominately during transient heating and is virtually complete by a temperature of 700 °C.

Freihaut et al. also demonstrated a striking parity between the mass fraction of coal evolved as tar and the mass fraction of nitrogen evolved as tar. This indicates that tar is perhaps the dominant primary nitrogen-bearing volatile component especially for highly aromatic coals. This is in agreement with earlier work by Blair et al.[70] which showed that approximately 85% of the volatile nitrogen does not evolve as HCN

or NH_3. The balance was presumed to be contained in heavier components such as tars.

Simultaneous with evolution is the cracking of aromatic rings to form light gas species such as HCN and condensation to form char.[64,67] This apparently presents a competition between diffusional escape of primary tars and secondary reactions which alter the devolatilization product distribution.[63,66] Conditions resulting in a decrease in tar yield also typically produce increased HCN yields. Thus, HCN probably results from secondary reactions of coal tars. The susceptibility of primary tars to secondary reactions is a strong function of the chemical characteristics of the parent coal. As a result, lignite tars are more stable and less likely to undergo secondary reactions than bituminous tars.[67]

Pyrolysis Parameters

Pyrolysis is by definition thermally induced, and temperature is, therefore, of extreme importance in determining both the quantity and speciation of coal volatiles produced. As the pyrolysis temperature increases, more stable bonds in the coal structure can be broken, yielding a greater quantity of volatile products. Also, secondary reactions of primary decomposition products are increased so that gas-phase products that were stable at lower temperatures are decomposed causing a shift in volatiles composition.

Kobayashi et al.[65] studied devolatilization of a lignite and a bituminous coal in a flow furnace and found that volatile yields of both coals increased significantly with

temperature. The yield ranged from about 30% (dry ash free) at 1260 K and 20 ms to about 63% at 2100 K and 25 ms. Thus, maximum volatile yields can significantly exceed the value given by the ASTM proximate volatile test, which in the case of these coals was approximately 46%.

Temperature also has a significant effect on the distribution of nitrogen between volatiles and char. Blair et al.[70] studied two bituminous coals and one subbituminous coal and found that nitrogen evolution is much more sensitive to pyrolysis temperature than total mass evolution. Their tests also showed that the mass fraction of nitrogen lost increased with temperature with roughly the same slope for all three coals even though the dependence of total mass fraction lost varied widely. This led the authors to suggest that nitrogen evolution kinetics may be similar even for very diverse coals.

Temperature also influences the gas-phase speciation of nitrogen-bearing volatiles. Gay et al.[73] found that HCN yield increased monotonically with temperature up to 1100 °C. Freihaut et al.[67] also found that HCN yields increased with temperature but noted that increases in HCN were accompanied by decreases in tar yield. As noted previously, this is probably due to secondary reactions involving tar within or on the particle.

The effect of heating rate on volatile yield has been studied by several investigators.[63,66,70] Anthony et al.[66] studied the rapid devolatilization of a lignite and a bituminous coal with heating rates from 10^2 to 10^4 °C/s and final temperatures from 400 to 1100 °C. They found no heating rate dependence for the bituminous coal. Suuberg et al.[63] also investigated the effect of heating rate on pyrolysis over a similar

temperature range and found no appreciable effect on total volatile yields or major product distribution. Blair et al.[70] found that heating rate may be important below 50 °C/s but for heating rates of interest in combustion there was no significant effect.

In contrast, Freihaut et al.[67] reported that increases in heating rate did result in decreased tar yield and increased HCN. This is consistent with the theory of competition between diffusional escape and secondary reaction of primary tars.

Other factors including pressure, particle size and particle dispersion have also been shown to be important in the tar yield. Increasing pressure or particle size or decreasing particle dispersion results in decreased tar yield and increased char and light gas evolution.[63,67] This is also probably due to secondary reaction of the tars. Since altering these parameters in the manner described inhibits diffusional escape of the tars from the particles, secondary reactions become more likely.

Reburning

Reburning or fuel-staged combustion is the name given to a NO_x reducing combustion modification proposed by Wendt et al.[74] in 1973. Reburning, like air-staged combustion, makes use of the reducing properties of hydrocarbons, but the physical setup is different.

Reburning utilizes a three-stage combustion process. The first stage typically consumes 80-90% of the fuel in a flame which is fuel lean. In the second stage, the remaining fuel is added but usually no additional air. Thus, the second-stage stoichiometry is fuel rich providing a reducing environment. The third stage is a

burnout phase in which enough air is added to complete the combustion process with an overall lean stoichiometry.

In a typical reburning application, the first-stage flame would burn coal. Since coal has a high fuel nitrogen content and the first-stage flame is fuel lean (promoting a high conversion of fuel nitrogen to NO), the concentration of NO_x at the exit of the first stage may exceed 1000 ppm. However, other fixed-nitrogen compounds such as HCN and NH_3 are minimal due to the lean stoichiometry.

In the second stage, the NO is reduced by adding fuel to provide a fuel-rich environment. The excess oxygen from the first stage promotes the breakup of the reburning fuel producing a rich pool of hydrocarbon fragments such as CH and CH_2 which attack the NO. One example of such a reaction is given by

$$CH + NO \rightarrow HCN + O \qquad (16)$$

This and other similar reactions combine to give an effective reduction of NO in the second stage. Although these initial hydrocarbon attacks result in a reduction of NO, the total fixed nitrogen (TFN is the sum of all nitrogen-bearing compounds except N_2) is not reduced and other reactions must follow if the NO is ultimately to be converted to N_2.

There are numerous plausible reactions by which NO is reduced to various intermediate compounds and by which the intermediate compounds are reduced to N_2. Thus, the form and oxidation mechanism of the reburning fuel are important in

determining the ultimate success of reburning.

In the third or burnout stage of the reburning process, additional air is supplied to complete the combustion process and eliminate the hydrocarbons from the furnace exhaust. Since part of the NO reduced in the second stage remains as fixed-nitrogen compounds, the lean stoichiometry of the burnout stage promotes a reconversion of these compounds to NO.

Current Status of Reburning Research

It has been more than three decades since the reductive powers of hydrocarbons in the conversion of NO_x to N_2 was first discovered. However, the concept of reburning accomplishing 50% NO_x removal was not demonstrated until 1983 when Takahashi, et al.[75] reported results from tests at Mitsubishi Heavy Industries using natural gas as a reburning fuel. These attractive results led to subsequent efforts at Acurex Corporation (Mulholland and Lanier[76]), at Energy and Environmental Research Corporation (Greene et al.[77], Overmoe et al.[78]), and at the U.S. Environmental Protection Agency (Mulholland and Hall[79]). A number of operational variables have been identified including the nature of the reburning fuel, the second-stage stoichiometry, the second-stage temperature, and the second-stage residence time.

Of all possible reburning fuels, the most economical would be coal owing to its lower energy cost. Also, reburning would typically be applied to a coal-fired facility, so the necessary coal handling and processing equipment would already be in place. However, there are some practical problems with coal reburning that may diminish its

effectiveness. The reburning stoichiometry is fuel rich, which tends to make char burnout incomplete or slow at best. High rank coals featuring a high fixed carbon content would require an extensive and perhaps impractical reburning residence time. Also, the considerable fuel-bound nitrogen in coal may contribute to additional TFN at the reburning exit which would subsequently be converted to NO in the burnout stage.[80]

Other potential fuels include natural gas, fuel oil, and possibly alcohol. Of these, natural gas has been studied most often and its effectiveness as a reburning fuel has been demonstrated. Potential reburning fuels other than coal and natural gas have received little attention in the literature, and their comparative effectiveness is unknown.

The reburning stoichiometry has received much attention in previous studies. As the reburning zone stoichiometry (SR_2) is decreased and approaches fuel-rich conditions, the NO_x reduction is enhanced. This is thought to be due to the build up of reducing hydrocarbon fragments in the richer flames. At some point, however, the pool of hydrocarbon radicals becomes excessive and fixation of atmospheric nitrogen and/or retention of fuel-bound nitrogen as TFN becomes dominant. Thus, any further decrease in SR_2 causes an increase in the ultimate NO concentration at the exit of the burnout stage. This results in a characteristic minimum in the NO when plotted versus SR_2 as shown in Figure 6.

This feature is very similar in nature to the minimum exhibited by air-staged combustion. However, for air-staged combustion, the minimum typically occurs at SR_2

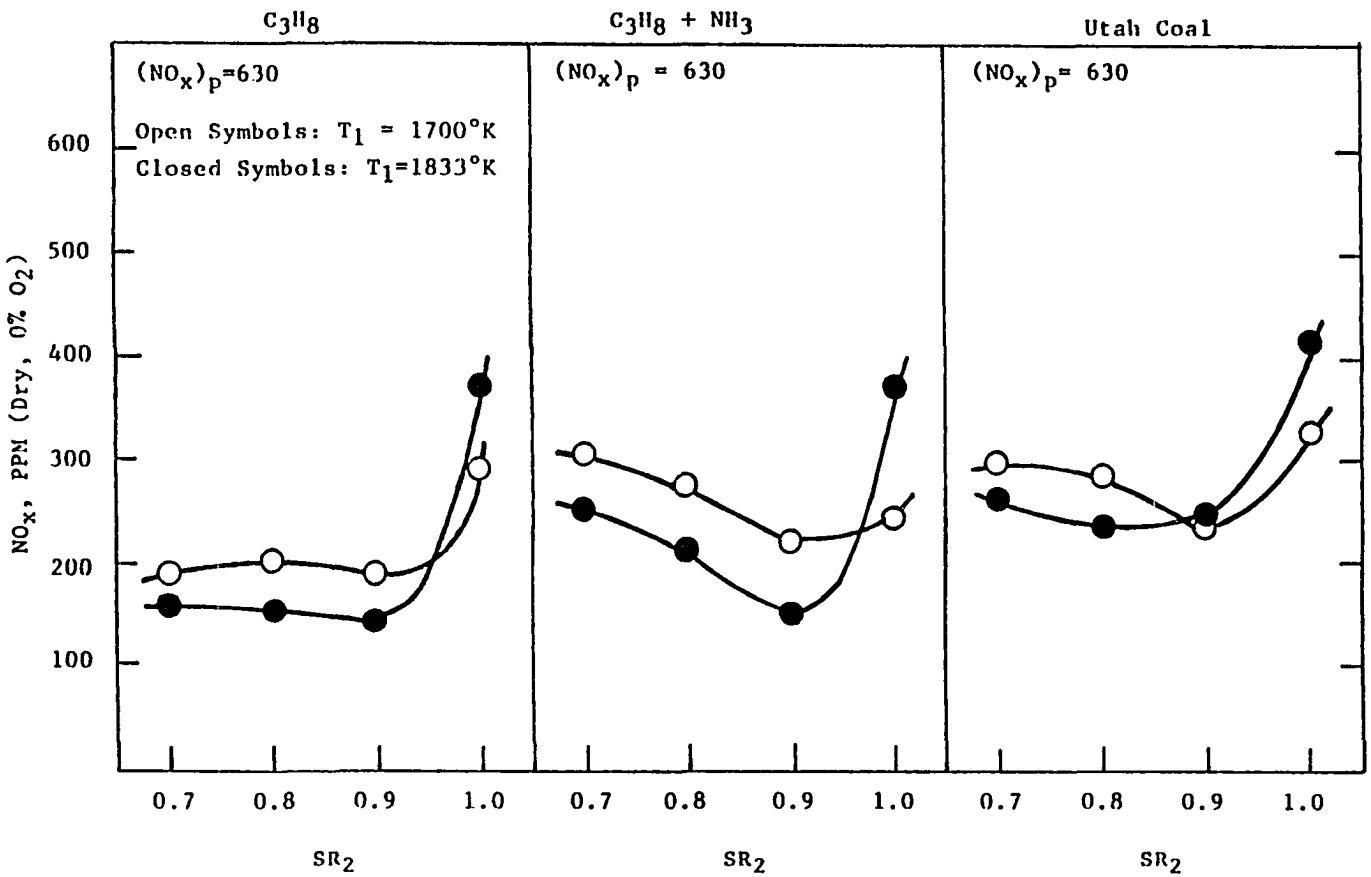

Figure 6. Influence of reburning zone temperature and stoichiometry. (Greene et al., Ref. 77)

= 0.7, whereas the reburning minimum is closer to SR_2 = 0.9. This difference has not been addressed in the literature and several factors including temperature may contribute to this behavior. One possible explanation involves the initial availability of OH radicals. In the reburning application, the water vapor produced in the primary flame provides a substantial pool of OH radicals to assist in the fragmentation of the reburning fuel. Also, the lack of available oxygen in reburning slows the rate of chain terminating reactions consuming the hydrocarbon fragments. This combination facilitates a buildup of hydrocarbon radicals in reburning at leaner stoichiometries than in air staging.

The reburning temperature also appears to be important although not to the extent that was once thought. As the reburning temperature increases, the reduction of NO to N_2 is accelerated. The conversion of N_2 to NO is also accelerated, but the net effect is a shift in equilibrium favoring N_2 formation. This produces both lower NO and lower TFN at exit of the reburning zone. However, this apparent advantage is offset by higher conversion of the remaining TFN to NO at elevated temperatures in the burnout stage. The result is typically no net effect on NO concentrations at the burnout stage exit.

Although the direct effect of temperature is small, secondary effects related to temperature can be significant. First, the thermal history has a substantial impact on the speciation of TFN. This is dramatically illustrated in coal-fired reburning where low temperatures may cause significant quantities of fuel nitrogen to be retained in the char and subsequently converted to NO in the burnout stage. Similar consequences

might be experienced with liquid fuels.[81] Johnson et al.[82] found that with pulverized coal, significant heat removal was beneficial with respect to overall NO_x emissions and postulated that selective reduction of NO by NH_i species in the burnout region was responsible.

Another secondary temperature effect that is present but not addressed anywhere in the literature is the apparent shift in optimal stoichiometry with reburning temperature changes. This is exemplified by the data of Greene et al.[83] shown in Figure 6. These data demonstrate a perceptible shift in minimum NO_x to richer stoichiometries as the temperature is increased. An explanation of this effect might also be applicable in reasoning out the differences in optimum stoichiometry for reburning as opposed to air-staged combustion.

The effect of second-stage residence time has also been investigated by Greene et al.[83] with a variety of fuels including propane and a Utah coal. In all cases, the NO_x reduction efficiency was increased by increasing the reburning residence time. However, it is interesting to note that the residence time also influences the optimum reburning stoichiometry but not in a uniform manner. For the Utah coal, increased residence time (from 140 ms to 750 ms) shifted the optimum from approximately SR2 = .95 down to SR2 = 0.8. However, in the propane experiments increased residence times seem to favor leaner stoichiometries.

Some numerical work (notably that of Glarborg et al.[84]) has been produced to simulate NO reduction under fuel-rich conditions. Their work included computer simulations of experimental stirred reactor data for combustion of natural gas doped

with NO. Their 213 reaction model was unique in that it included the C_2 - chemistry which is known to be an important part of the methane oxidation scheme. Although the trends of these results were consistent with the experimental data, the model predicted too much NO in the fuel-lean experiments and too little NO in the fuel-rich. This substantial effort required to simulate rather simplified experiments illustrates the complexity involved in the computer modeling of full scale combustors.

The work of Glarborg et al. was updated and extended by Miller and Bowman[85]. In their efforts, sensitivity analysis was used to identify the major kinetic pathways for NO destruction and production. An interesting outcome of this work is the graph shown in Figure 7, which depicts the principal mechanisms of reburning. In this figure, the width of the lines are indicative of the importance of that route in the NO reduction scheme. The pathways shown in Figure 7 result from modelling of experimental data for a fuel-rich (SR = 0.67) H_2/O_2/AR flame at 25 Torr to which 2.9% C_2 H_2 and 1.4% NO were added. While the pathways for NO reduction probably remain intact, the most important mechanisms almost certainly change with experimental conditions and fuel type.

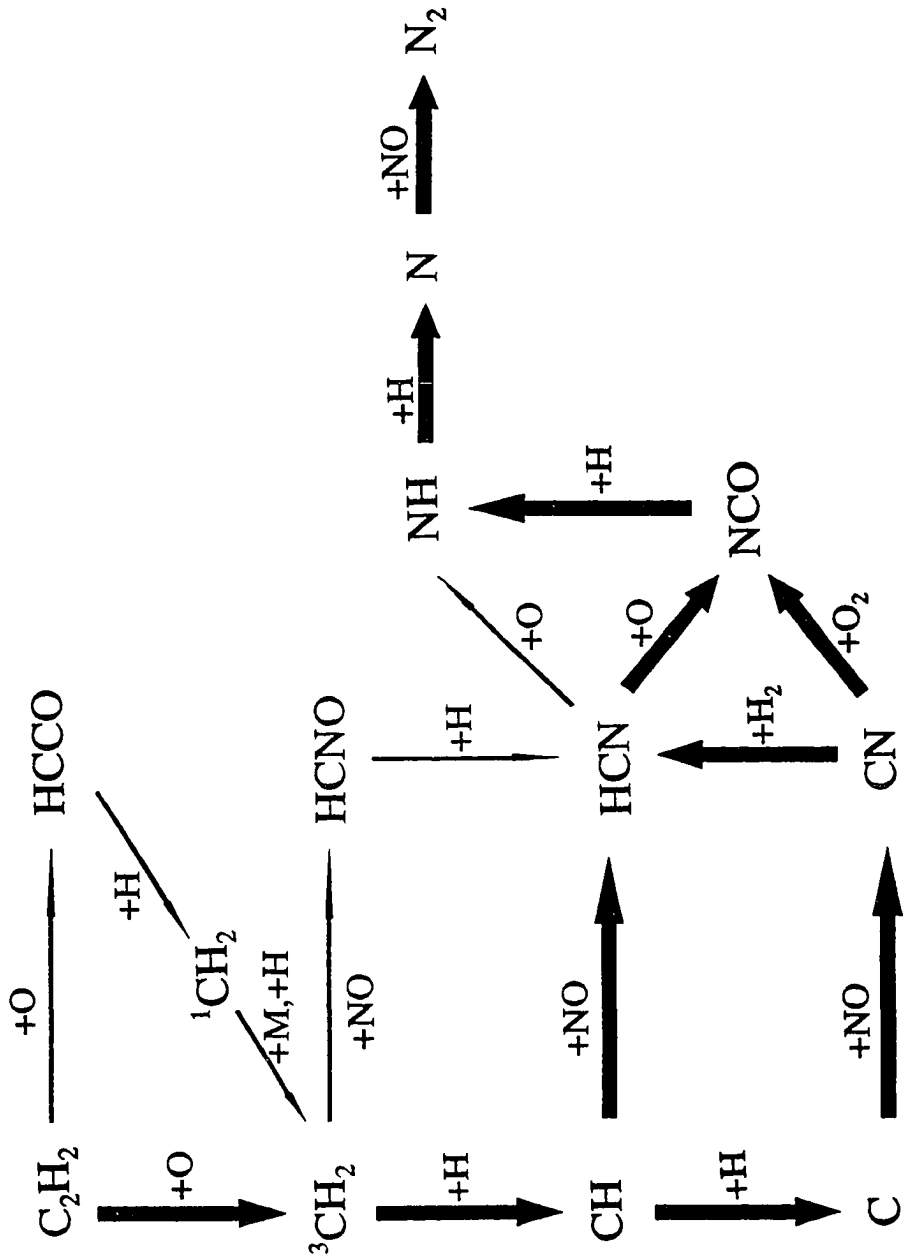

Figure 7. NO reducing pathways in fuel-rich flame. (Miller and Bowman, Ref. 85)

CHAPTER III

Preface to Experimental Work

Equilibrium TFN calculations performed by Chen, et al.[86] and Chen et al.[87] for fuel-rich hydrocarbon flames show that TFN levels below 10 ppm are possible. However, actual reburning experiments routinely produce minimum TFN levels in excess of 100 ppm. Thus, reburning effectiveness is concluded to be kinetically controlled. The realization that kinetic barriers govern reburning suggests that significant opportunity exists for reburning enhancement through manipulation of various intermediate and secondary species concentrations.

Objectives

The understanding and optimization of reburning is made difficult by the complex interaction between nitrogen chemistry and fuel-rich hydrocarbon oxidation mechanisms. With coal, the interaction is complicated further by pyrolysis, heterogeneous reactions, and the possibility of catalyzed reactions on the char or ash.

The overriding objective of this research is to scrutinize the behavior of coal as a reburning fuel. This primary objective comprises two important secondary thrusts which are:

* Determination of the importance of reburning fuel type, and
* The interaction of fuel nitrogen from coal with gas-phase nitrogenous species.

The importance of fuel type is studied to determine if the effects of the unique oxidation mechanisms associated with particular fuels substantially affect the kinetic barriers observed in reburning. Methane, hexane, and benzene are used to give variety in fuel composition without introducing heterogeneous effects. Experimental results from these fuels give some insight into the effect of fuel type on homogeneous gas-phase reactions. Two coals, one lignite and one bituminous, are tested and the results compared to the gaseous fuels. Nitrogen species reaction mechanisms specific to coal reburning are also investigated.

One important characteristic distinguishing coal from other candidate reburning fuels is fuel-bound nitrogen. Most liquid and gaseous fuels considered practical for reburning have little or no fuel-bound nitrogen. However, coal may contain 2 percent by weight nitrogen or more, which can contribute substantially to the TFN. Thus, the evolution of fuel nitrogen and the subsequent interaction with gas-phase nitrogen species is a critical concern in coal reburning. This interaction is studied by using isotopically labeled $N^{15}O$ in the gas phase to distinguish nitrogen originating in the gas phase from nitrogen originating in the coal.

Choice of Experimental Technique

Many experimental techniques including shock tubes, stirred reactors, laminar flow reactors, and large-scale turbulent furnaces have been used to study NO_x formation and destruction. Each of these techniques inherently possesses advantages and disadvantages arising from the physical equipment and processes involved. The

best technique is determined by the objectives to be accomplished in the research.

The focus of this study is on the mechanisms by which nitric oxide and other fixed-nitrogen species are converted to diatomic nitrogen in reburning. However, the ultimate practical goal is to determine the viability of coal as a reburning fuel. Thus, the paramount feature of the experimental technique must be to emulate practical reburning environments as closely as possible. At the same time, the technique must provide reasonably controlled environments to allow the evaluation of specific variable changes.

Shock tubes are very useful for kinetic studies because of precise determination of temperature and reaction time. However, the reaction time achievable in shock tubes is very short compared to industrial furnaces and the small gas volume available limits analysis techniques. Stirred reactors can achieve the reaction times desired, but the intense back mixing does not represent the species environment encountered in practical reburning.

Large-scale turbulent reactors are most representative of actual reburning environments since all of the physical as well as kinetic features are retained. However, physical attributes such as turbulence, mixing effects, and varying temperature profiles make the definition of experimental conditions troublesome at best.

The technique chosen for this research is the laminar flow reactor which represents a compromise, retaining the salient features of actual reburning environments while allowing good definition of experimental conditions. The

externally heated walls of the flow reactor are not isothermal, but they do provide a very reproducible thermal environment. The low Reynolds number of the small diameter reactor tube ensures laminar flow so turbulence effects can be neglected. Also the reactant gases (and solids) can be pre-mixed to eliminate nonuniform species concentrations that plague larger furnaces.

Target Compounds and Analysis

The variety of reaction paths by which NO is reduced to N_2 under fuel-rich conditions produces many intermediate nitrogenous species. However, only two stable intermediates, namely HCN and NH_3, appear in significant concentrations. Nitrous oxide (N_2O) has been measured in significant quantities in fluidized-bed boilers, but concentrations are generally less than 5 ppm when firing pulverized coal. Thus the nitrogenous species of interest here are NO, HCN, NH_3 and N_2. The fact that this list is sufficient is borne out in the nitrogen balances performed for coal reburning presented in the next chapter. Analysis of these species is carried out using the most appropriate techniques available.

The most versatile analytical tool employed in this work is the gas chromatograph/mass spectrometer (GC/MS). Quantification of each of the target compounds is possible using the GC/MS technique developed as part of this work, but more accurate analytic results for all nitrogen species concentrations except N_2 were obtained using other means.

Nitric oxide (NO) is susceptible to fairly rapid conversion to NO_2 in the

presence of O_2. Thus an on-line measuring technique is preferred. For this purpose, a chemiluminescent NO_x analyzer (Thermoelectron) was used. This on-line analyzer provided an almost immediate display of residual NO levels that aided in troubleshooting reactor problems as well as producing accurate data.

HCN and NH_3 are strongly adsorbed on most materials making analysis of grab samples by GC/MS difficult. Also, the sensitivity of the chromatographic technique was limited to concentrations on the order of 100 ppm. Thus, quantitative HCN and NH_3 data were obtained by capturing these species in water and analyzing with specific ion electrodes (Orion Research).

For studies of the interaction of fuel nitrogen from coal with gaseous nitrogen species, isotopically labelled $N^{15}O$ was used. Isotope separation was then accomplished using GC/MS. Isotope distributions derived from the GC/MS data, along with quantitative NO, HCN, and NH_3 measurements from the other methods stated, gave the most accurate results.

Experimental Prerequisites

Three major experimental developments were required to complete the experimental program. These were;

*Development of a suitable chromatographic technique
for the separation of NH_3 and HCN,

*Definition of the reaction time and temperature for
the flow reactor, and

*Development of a coal feeder for stable entrainment at low feed rates.

Developing a chromatographic technique for the separation of NH_3 and HCN proved to be the most difficult and tedious technical problem encountered. The strong adsorption of these species on common materials is exacerbated by the fact that NH_3 is a base while HCN is an acid. Thus, separation media and system preparation techniques conducive to good resolution of one of these compounds is detrimental to the other. A literature survey produced little useful information. Reported techniques were invariably specific for one of the species only and used exotic materials not commonly available.

The most workable solution for separation of these species was found to be a porous polymer column manufactured by Hayes Separations (Hayesep C). This column is designed to be inert, so separation of both species on a single column was possible. However, active sites in the remainder of the system required total replacement of the injection system, valves, and transfer lines. Even with the most carefully-controlled conditions, saturation injections were required to give readable peaks at concentrations below 100 ppm. A complete description of the chromatographic technique used is given in Appendix I.

The thermal environment of the flow reactor was defined by measuring the wall temperature profile and calculating the gas temperature profile. The wall temperature profile was measured using wall mounted thermocouples. The gas temperature was then calculated by the method of Sellars et al.[88], which gives an average gas temperature at any cross section based on ideal fully developed laminar flow. Details

of the calculation scheme used are given in Appendix II.

Coal reburning experiments in the flow reactor required the use of a coal entrainment device to feed and disperse pulverized coal in the gas stream. The requirements for this device were unique in that uniform mass flow rates as low as .025 gm/min of coal were needed. Other coal feeders documented in the literature were used for feed rates at least one order of magnitude higher. Also, the nature of the experiments conducted here required that the flow rates be maintained for at least 45 minutes to allow ample time for equilibration and data collection.

Several promising coal feeder designs were tried but were found to be inadequate for the low feed rates needed. Eventually, a novel coal feeding device was developed to meet these requirements. This device is documented in the following paper which is to be submitted for publication.

A Practical Pulverized Coal Feeder for Bench-Scale Combustion Requiring Low Feed Rates

T.E. Burch, R.B. Conway, and W.Y. Chen*

Mechanical Engineering Department
Louisiana State University
Baton Rouge, Louisiana 70803

May, 1990

* Present Address: Department of Chemical Engineering, University of Mississippi, University, Mississippi 38677

Abstract

A laboratory coal metering device for the entrainment of pulverized coals is described. The system uses controlled aerodynamic stripping of the powder surface by a carrier gas to effect the coal feed. It has been used for approximately one year in bench-scale combustion studies requiring exacting feed rates with very satisfactory results.

Introduction

The study of pulverized coal and coal-derived char combustion has been the subject of increasing interest in recent years. This has necessitated the development of laboratory-scale feeding devices to provide feed gas streams with known and reproducible quantities of entrained particles. In industrial pulverized coal facilities, raw coal is fed into a pulverizer where size reduction and entrainment take place concomitantly. In these systems, the pulverizer acts as a buffer which dampens variations in the raw coal feed to provide a uniform feed rate to the combustion process. However, the scale of laboratory combustors makes on-line pulverizers impractical. Thus the use of previously pulverized and stored coal is required.

The problems encountered in feeding pulverized coal powder are formidable. The generally irregular shape of the individual particles leads to variations in powder density due to particle orientation differences and compaction. Also, the rough surfaces of particles in contact with each other produce varying inter-particle friction so that smooth flow is difficult to maintain. These factors combine to cause common feeder

problems such as bridging and sloughing. In laboratory feeders, where the coal feed rate is small, the individual particles or groups of particles forming a cluster become more important and these problems are amplified.

Most laboratory feeders can be classified as either mechanical (eg., screw feeders), gravity, or aspirated. Mechanical feeders are useful for larger laboratory needs (eg., greater than 1 lb/hr) but suffer greatly at low feed rates particularly on short time scales. Most bench-scale coal feeders delivering a few grams per hour are some variation of the gravity-feed system such as those used by Solomon and Hamblen (1983) and Song et al. (1981). However, some have used the aspirated type, such as the fluidized bed employed by Altenkirch et al. (1978). The gravity-feed devices depend on a smooth flow of material through a controlled opening similar to sand flowing in an hour-glass. The success of this method is strongly dependent on particle geometry and desired flow rate. The aspirated feeders suspend the coal in a gas then bleed off the required amount of suspension. Long-time-scale stability (ca. 30 min.) and reproducibility of volumetric gravity feeders is inherent, but short-time-scale variations (ca. 1 s) are more pronounced due to bridging and sloughing.

This paper describes the design and construction of a volumetric feeder that incorporates the best features of the previously described designs; one that has both long and short time scale stability coupled with reproducability and ease of calibration.

Apparatus Design

The coal entrainment technique used in this work retains the salient features of that used by Solomon and Hamblen (1983). The concentric tube design seemed to offer the greatest promise of accurate control and repeatability at the low flow rates required for these experiments (i.e., 0.025 to 0.14 gm/min). Solomon and Hamblen's feeder consisted of a vertical, cylindrical coal reservoir with a feed tube extending up through the bottom along the reservoir axis to the surface of the coal. Carrier gas flowed from the top of the reservoir and exited through the coal feed tube. Coal was fed by lowering the top of feed tube beneath the surface of the coal contained in the reservoir. The coal feed rate was thus determined by the relative motion between the feed tube and the reservoir.

This design was replicated and tried, but the feed rate was found to be inconsistent at best. The poor performance of this design was attributed to the extremely low coal delivery rates required by the present work. The feed rates needed in our experiments are approximately two orders of magnitude lower than those used by Solomon and Hamblen. The low delivery rates (and thus low relative motion of the feed tube) amplify the effects of sloughing of the coal surface and adherence to the walls, even for the coal samples at the optimal size range of 200 - 270 mesh. Efforts to rectify these problems by vibrating the feeder were not fruitful.

Several new designs were incorporated before settling on the design shown in Figure 1. A 12 mm o.d. glass tube (the coal reservoir) is contained in a slotted 1 in. o.d. housing and sealed on each end with 1/2 in. Teflon ferrules. The glass tube and

slotted housing allow visual inspection if feeding irregularities occur. The 1/8" o.d. feed tube extends through the bottom of the feeder and a sliding seal is provided by a Teflon ferrule.

The most pronounced modification incorporated in the design is the addition of a stainless steel piston and piston guide (upper portion of the piston, Figure 1) to follow the feed tube. The piston and piston guide are actually machined from a single piece and are separated only by a groove. The diameter of the piston guide is approximately 0.003 inches smaller than the inside diameter of the glass tube. To allow ample gas flow, the guide is slotted vertically. The diameter of the piston is approximately 0.020 inches smaller than the inside of the glass tube. The groove separating the piston and piston guide is intended to provide a more even distribution of gas flow around the piston.

The end of the piston is concave and center drilled with a 0.125 in. drill bit. The drilled hole mates the piston to the coal feed tube, thus ensuring both horizontal and vertical alignment for the feed tube relative to the piston. The top of the feed tube is slotted to provide a visible gap of approximately 1/32 in. when the feed tube is inserted into the piston.

This design allows effective flow control at extremely low coal feed rates. The piston, centered by the piston guide, continuously eliminates coal adherence to the walls by producing a high gas velocity in the annular space between the piston and reservoir walls. The concave piston forces a coal accumulation in the center of the reservoir so that coal is fed by aerodynamic stripping rather than gravity.

The coal feeder is shown mounted to its drive mechanism in Figure 2. The coal feeder is positioned on a solid carriage via two mounting studs and is held in place with wing nuts. The solid rod extending through the top of the coal feeder is held in place by a locking collar so that the vertical position of the piston and coal feed tube is fixed.

The vertical motion of the carriage assembly and reservoir is provided by a threaded feed screw. The feed screw is driven by a 1/100 H.P. 12 volt DC drive motor and gear box located at the top of the drive mechanism. The gear box produces a final drive maximum of 3.4 RPM (0.170 in/min of carriage travel) which can be controlled by a variable voltage DC power supply down to approximately 0.25 RPM (0.0125 in/min).

To provide a smooth linear motion of the coal feeder, wobble of the carriage must be minimized. The carriage is stabilized via four linear bearings riding on 0.5 in. ground shafts. The feed screw is machined to a maximum eccentricity of 0.002 inches peak to peak and provides translation of the carriage through a threaded coupling and rubber grommet to minimize transmission of eccentric motion to the carriage.

The coal feeder is charged by removing the 1/2 in. x 1/8 in. conversion fittings at the top of the coal feeder and gently adding coal with the aid of a funnel. Although this operation can be conducted while the feeder is mounted to the carriage it is usually more convenient to remove the feeder before charging.

The volumetric nature of this feeder provides inherent long-time-scale stability

since the only variable is the density of the powder. Although variations in powder density can be considerable (ca. 10%) depending on the amount of vibration induced settling experienced, reasonable care and consistency during loading and handling of the coal feeder easily reduces these variations to less than 2%.

Experimental

Calibration of the feeder was performed by collecting the entrained coal on pre-weighed filter paper for a specified number of revolutions of the feed screw. The coal feed per revolution calculated from this test was then used to calculate the RPM required for a given coal feed rate. To further simplify the process, a plot of coal feed rate versus applied voltage was constructed. This plot was very useful and extremely accurate (± 3% of feed rate) for feed rates in the upper half of the feeding rate range. However, at lower rates, directly measuring RPM was necessary to achieve the same accuracy.

Short-time-scale stability of coal feed was evaluated indirectly. The coal feeder was developed for use in a study of reburning; a method of controlling nitric oxide emissions. For a given gas flow rate, initially containing 1000 ppm of NO, the surviving NO was found to vary with coal addition according to the curve shown in Figure 3. The linearity of this curve for feed rates below 0.05 gm/min allows short-time-scale stability to be evaluated by observing the surviving NO levels versus time.

The typical strip-chart recording presented in Figure 4 shows fluctuations to be contained in a 40 ppm band for a 30 min. run (excluding large upsets at each end of

the cycle caused by valve switching). The results shown in Figure 4 are for a nominal coal input of 0.027 gm/min. Based on the linear relationship exhibited in Figure 3 the fluctuations observed in Figure 4 correspond to feed-rate fluctuations of ±.0019 gm/min. The actual fluctuations may be slightly larger than the calculated value due to mixing in the sampling train.

The magnitude of the fluctuations described above correspond to feed-rate changes of ±7% for a feed rate of 0.027 gm/min. However, the fluctuations have been shown to be relatively constant in magnitude and thus represent a decreasing percentage at higher feed rates.

Experience has shown this coal feeder to work best with particles in the range of 50 μm-100 μm. With smaller particles, the cohesive forces between particles prevent smooth aerodynamic stripping. Large particles require high gas velocities for entrainment and are more prone to form blockages at the coal feed tube entrance. Acceptable carrier gas flows for helium are found to be between 0.8 and 1.7 L/min. Lower rates fail to properly strip the surface and walls, while higher rates are prone to siphon coal from the reservoir well ahead of the piston.

Although the design principles incorporated in this feeder can readily be extended to other feed-rate ranges, practical limitations of motor speed and useful run times restrict the present feeder to the approximate feed rate range of 0.02 to 0.20 gm/min. The design presented here has been found to be simple to construct from readily available parts and materials at reasonable cost (approximately $500). In addition, the performance and reliability within the designated ranges of particle size,

feed rate and carrier gas flow are extremely good.

Acknowledgement:

The work reported in this paper was funded by the U.S. Department of Energy, Pittsburgh Energy Technology Center under contract DE-AC22-88PC8859.

References:

Altenkirch, R.A., R.E. Peck, and S.L. Chen, "Fluidized Bed Feeding of Pulverized Coal", Powder Technology, 20: 189-196 (1978).

Solomon, P.R. and D.G. Hamblen, "Analysis of Coal Devolatilization in a Laboratory-Scale Entrained Flow Reactor", Final Report AP-2603 under EPRI Project 1654-8, July, 1983.

Song, Y.H., J.M. Beer, and A.F. Sarofim, "Coal Devolatilization at High Temperatures", Sixteenth Symposium (Int.) on Combustion, 16: 411-425 (1977).

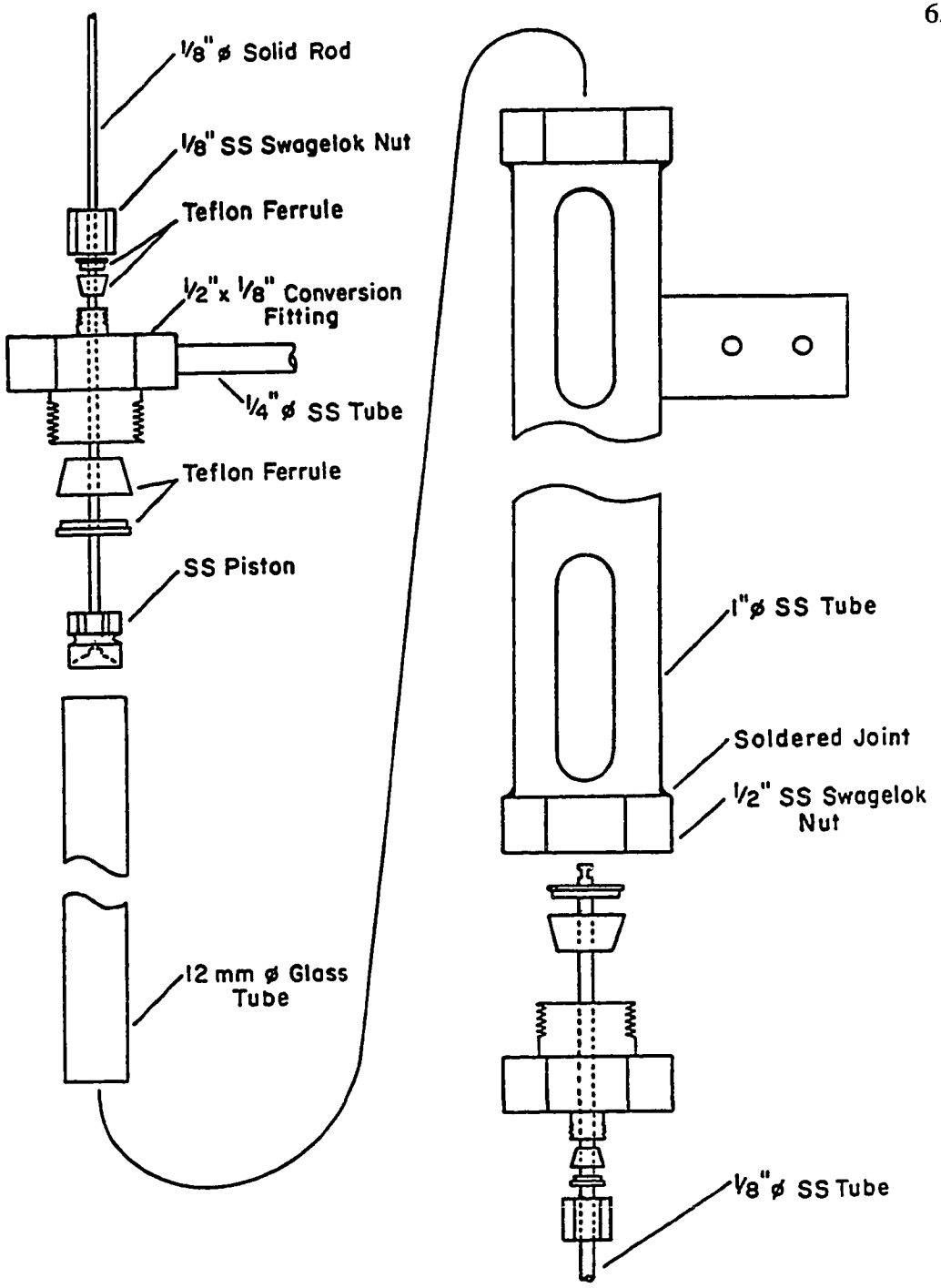

Figure 1. Exploded view of coal feeder assembly.

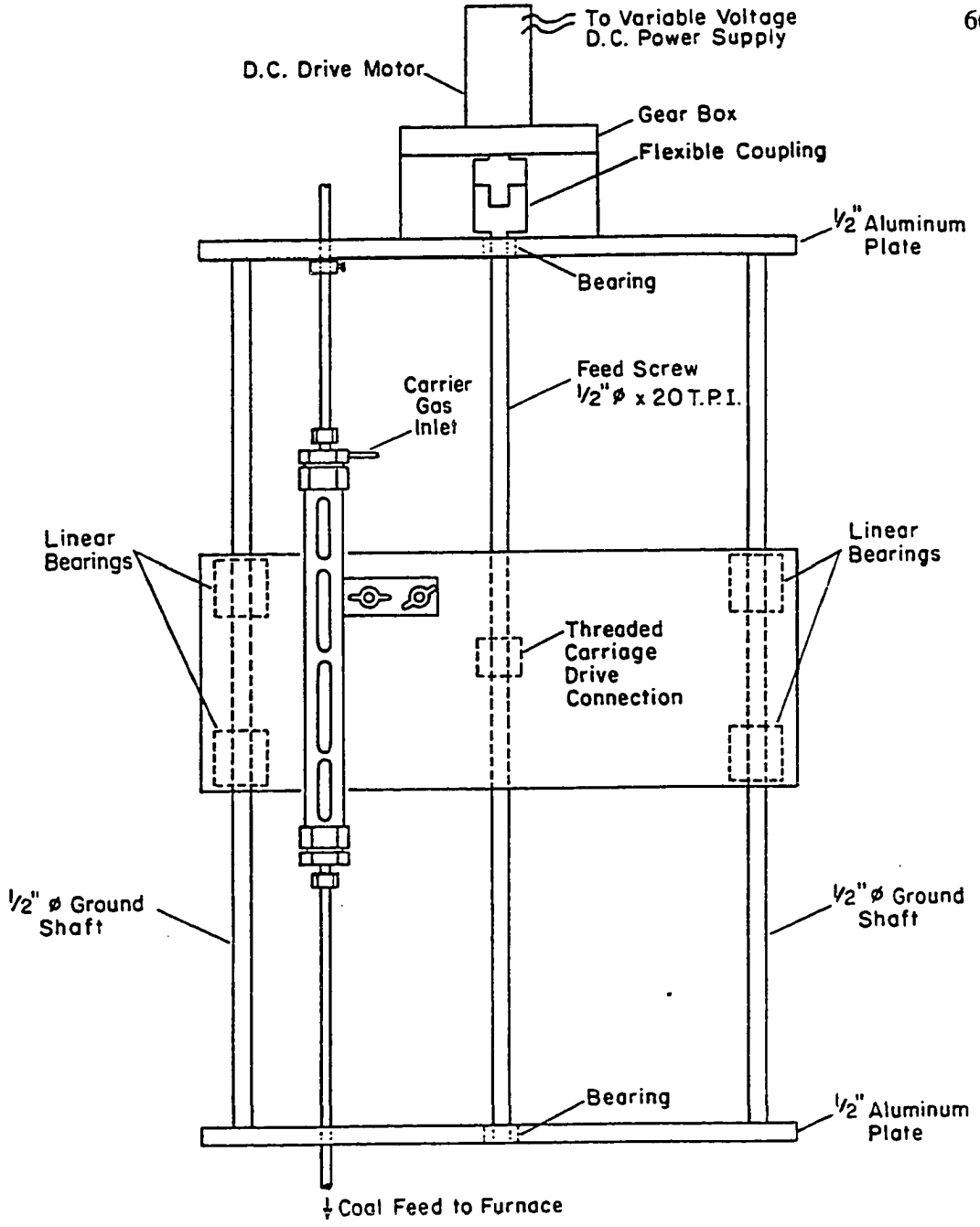

Figure 2. Coal feeder with carriage and drive mechanism.

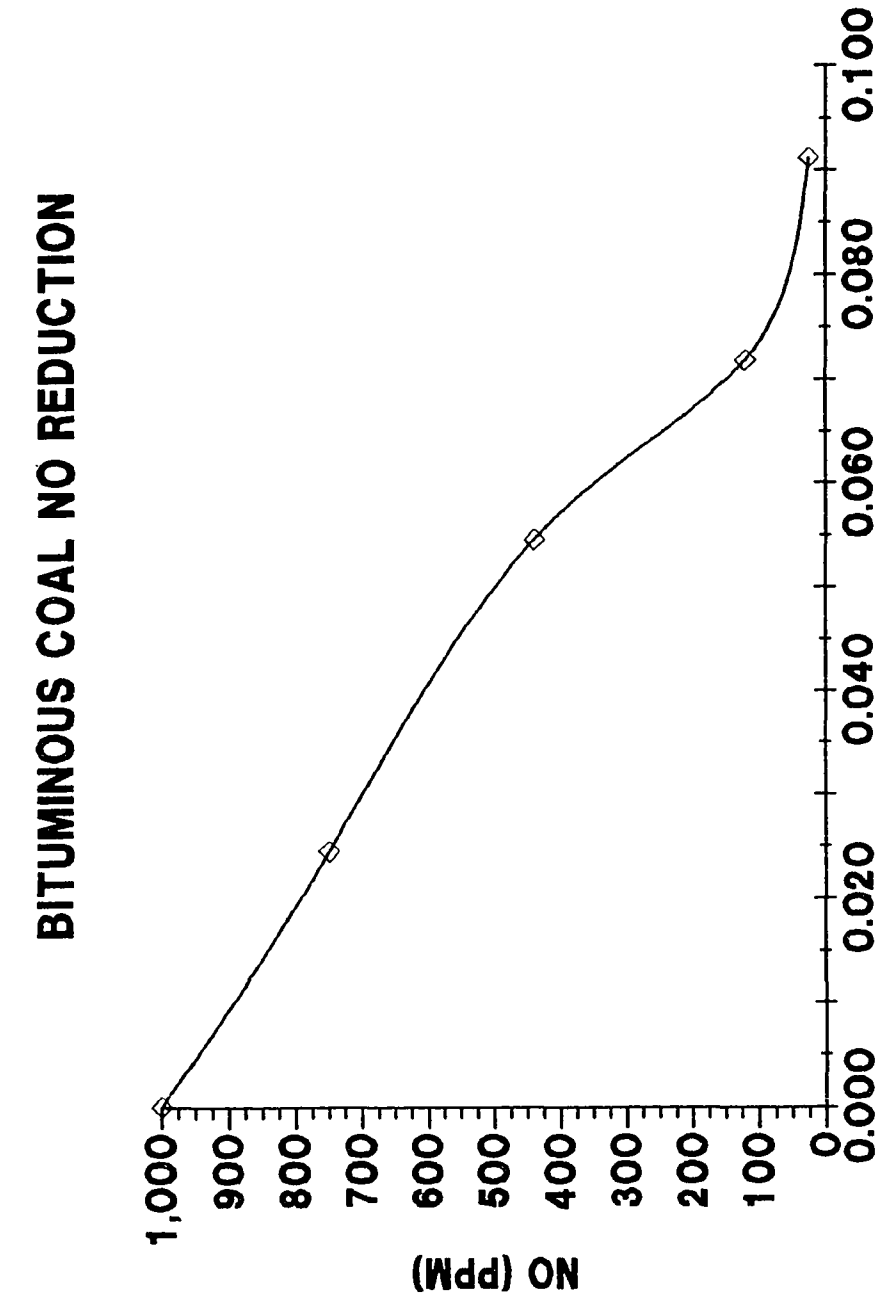

Figure 3. Surviving NO from coal reburning.

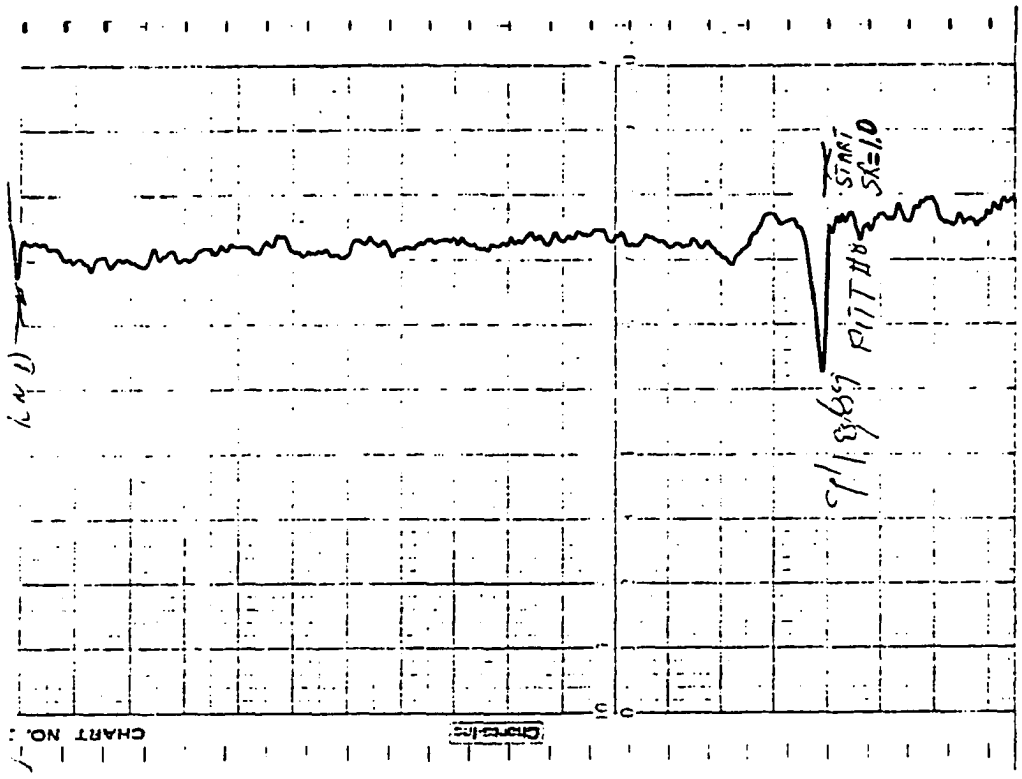

Figure 4. Strip chart recording of surviving NO for preset coal feed rate. Verticle scale is 100 ppm per major division. Horizontal scale is 2 min. per major division.

CHAPTER IV

Experimental Results

The results of the experimental work are presented in two separate papers. These results consist of mole fraction measurements of fixed-nitrogen species (and N_2 for coals) in the reactor effluent. Pertinent experimental details are described in the papers. Additional information about the thermal environment and data reduction techniques are given in the Appendices II and III of this dissertation.

The first paper compares the fixed-nitrogen speciation for methane, hexane, benzene, lignite and bituminous coal. Speciation variations are interpreted using results of numerical studies and mechanisms published in the literature. NO reduction and HCN conversion mechanisms unique to lignite reburning are investigated. The results and analysis presented in this paper accomplish the first objective listed in Chapter III.

The second paper details the results of experiments using isotopically labelled $N^{15}O$. Isotope separation with GC/MS is used to trace the various nitrogen species to their source (i.e., fuel nitrogen or NO). Probability analysis, described in Appendix III, is used to extract plausible mechanisms involved in NO reduction and N_2 production. The interaction of fuel nitrogen with NO demonstrated in this paper accomplishes the second objective given in Chapter III.

Partitioning of Nitrogenous Species in the Fuel Rich Stage of Reburning

T.E. Burch, F.R. Tillman, W.Y. Chen*, T.W. Lester,
R.B. Conway, and A.M. Sterling

Mechanical Engineering Department
Louisiana State University
Baton Rouge, Louisiana 70803

May, 1990

*Present address: Department of Chemical Engineering, University of Mississippi,
University, Mississippi 38677

Abstract

The partitioning of fixed-nitrogen species in the fuel-rich stage of reburning with methane, hexane, benzene, bituminous coal and lignite has been studied in a bench scale flow reactor. A simulated flue gas consisting of CO_2 (16.8%), O_2 (1.95%), NO (1000 ppm) and helium was used for experiments at 1100 °C and ca. 0.2 s residence time. The total fixed nitrogen (TFN) speciation was found to depend strongly on fuel type and stoichiometric ratio (SR). Rich stoichiometries promoted conversion of NO to HCN, whereas conversion of HCN to N_2 was promoted by lean stoichiometries. The optimum stoichiometry for gaseous fuels was ca. SR= 0.95. For bituminous coal and lignite, the optimum stoichiometry was lower (ca. SR=0.85). For the gaseous fuels, the HCN contribution to TFN increased as the C/H ratio of the fuel increased. The dominant TFN species for bituminous coal was HCN, but for lignite NH_3 dominated. Lignite reburning results were strongly influenced by heterogeneous conversion of NO to N_2 on char and catalytic conversion of HCN to NH_3 on fly ash. Due to these effects, which overcome kinetic barriers in reburning, lignite produced the lowest gas-phase TFN of any of the fuels tested. Consequently, enhanced reburning, by injection of lignite char/ash in the reburning zone has been proposed.

Introduction

The reductive powers of hydrocarbons in the conversion of NO_x to N_2 were first demonstrated almost four decades ago by Engle (1950). Application of this knowledge in the concept of fuel-staged combustion or reburning was proposed by Wendt et al. (1973) as an alternative to air-staged combustion.

Reburning comprises three zones in the combustion process. The primary zone is the main heat release zone in which approximately 80% of the fuel is burned in a fuel-lean (SR = 1.1) environment. This is followed by a reburning zone where additional fuel is added to give an overall fuel-rich stoichiometry (ca. SR = 0.9). Finally, additional air is provided in the burnout zone to complete the combustion process by burning off residual hydrocarbons in a fuel-lean environment. Air-staged combustion, in contrast, has only two stages, a fuel-rich primary zone (ca. SR = 0.7) followed by a fuel-lean burnout zone.

Reburning has advantages over air-staged combustion, particularly when applied to coal. The fuel-lean primary zone of reburning produces better flame stability and char burnout. However advantageous from a practical viewpoint, reburning accomplishing 50% NO_x removal was not demonstrated until Takahashi et al. (1983) reported results from tests at Mitsubishi Heavy Industries using natural gas as a reburning fuel. This success led to subsequent efforts at Acurex Corporation (Mulholland and Lanier, 1984), at Energy and Environmental Research Corporation (Overmoe et al., 1986), and at the U.S. Environmental Protection Agency (Mulholland and Hall, 1986).

A number of operational parameters have been identified including the nature of the reburning fuel, second-stage stoichiometry, second-stage temperature, second-stage residence time, and mixing effects. However, the relative importance of these parameters is not well understood and there is conflicting information in the literature. Consequently, the need for better understanding of NO_x destruction mechanisms, as stressed by Levy (1982), persists.

Equilibrium studies, such as those conducted by Chen, et al. (1987) and Chen, et al. (1989), show equilibrium total fixed nitrogen (TFN) to be less than 10 ppm under most conditions of interest in reburning. The extremely low equilibrium TFN levels serve to emphasize the relative crudeness of current technology in overcoming kinetic barriers presented in reburning.

Recently, kinetic modelling with mechanisms such as those developed by Miller and Bowman (1989) has been developed to the point of producing useful insight into important mechanisms of NO_x reduction as well as identifying kinetic barriers. However, detailed oxidation mechanisms are only available for small hydrocarbons (e.g., C_2 and smaller). Even the best methane sets suffer from unreliable and insufficient data for some important reaction steps. Thus many prospective reburning fuels cannot be modelled adequately.

One potentially important variable that has received only nominal attention in the literature is fuel type. Fuels of different composition under the oxidation/pyrolysis conditions of reburning would be expected to produce different hydrocarbon fragment speciations which, in turn, could radically affect reburning characteristics. In fact,

Myerson (1974) reported variation in TFN levels with a variety of fuels ranging from methane to "regular" gasoline, but he did not give details of the TFN speciation. S.L. Chen, et al. (1989) also tested a variety of fuels, but reported only the NO levels found in the effluent of the full three-stage operation. Again important details were obscured.

The purpose of this paper is to present the results of a comparative study showing variations in reburning-stage TFN speciation with fuel type and stoichiometric ratio. The emphasis is on possible utilitarian effects. Fuels included in this study are methane, hexane, benzene, lignite, and bituminous coal. The lignite and bituminous coal are included because of their economic attractiveness as reburning fuels.

Experimental

The experiments reported here were carried out in a ceramic flow reactor (Figure 1) with a simulated flue gas consisting of 16.8% CO_2, 1.95% O_2, and 0.1% NO in a helium base. These concentrations of CO_2, O_2, and NO were chosen to be consistent with those of a coal primary flame operated at a stoichiometric ratio of 1.1. Helium, instead of nitrogen, was used as the base gas to minimize heating time due to its low heat capacity.

The flow reactor used for this research was an alumina tube (Coors Ceramics Co.) with an inside diameter of 0.75 in. and an overall length of 24 in. The central portion of the reactor tube was enclosed in a 12-in. long, electrically heated furnace (Lindberg Model 55035), which provided tube temperatures up to 1150 °C.

Furnace temperature profiles were determined by both centerline traverse and

wall mounted type K thermocouples. These two methods agreed within ±5 °C. The furnace produced a parabolic axial temperature profile common to all flow reactors with a relatively flat peak (±20 °C) over approximately 8 in. of the heated length. Outside the zone of maximal heating, the temperature fell rapidly at a rate of approximately 150 °C/in. For typical flow conditions this corresponds to heating and cooling rates on the order of 2000 °C/s. Furnace temperature profiles with and without combustion produced identical temperature profiles except for a narrow zone of maximum heat release where both wall mounted and centerline thermocouples exhibited an approximate 10 °C rise.

The centerline temperature measurements were taken using a 0.125 in o.d. sheathed but unshielded thermocouple. Due to high radiation from the walls, the temperature profiles obtained by this method are more representative of the wall temperature than the mean gas temperature at any given location. Using property data for the simulated flue gas composition and the method of Sellars, et al. (1956), the maximum gas temperature is estimated to be 50 °C lower than the maximum wall temperature and to be maintained for only 4 in. of the furnace length. The estimated average gas temperature and reaction time for this 4-in. zone are the basis for the data presented here.

The assignment of an accurate reaction temperature is complicated by the variety of fuels used. Variations in the required induction time may cause the bulk of the reaction to take place before the maximum gas temperature is reached. Since many of the radical species important in reburning are short-lived, the most appropriate

reaction temperature may be somewhat lower than that reported.

All of the gas flows were measured individually with specifically calibrated rotameters, as shown in Figure 1. The gas mixtures, with certified composition, were purchased from Matheson Gas Products Inc., Liquid Air Corp., or Liquid Carbonic. Liquid fuels (hexane and benzene) were metered and continuously vaporized in a 300 cm^3 stainless steel cylinder heated to approximately 110 °C. This relatively large volume also provided good mixing of the fuel with other feed gases prior to entering the flow reactor.

For experiments with coal as the reburning fuel, the delivery system was modified to incorporate a laboratory-scale coal feeder, shown schematically in Figure 2. Details of this device have been reported elsewhere (Burch, et al. 1990). Part of the gas flow (usually helium) was diverted through the coal feeder as a carrier gas.

The sampling train consisted of 0.25-in., stainless steel transfer lines and a switching manifold with stainless steel valves. Transfer lines from the reactor tube exit to the impinger were heat traced (80 °C) to minimize adsorption of HCN and NH_3. The effluent was desiccated with anhydrous calcium sulfate before transfer to the instrument package through 0.25-in. teflon tubing. For coal experiments, the sampling train was modified to allow the gaseous products (and particulate matter) to pass straight through the end of the reactor tube onto a paper filter before entering the transfer lines. The filter was enclosed in a glass housing and heated to 100 °C. Recovery tests showed no loss of HCN or NH_3 in the filter. A 10 μm filter was also added upstream of the desiccant dryer for coal experiments. The flow reactor was

maintained near atmospheric pressure by providing an atmospheric vent downstream of the instrument package and monitoring the supply gas pressure in the mixing chamber.

Fixed gas species of interest were monitored by an on-line instrument package. The analysis included NO_x (chemiluminescence, Thermoelectron), O_2 (paramagnetic, Beckman), CO and CO_2 (infrared, Beckman). Differences between the base gas used for the calibration gas and sample gas were found to produce significant instrument error. This is particularly true for chemiluminescent NO_x measurement which relies on a constant gas flow through capillary tubes. Thus, each of these instruments was calibrated with a gas mixture representative of the feed gas composition.

HCN and NH_3 were collected by diverting the reactor effluent through a straight tube impinger filled with 0.5 L of 0.1N HNO_3 aqueous solution for a specified time interval. The captured solutions were pH adjusted with NaOH and analyzed for CN^- and dissolved ammonia with specific ion electrodes (Orion Research). Poisoning of the cyanide electrode by sulfur ions was prevented by adding an aqueous solution of $Pb(NO_3)_2$ prior to adding the NaOH. Sulfide ions were precipitated as PbS. Recovery of HCN and NH_3 by this method was tested using known standards and found to be near quantitative for NH_3 but only 70% for HCN. Thus NH_3 values have been presented as measured while HCN values reported have been corrected for collection efficiency.

To insure the integrity of the data, replicate experiments were run at most conditions. Also, the reactor tube was cleaned frequently to minimize wall buildup of

soot or ash. For coal reburning, the tube was cleaned after each run. To eliminate any transient phenomena due to adsorption/desorption, operating conditions were stabilized for at least fifteen minutes before data collection began.

Gaseous Fuels Results

Reburning experiments were conducted for methane, hexane and benzene at a reburning temperature of 1100 °C and an estimated reaction time of 0.2 seconds. The stoichiometry for these tests was varied from SR = 0.7 to 1.0. The resulting TFN speciation profiles are illustrated in cumulative fashion by the curves in Figures 3 through 5.

The minimum TFN for each of these fuels occurred near SR=0.95 under these conditions. However, the minimum value attained and the sensitivity to stoichiometry were found to be considerably different for the three fuels. Also, the TFN speciation in the neighborhood of the minimum TFN was radically different.

For methane, the dominant fixed-nitrogen species at the optimum stoichiometry was NO, which accounted for more than 85% of the total. HCN comprised only 4% of the TFN. In benzene reburning, the contribution of NO at the optimum stoichiometry was only 2% of the total, with HCN making up 75%. Hexane fell in between these two extremes with NO and HCN contributions of 33% and 60% respectively. It is interesting to note that hexane exhibited the lowest TFN.

Based on the mechanisms and sensitivity analysis of Miller and Bowman (1989) and the calculations performed by W.Y. Chen et al. (1989), it seems reasonable

to view reburning as possessing two major kinetic barriers. The first barrier is the conversion of NO to HCN by combination with various hydrocarbon fragments as in the following examples.

$$C + NO \rightarrow CN + O$$

$$CH + NO \rightarrow HCN + O$$

$$CH_2 + NO \rightarrow HCNO + H$$

The accepted rate constants for these reactions are all within roughly one order of magnitude, so the dominant mechanism in the conversion of NO to HCN is strongly dependent on the relative concentrations of the reducing species produced. Regardless of which mechanism dominates, there is general agreement that the end product is HCN, whether formed directly or by rapid conversion of intermediates, such as CN or HCNO.

The second major kinetic obstacle appears to be oxidation of HCN via one of the following reactions.

$$HCN + OH \rightarrow HOCN + H$$

$$HCN + OH \rightarrow HNCO + H$$

$$HCN + O \rightarrow NCO + H$$

$$HCN + O \rightarrow NH + CO$$

Once oxidation of HCN is accomplished, the subsequent conversion of products to N atoms is rapid. N atoms are then recycled to form NO or react with NO to form N_2.

With this two-barrier concept, many of the salient features of reburning can be interpreted. First, the concentration and longevity of reducing species at near-stoichiometric conditions is so low that substantial quantities of the initial NO remains unreacted. As the stoichiometry is shifted to more fuel-rich conditions, competition from other oxidizing species decreases allowing concentrations of reducing species to build and react with NO. Thus, at richer stoichiometries, most of the NO is converted to HCN. Actually, the concentration of reducing species appears to peak somewhere around SR = 0.9, then slowly decline as the stoichiometry becomes more fuel rich. However, the general trend described above appears valid.

The concentration of oxidizing species needed to overcome the second barrier follows an opposite trend. At lean stoichiometries the populations of O and OH are high, effectively converting most of the HCN to subsequent species. As the stoichiometry becomes richer, the concentration of oxidizing species is depleted by reaction with the abundant reducing species.

Thus in lean stoichiometries, the dominant kinetic barrier appears to be the initial reduction of NO, whereas in rich stoichiometries, the conversion of HCN to subsequent species is the major barrier. The optimum stoichiometry is then defined by a compromise between these processes. This concept, admittedly simple, allows the behavior exhibited in Figures 3 through 5 to be interpreted.

For methane, the fact that the minimum TFN contains primarily NO indicates that reduction of NO to HCN is the limiting factor. The carbon to hydrogen ratio of methane (1 to 4) may not provide sufficient concentrations of the appropriate reducing species to effectively convert NO to HCN until the stoichiometry becomes too fuel rich to sustain good populations of O and OH.

Although any comment on the oxidation mechanisms of hexane and benzene is somewhat speculative, one might expect these carbon-rich fuels to produce CH_i (i = 0, 1, 2) fragments in greater concentration at stoichiometries still lean enough to support substantial O and OH populations. The hexane curves (Figure 4) seem to follow this reasoning in that more of the NO has apparently been converted to HCN at SR = 0.95. A substantial quantity of the HCN produced was then converted to subsequent species leading to N_2.

Benzene, shown in Figure 5, continued the trend of increasing reduction of NO to HCN as the carbon content of the fuel increased. However, the expected attending conversion of HCN to N_2 at this relatively lean stoichiometry was not observed. Perhaps the benzene oxidation mechanism is such that O and OH species are consumed too rapidly (or not produced at all) to allow for the conversion of HCN.

The timing of peak concentrations of important species is also critical. Since the conversion of HCN to N_2 by necessity succeeds the reduction of NO to HCN, high populations of NO reducing species occurring after O and OH have been depleted serve to reduce NO but not TFN.

One final observation is that the true optimum stoichiometry for benzene (or

methane) may not have been found. The high levels of HCN at SR = 0.95 would seem to suggest that a leaner stoichiometry might yield a better conversion of HCN to N_2 without seriously impairing the reduction of NO to HCN. Similarly, the high NO and low HCN levels exhibited by methane at SR = 0.95 would indicate that a slightly richer stoichiometry might improve overall TFN levels.

Coal Results

Reburning experiments were conducted for a Pittsburgh #8 bituminous coal and a North Dakota lignite with reburning conditions identical to those used for gaseous fuels. The analyses of the two coals used are given in Table I. Each of the coals were sieved between 200 and 270 mesh to provide a uniform particle size for feeding and to eliminate particle size considerations in comparison of results.

Char samples were collected from reburning experiments ranging from SR = 0.7 to SR = 1.0. Analysis of these samples for each coal showed no dependence on stoichiometric ratio for either nitrogen or carbon retained in the char. On average, lignite char retained 50% of the nitrogen contained in the coal whereas bituminous char contained 58% of the original nitrogen. Apparently, reburning with the conditions used here involves primarily devolatilization with little or no char oxidation taking place. Since no dependence on stoichiometry was observed, the average char composition for all stoichiometries was used to calculate the char nitrogen content. For these calculations ash was used as a tracer.

The cumulative TFN speciation for the Pittsburgh #8 coal is shown in Figure

6. The most notable feature of this graph is that the minimum gas-phase TFN occurs at SR = 0.85 whereas for gaseous fuels SR = 0.95 produced the minimum TFN. This is reasonable if reburning is considered to be controlled primarily by homogeneous gas-phase reactions. Since part of the hydrocarbons were retained in the solid phase as char, the gas-phase stoichiometry was somewhat leaner than the overall stoichiometry.

The gas-phase TFN exhibited by the Pittsburgh #8 coal appears very similar to the hexane distribution both in minimum TFN value and speciation. However, the retained char nitrogen added considerably to the fixed-nitrogen pool and accounted for more than 65% of the total at SR = 0.85.

Lignite reburning produced more novel results as shown in Figure 7. The minimum TFN for lignite occurred at SR = 0.9 owing partially to higher volatility of combustible species. Surprisingly, reduction of NO was nearly complete for stoichiometries below SR = 0.85, achieving levels below 1 ppm. Another unusual feature is that for all stoichiometries below SR = 0.90 the gas-phase TFN is totally dominated by NH_3. HCN levels never exceeded 17 ppm at any stoichiometry.

Although fuel-rich combustion and pyrolysis experiments reported in the literature (e.g., Bose et al.,1988) have shown high levels of NH_3 from lignites, the results presented here differ in that much of the gas-phase nitrogen in these experiments did not originate in the coal. The extremely low NO and HCN levels (normally the dominant species in reburning) suggest that most of the original NO has been converted to either NH_3 or N_2. These peculiar results spawned an effort to isolate

the reason for this behavior and to see if the low NO, low HCN, and high NH_3 levels were related.

Heterogeneous reactions of NO are usually discounted in reburning as too slow to be of any consequence. However, a suitable gas-phase mechanism could not be found, so the search was directed toward heterogeneous mechanisms.

The effect of char addition rate on surviving NO levels with varying gas composition was studied. The char was collected from lignite reburning at SR = 0.85. First, the standard gas composition used for other reburning experiments (i.e., 16.8% CO_2, 1.95% O_2, 1000 ppm NO, balance He) was used. For reference a char feed rate of 0.029 gm/min corresponds to the char loading found in lignite reburning at SR = 0.9. The results are shown in Curve 1 of Figure 8. As the char feed rate was increased, the surviving NO levels gradually decreased and then abruptly fell to less than 10 ppm. This precipitous decline was accompanied by the disappearance of measurable O_2 in the reactor effluent. This suggested competition for active sites on the char surface.

The results shown in Curve 2 of Figure 8 were obtained by replacing the O_2 in the feed gas with helium so that CO_2 remained the only oxidizer competing with NO for active sites. The elimination of O_2 had a profound effect in that significantly lower char feed rates produced very low surviving NO levels. However, some competition for active sites persisted. When char was fed, some of the CO_2 was reduced to CO.

Finally, the effect of char on surviving NO with only NO and He in the feed

gas is shown in Curve 3 of Figure 8. Eliminating the CO_2 from the feed gas further reduced the required char feed rate to the point that any char feed resulted in almost total elimination of NO from the reactor effluent.

In all of the above tests only low levels of HCN and NH_3 were formed because of the absence of available hydrogen. Also, the reaction was almost certainly heterogeneous instead of surface-catalyzed gas-phase since gas-phase reactants were almost non-existent. DeSoete (1980) gives an excellent review of possible mechanisms.

Next attention was turned to the unusually high production of NH_3 in lignite reburning. Again heterogeneous effects were suspected. To confirm this, a methane reburning experiment was conducted at SR = 0.9 with char addition at a rate of approximately 0.0194 gm/min. The results of this experiment (shown in Table 2) were very similar to those from lignite reburning. The only difference of note was the lower NO level produced by methane/char reburning because of the richer gas-phase stoichiometry.

Next, lignite ash was produced by burning char in excess O_2 at 1100 °C and fed with methane at SR = 0.9. Again, high levels of NH_3 were produced as shown in Table 2. However, in this experiment the surviving NO level was similar to that when reburning with methane alone. Also, the NH_3 level was almost twice that of methane/char reburning. Since the ash contained very little carbon, the direct heterogeneous reduction of NO on carbon was eliminated. This caused more of the nitrogen to be converted to HCN as in reburning with methane alone.

In the final experiments, (shown in Table 2) NO was replaced with approximately 500 ppm of HCN in methane/char reburning. Again the final TFN distribution was weighted heavily in favor of NH_3. Although not conclusive, these tests strongly indicate that increased NH_3 production with lignite reburning was the result of HCN conversion in an ash-catalyzed reaction. However, direct conversion by addition of H_2 would seem unlikely. A mechanism such as the sequence

$$HCN + OH \xrightarrow{catalyst} HOCN + H$$

$$HOCN + H \rightarrow HNCO + H$$

$$HNCO + H \rightarrow NH_2 + CO$$

$$NH_2 + H_2 \rightarrow NH_3 + H$$

would be more plausible. In this mechanism, some of the HCN converted to NH_2 would be subsequently converted to N_2 via

$$NH + NH_2 \rightarrow N_2H_2 + H$$

$$N_2H_2 + M \rightarrow NNH + H + M$$

$$N_2H_2 + H \rightarrow NNH + H_2$$

$$NNH + M \rightarrow N_2 + H + M.$$

Thus the lower total fixed nitrogen found in methane/ash versus methane alone would be accounted for.

The strong heterogeneous and/or catalytic effects observed with lignite char are particularly interesting in light of the apparent absence of such effects with bituminous char. The reason for this disparity is not known, but may be due to differences in the ash composition.

The lignite ash (PSOC 1507) composition as reported by the Pennsylvania State University Coal Research Section was unusually rich in calcium oxide (23.2%), barium (6570 ppm), and strontium (4900 ppm). On the basis of concentrations alone, these seem to be the most likely candidates for catalysts.

The heterogeneous reduction of NO to N_2 is most likely due to the large surface area of the very porous and friable lignite char. However, this may also be a catalytic effect. Several authors including Walker (1968) have observed enhancement of char oxidation rates when the chars were impregnated with various transition metal compounds.

Conclusions

The choice of fuels has a very definite impact on the TFN speciation and minimum TFN achievable in reburning. The estimated NO concentrations after burnout for the fuels tested in this work are shown in Figure 9. These estimations are based on 80% conversion of gas-phase fixed nitrogen and 20% conversion of char

nitrogen to NO. From this graph it would appear that the lignite has the greatest potential in spite of its fuel-bound nitrogen. However, because the NO after burnout is very sensitive to the char-nitrogen to NO conversion rate, these estimates may be subject to considerable error.

The strong heterogeneous/catalytic activity of the lignite char could have important consequences for practical reburning enhancement. It appears that lignite char at least partially removes the current kinetic barriers in reburning by directly converting NO to N_2 and by converting HCN to other nitrogenous species that are more readily converted to N_2.

Addition of lignite char in methane reburning reduced gas-phase TFN by 71%. If the char could be produced with low nitrogen content or used in smaller quantities without adversely affecting the desirable characteristics, overall TFN could be reduced to extremely low levels. Even the simple addition of lignite ash in methane reburning reduced TFN levels by 39% over methane alone. Although temperature, scale up, and mixing effects need to be studied, and may impact the utility of this scheme, enhanced reburning by injection of suitable char/ash may show some promise.

Acknowledgements

The work reported in this communication was funded by the U.S. Department of Energy, Pittsburgh Energy Technology Center under contract No. DE-AC22-88PC88859.

References

Bose, A.C., K.M. Danneker, and J.O.L. Wendt, "Coal Composition Effects on Mechanisms Goverening the Destruction of NO and Other Nitrogenous Species During Fuel-Rich Combustion"'Energy and Fuels, Vol. 2, No. 3, 1988.

Burch, T.E., R.B. Conway, and W.Y. Chen, "A Practical Coal Feeder for Bench-Scale Combustion Requiring Low Feed Rates", submitted to Review of Scientific Instruments, May, 1990.

Chen, J.K., W.Y. Chen and R.E.C. Weaver, "Nitric Oxide Emission under Reburning Conditions: Equilibrium Concentration", Spring National Meeting AIChE, Houston, Texas, Paper No. 76c, April 1987.

Chen, S.L., J.C. Kramlich, W.R. Seeker, and D.W. Pershing, "Optimization of Reburning for Advanced NO_x control on Coal-Fired Boilers", Journal Air Waste Management Association, Vol. 39, No. 10, October 1989.

Chen, W.Y., T.W. Lester, L.M. Babcock, T.E. Burch, and F.R. Tillman, "Formation and Destruction of Nitrogen Oxides in Coal Combustion", Sixth Quarterly Report, DOE Contract No. DE-AC22-88PC88859, July 1989.

DeSoete, G.G., "Mechanisms of Nitric Oxide Reduction on Solid Particles", Fifth EPA Fundamental Combustion Research Workshop, Newport Beach, January, 1980.

Engle, G., "Formation of Hydrogen Cyanide by the Action of Nitric Oxide on Natural Gas under Atmospheric Pressure,II. The Influence of Steam, Hydrogen and Oxygen", Compt. Rend., 231, p. 1493, 1950.

Levy, A., "Unresolved Problems in SO_x, NO_x, Soot Control in Combustion", Nineteenth Symposium (International) on Combustion, p. 1223, The Combustion Institute, 1982.

Miller, J.A. and C.T. Bowman, "Mechanism and Modelling of Nitrogen Chemistry in Combustion", Prog. Energy Combustion Science, Vol. 15, p. 287, 1989.

Mulholland, J.A., and R.E. Hall, Proceedings 1984 Symposium Stationary Combustion NO_x Control, Vol. 1, Utility Boiler Application, EPRI CS-4360, Jan. 1986.

Mulholland, J.A., and W.S. Lanier, "Application of Reburning for NO_x Control to a Firetube Package Boiler", EPA-600/D-84-170, U.S. EPA, June 1984.

Myerson, A.L., F.R. Taylor, and B.G. Faunce, Sixth Symposium (International) on

Combustion, p. 154, Rheinhold, 1957.

Myerson, A.L., "The Reduction of Nitric Oxide in Simulated Combustion Effluents by Hydrocarbon-Oxygen Mixtures", Fifteenth Symposium (International) on Combustion, p.1085, The Combustion Institute, 1974.

Overmoe, B.J., J.M. McCarthy, S.L. Chen, W.R. Seeker, G.D. Silcox, and D.W.Pershing, "Pilot Scale Evaluation of NO_x Control from Pulverized Coal Combustion by Reburning", Proceedings: 1985 Symposium Stationary Combustion NO_x Control, Vol.1. Utility Boiler Application, EPRI CS-4360, January, 1986.

Sellars, J.R., M. Tribus, and J.S. Klein, "Heat Transfer to Laminar Flow in a Round Tube or Flat Conduit-Gratz Problem Extended", Trans. ASME, Vol. 78, p. 441, 1956.

Takahashi, Y., T. Sengoku, F. Nakashima, S. Kaneko, and K. Tokuda, "Development of "MACT" In-Furnace NO_x Removal Process for Steam Generators", Proc. 1982 Joint Symposium Stationary NO_x Control, Vol. 1, "EPRI Report No. CS-3182, July, 1983.

Walker, P.L., M. Shelef, and R.T. Anderson, "Catalysis of Carbon Gasification", Chemistry and Physics of Carbon, Vol. 4 (Walker, P.L., Ed.), Marcel Dekker, New York, NY, 287, 1968

Wendt, J.O.L., C.V. Stemling, and M.A. Matovich, "Reduction of Sulfur Trioxides and Nitrogen Oxides by Secondary Fuel Injection", Fourteenth Symposium (International) on Combustion, p. 897, The Combustion Institute, 1973.

Table 1. Analysis of Coals

	Pittsburgh #8, Bituminous	North Dakota Lignite (PSOC 1507)
Moisture*	2.02	14.39
Carbon	70.48	60.63
Hydrogen	4.66	4.44
Oxygen (Diff)	8.53	22.63
Nitrogen	1.44	0.86
Sulfur	3.35	1.19
Ash	11.54	10.25
Vol. Matter	33.25	43.28
Fixed Carbon	55.21	46.47

*Moisture is reported on an as received basis all other results are on a dry basis.

Table 2. Total Fixed Nitrogen Speciation With Addition of Lignite Char/Ash.

Rebuming Fuel	CH_4	Lignite	CH_4/char	CH_4/ash	CH_4/char
N in Feed	NO	NO	NO	NO	HCN
Concentration, ppm	1000	1000	1000	1000	500
Effluent Species					
NO, ppm	90	32	5	70	1
HCN, ppm	308	12	9	10	12
NH_3, ppm	105	135	130	227	51

Gas phase SR=0.9 for all tests.

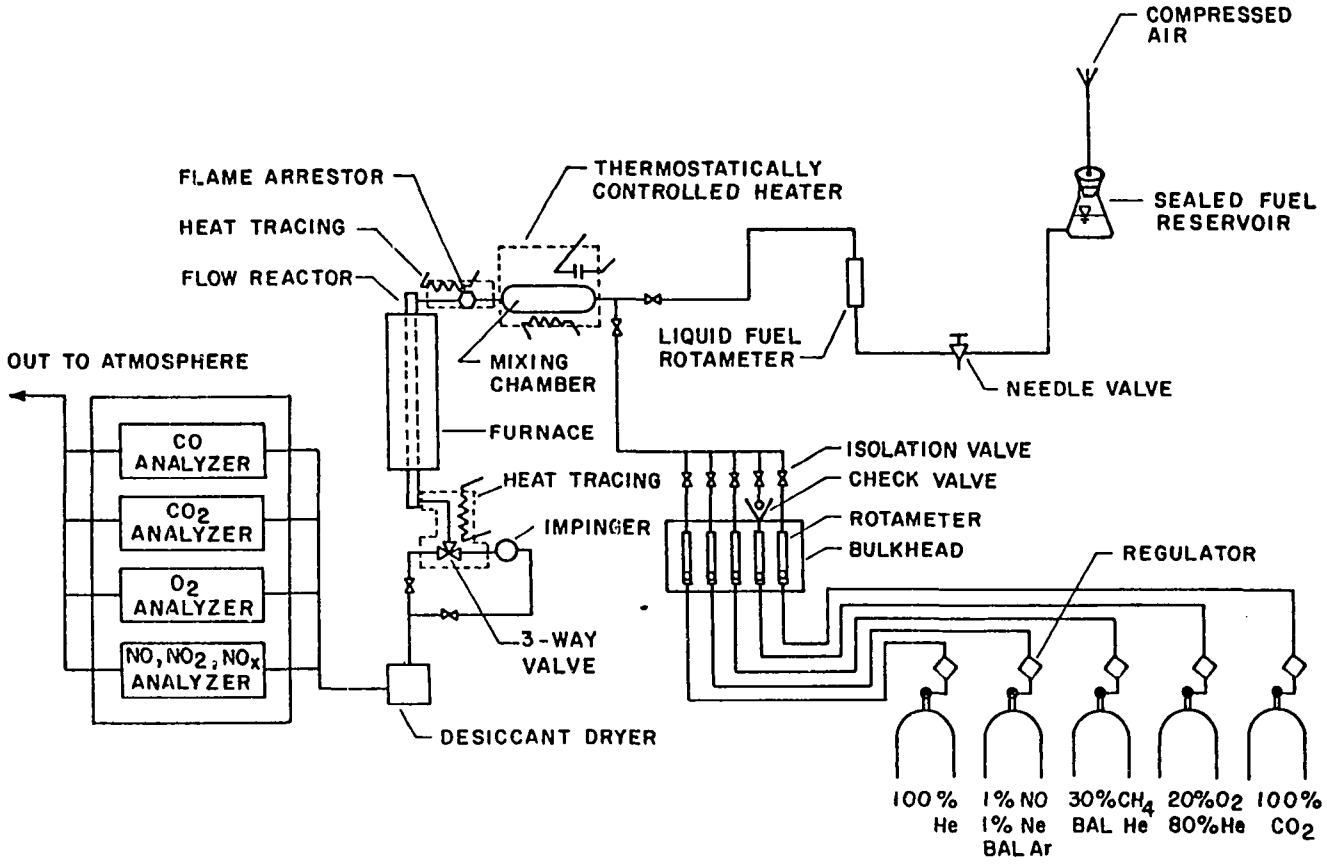

Figure 1. Schematic of experimental facility.

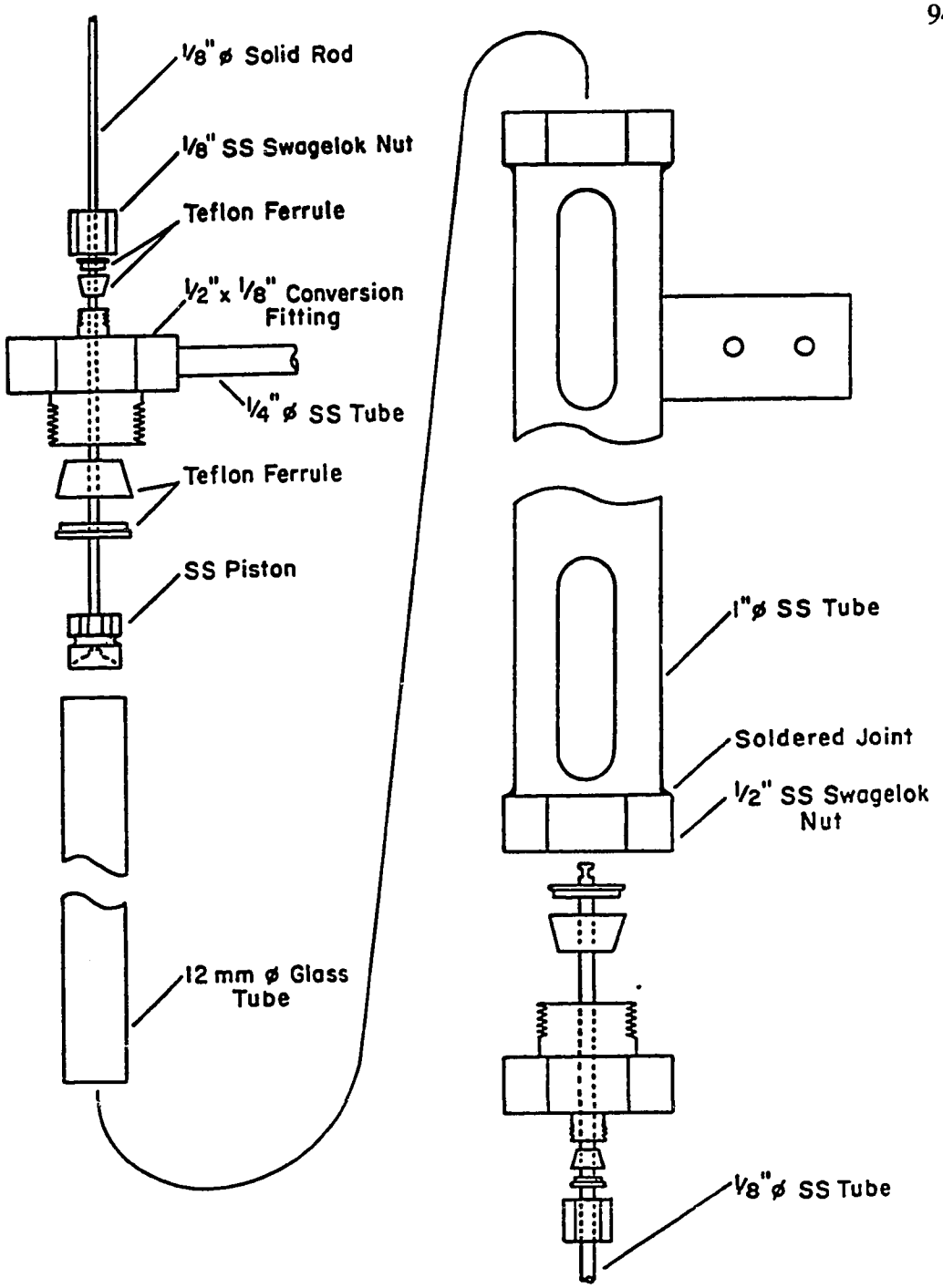

Figure 2. Exploded view of coal feeder assembly.

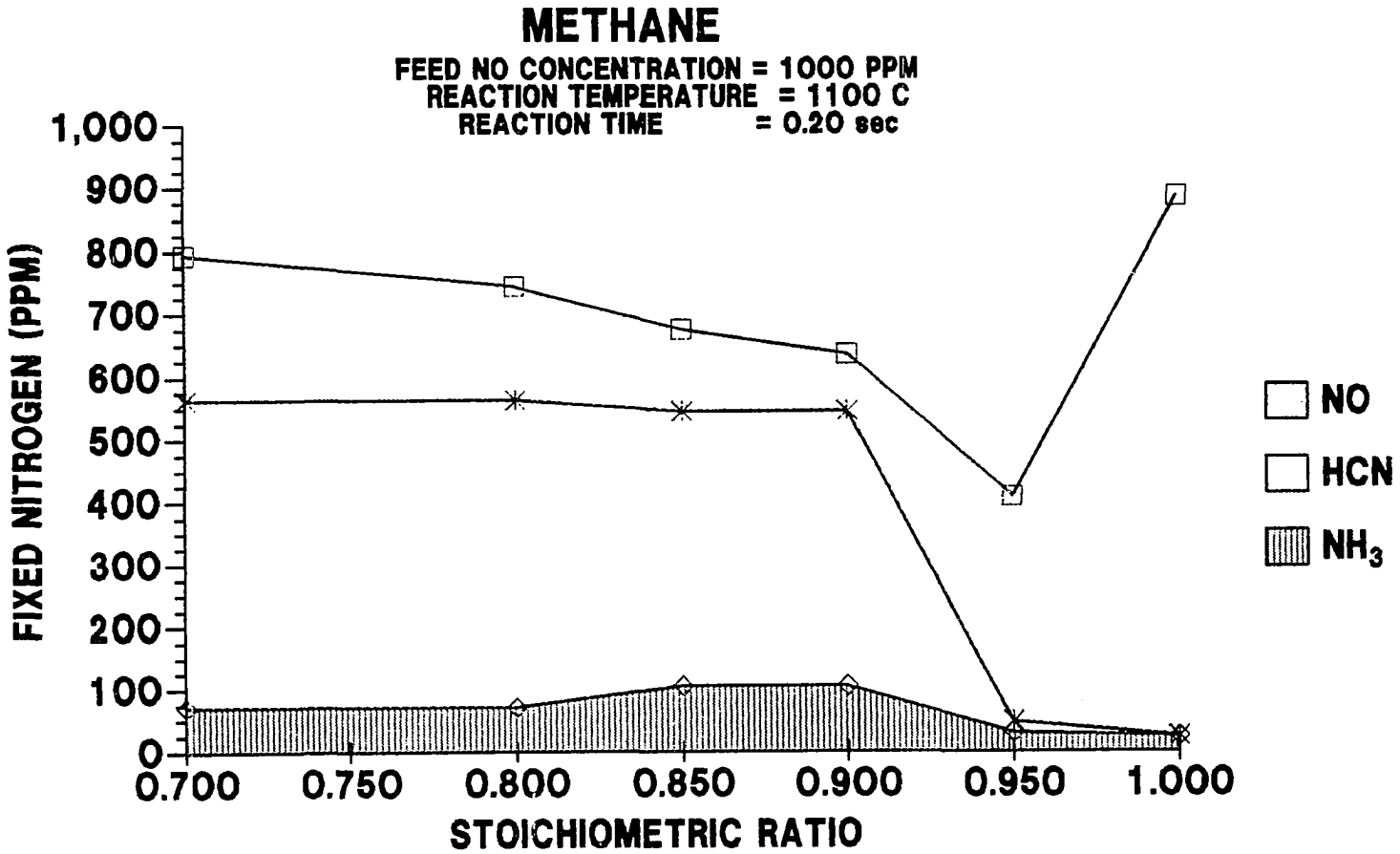

Figure 3. Cumulative total fixed nitrogen for methane reburning.

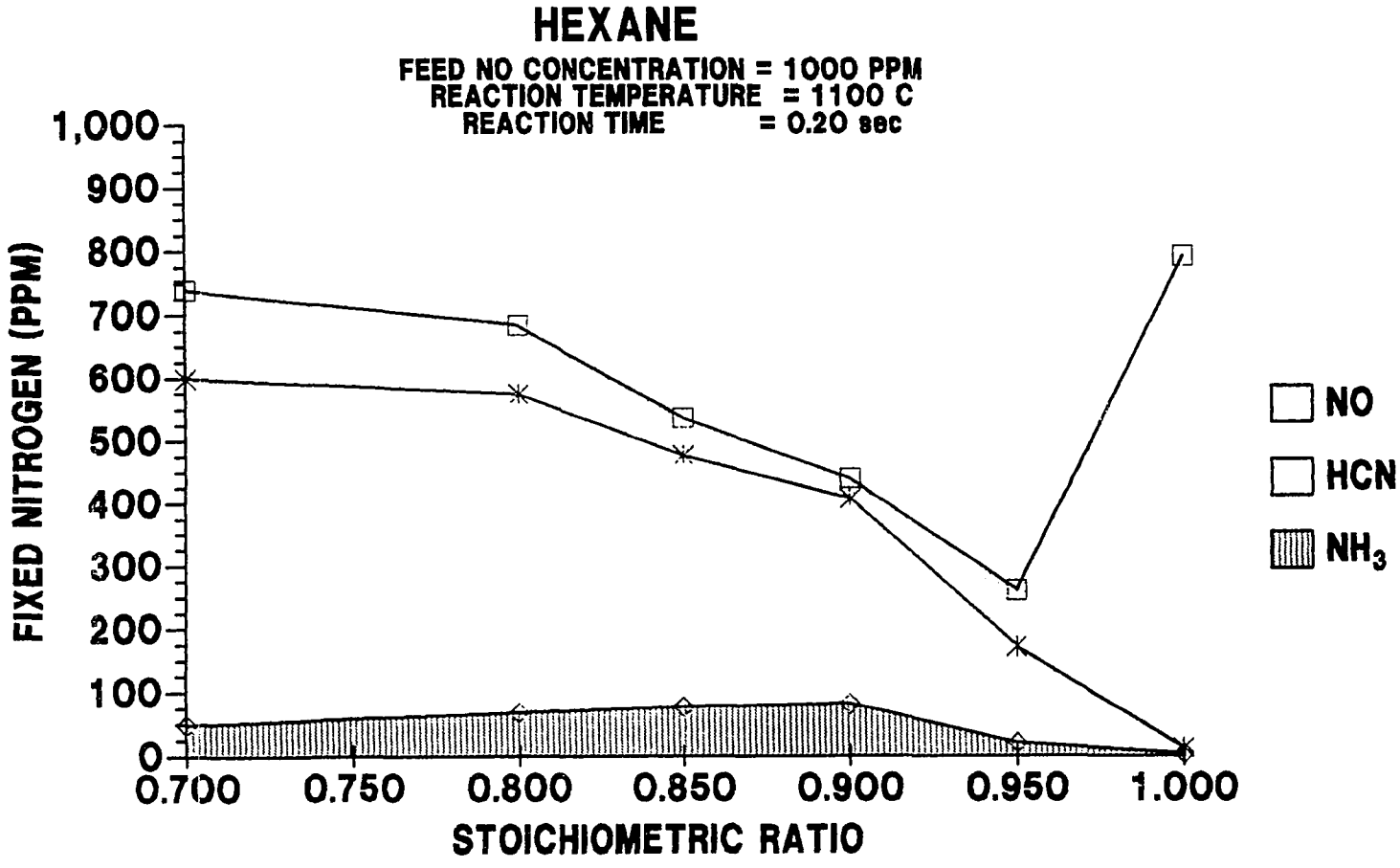

Figure 4. Cumulative total fixed nitrogen for hexane reburning.

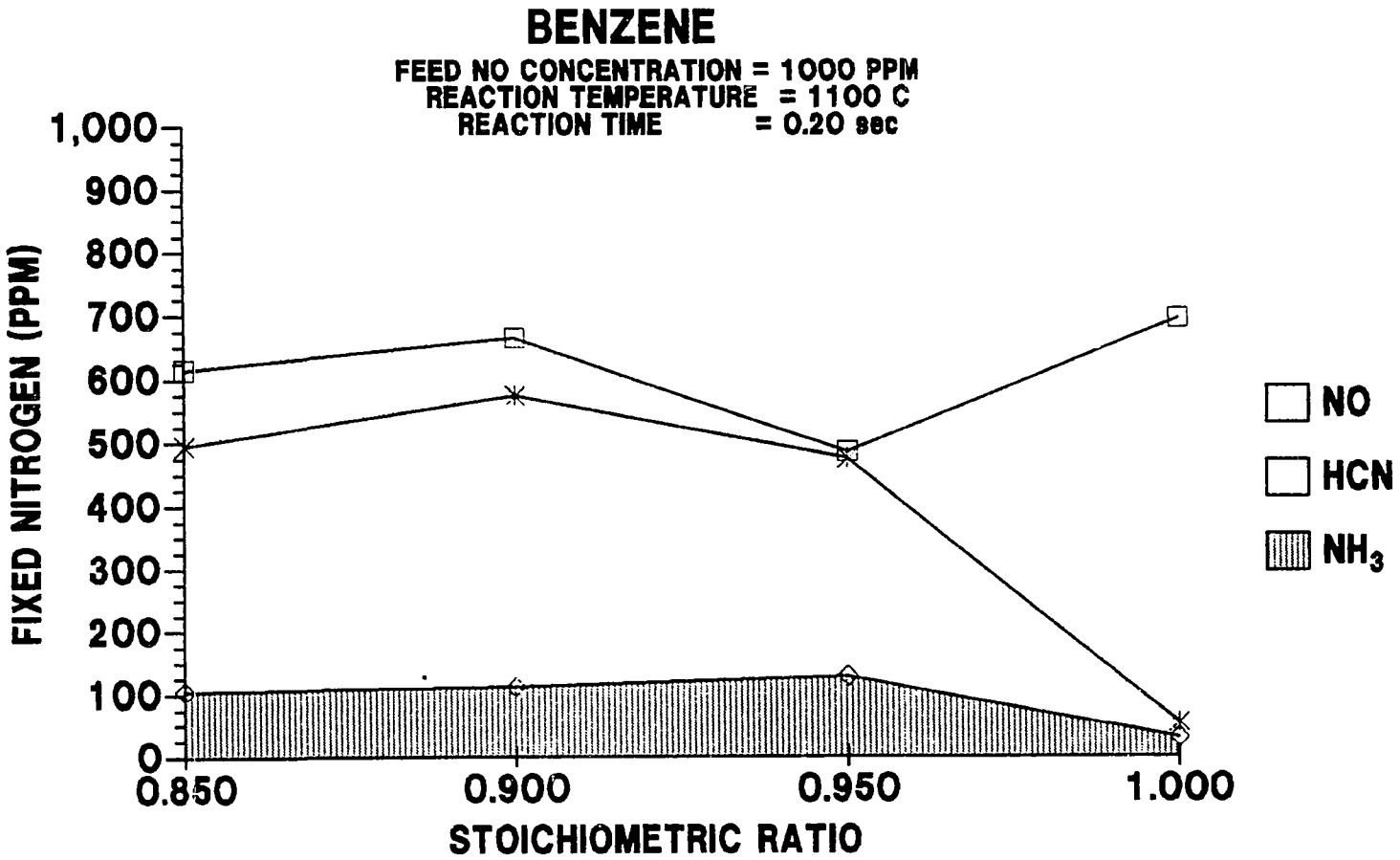

Figure 5. Cumulative total fixed nitrogen for benzene reburning.

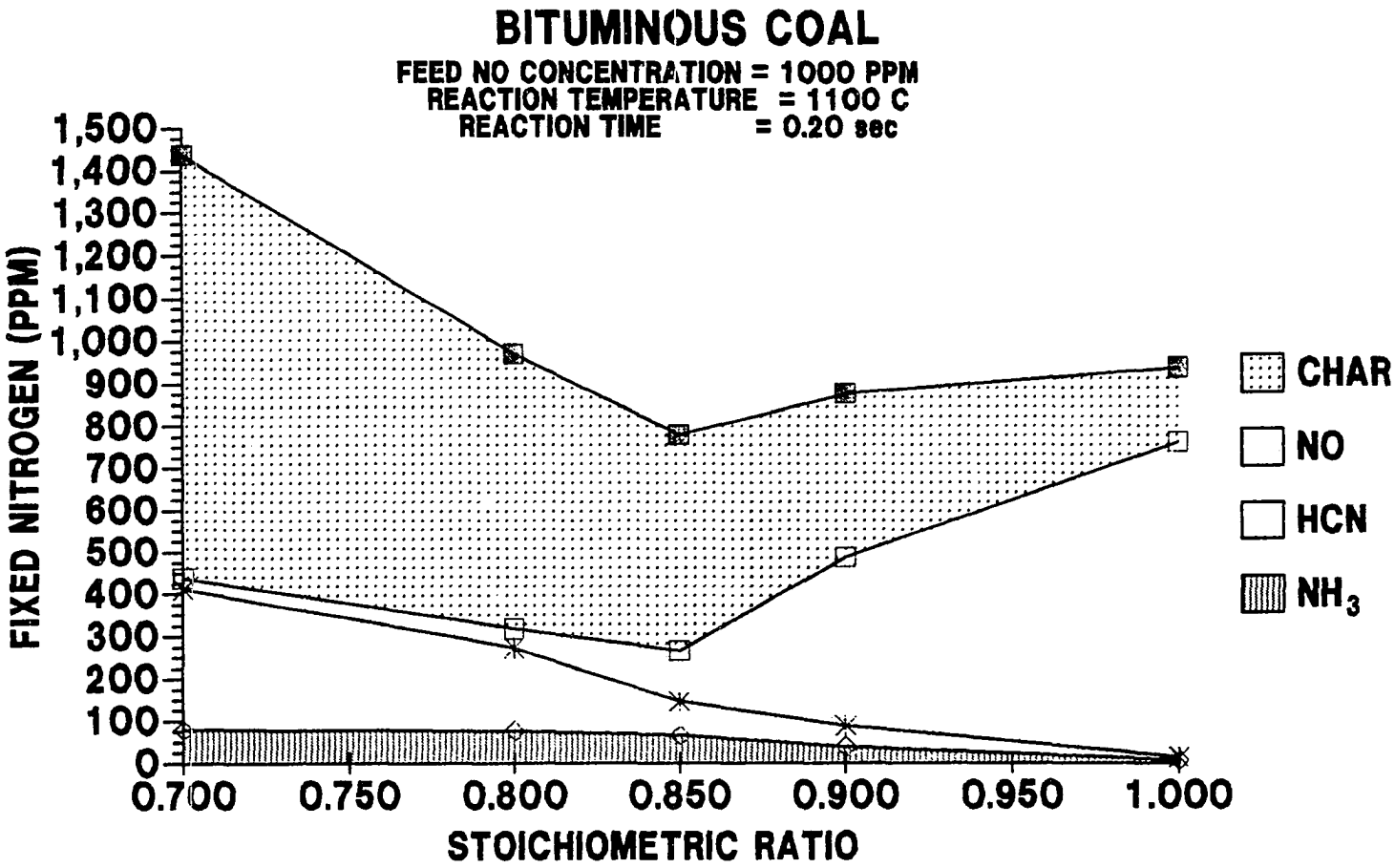

Figure 6. Cumulative total fixed nitrogen for reburning with Pittsburgh #8 bituminous coal.

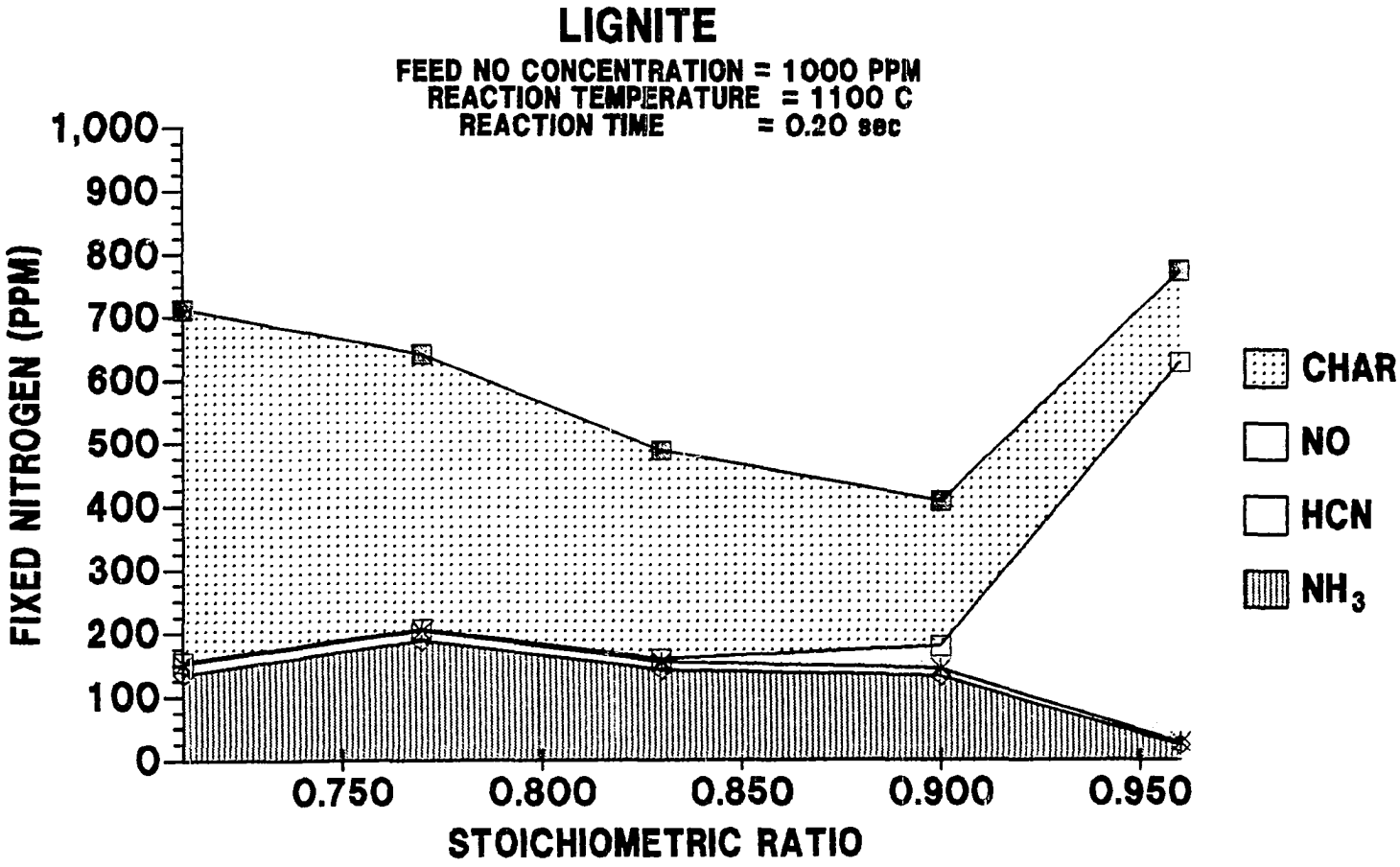

Figure 7. Cumulative total fixed nitrogen for reburning with Zap, North Dakota lignite.

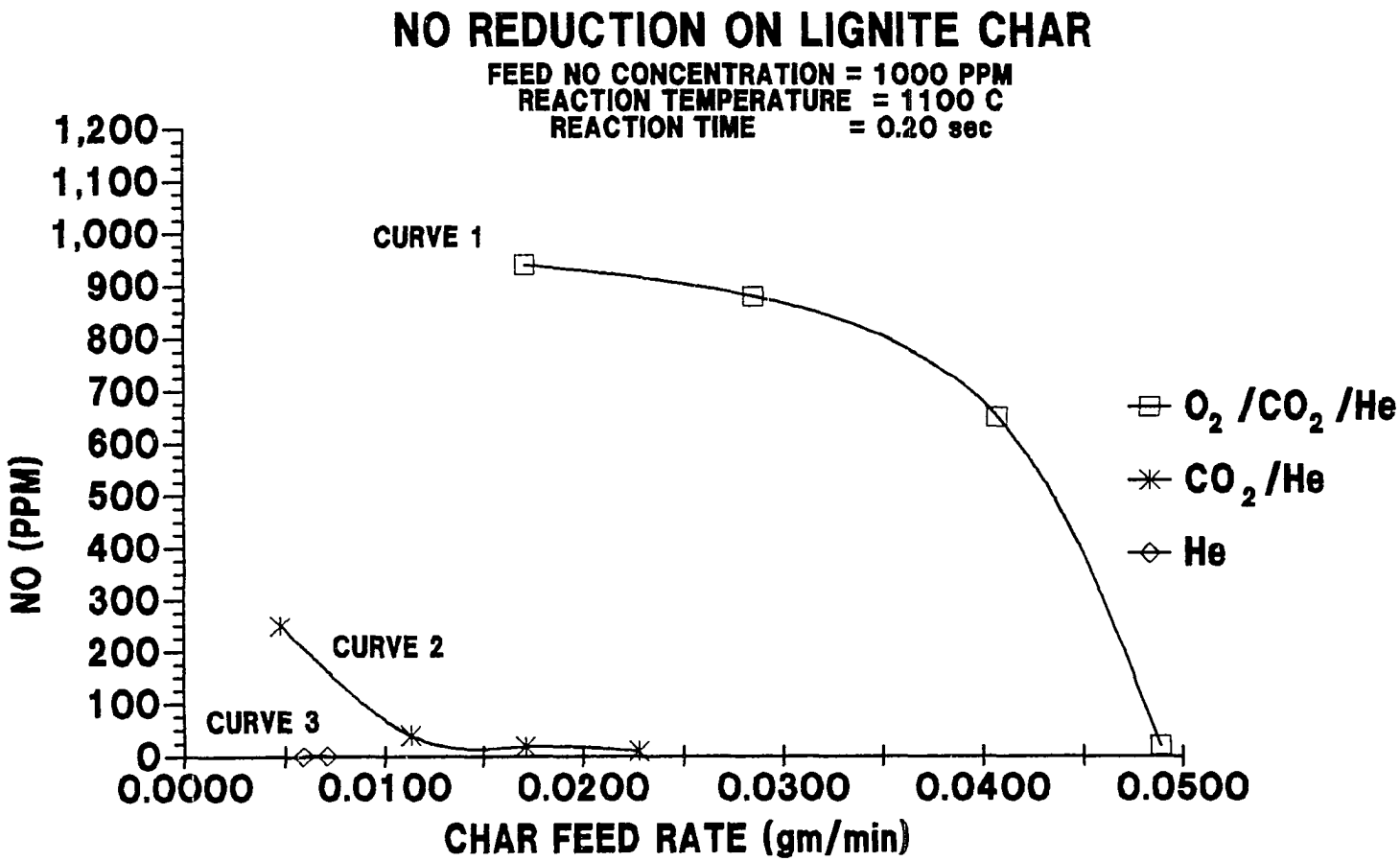

Figure 8. Influence of gas composition on heterogeneous reduction of NO with lignite char.

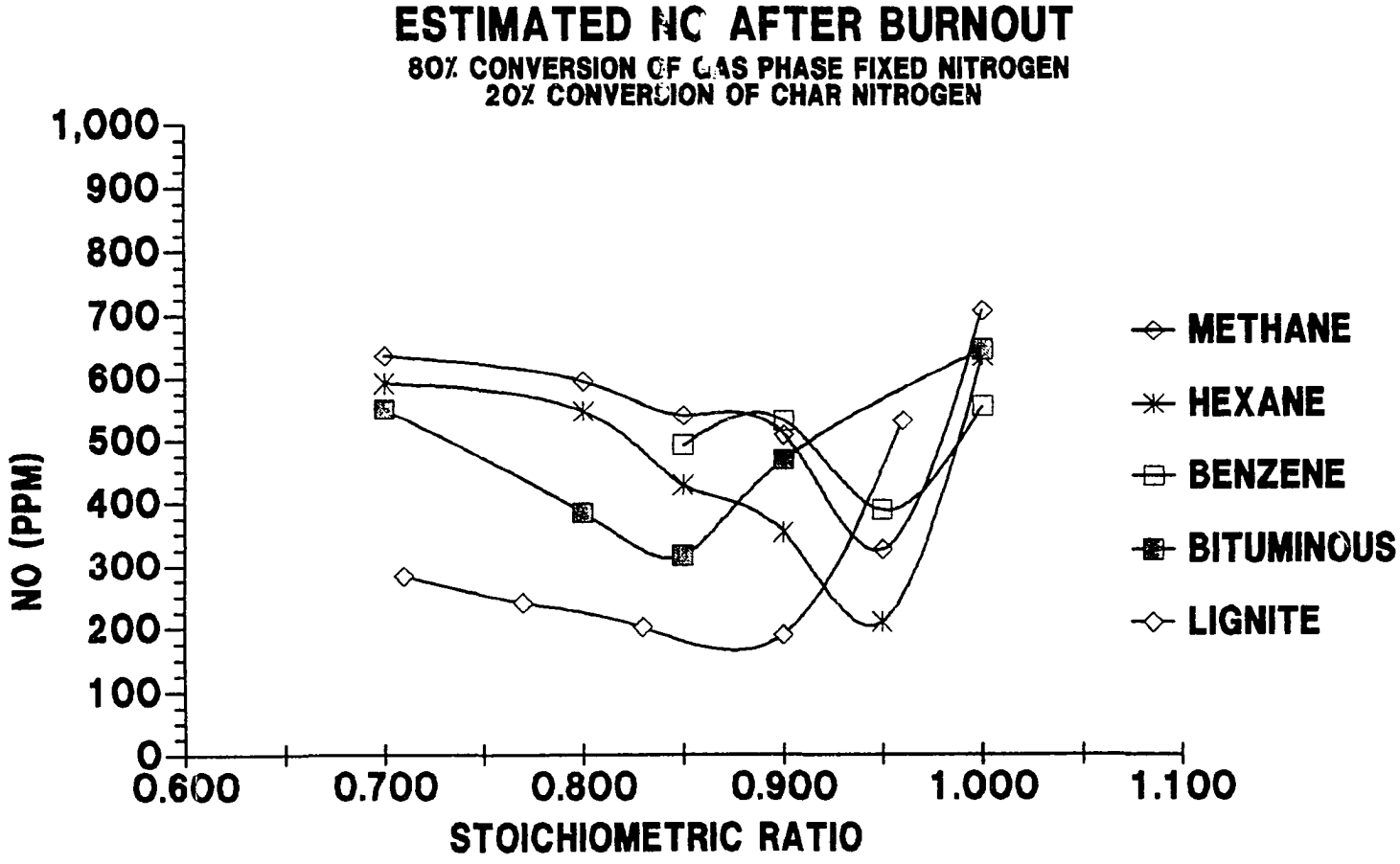

Figure 9. Comparison of estimated NO after burnout for fuels tested.

Interaction of Fuel Nitrogen with Nitric Oxide During Reburning with Coal

T.E. Burch, W.Y. Chen*, T.W. Lester,
and A.M. Sterling

Mechanical Engineering Department
Louisiana State University
Baton Rouge, Louisiana 70803

May, 1990

*Present Address: Department of Chemical Engineering, University of Mississippi,
University, Mississippi 38677

Abstract

Isotopically labelled $N^{15}O$ was used to study the interaction of fuel nitrogen with NO in reburning. Experiments were conducted in an alumina flow reactor operated at 1100 °C with a residence time of approximately 0.2 s. A North Dakota lignite and a Pittsburgh #8 bituminous coal were burned with a simulated flue gas. Species and isotope separation were accomplished using GC/MS. The ratio of labelled to unlabeled isotopes of each major nitrogen-containing species varied with stoichiometry, but not with coal type. Delayed nitrogen evolution from both coals was evident from the data. Data analysis showed that significant N_2 production (i.e., greater than 50%) occurred through non-NO pathways. Little $N^{14}O$ was observed, indicating low conversion rates of intermediates to NO after significant nitrogen evolution from the coal.

Introduction

Reburning or fuel-staged combustion is an in-furnace NO_x control process that utilizes the reductive powers of hydrocarbons. This concept, and the term reburning, were first proposed by Wendt, et al. (1973). However, reburning was not established as a practical NO_x reducing method until Takahashi, et al. (1983) reported greater than 50% reduction of NO in tests at Mitsubishi Heavy Industries.

Reburning has its greatest applicability in coal-fired facilities, where fuel-bound nitrogen produces high NO_x levels in the primary flame. Most of the reburning research, however, has concentrated on nitrogen-free reburning fuels, primarily natural gas. Coal is generally not regarded as a viable reburning-fuel candidate because the fuel-bound nitrogen in coal is thought to produce too much HCN and NH_3, which would be converted to NO in the burnout stage.

The economic attractiveness of coal as a reburning fuel has, however, prompted efforts by Glass, et al. (1982), Chen, et al. (1983), Bose, et al. (1988) and others to study the prospect of reburning with coal. Numerous questions remain to be answered regarding coal reburning. Among the more pressing issues are the timing and extent of fuel nitrogen release, the effect of fuel nitrogen form (i.e., HCN or NH_3), and the interaction of fuel nitrogen species with NO.

The work described here attempts to address these issues as well as elucidate important NO reducing and N_2 forming pathways. Specifically, isotopically labelled $N^{15}O$ was used in simulated reburning with diverse coals to determine the destiny of fuel nitrogen and gas-phase NO. The isotope distributions of nitrogenous species were

determined by GC/MS analysis. The important reduction mechanisms and interactions of fuel nitrogen species with NO were deduced from the N^{15}/N^{14} distribution among the various nitrogen compounds produced.

Experimental

Coal reburning experiments were conducted in a bench-scale flow reactor. The heart of this apparatus is a 0.75-in. i.d. alumina tube (Coors Ceramic Co.) enclosed in a 12-in. long electric furnace (Lindberg Model 55035). The furnace produces reaction temperatures of 1100 °C over approximately four inches of the heated length.

A simulated flue gas consisting of 16.8% CO_2, 1.95% O_2 and 0.1% NO in helium was used. The helium base produced rapid heating and cooling and also allowed diatomic nitrogen to be analyzed as a product of reburning. The simulated flue gas was produced from individual components or helium diluted components metered through calibrated rotameters. For all experiments a gas flow rate of 1840 cm^3/min was maintained, giving an estimated residence time of 0.2 s at the maximum temperature of 1100 °C.

Coal was fed from a custom-designed volumetric feeder. Part of the helium was diverted through the coal feeder for use as a carrier gas. Mixing of the entrained coal with the simulated flue gas was accomplished in a 6-in. long section of the reactor tube preceding the furnace. A more detailed description of the experimental apparatus is given elsewhere (Burch, et al. 1990).

To enhance the accuracy of the nitrogenous species measurements, quantitative and qualitative measurements were made separately. Quantitative measurements of fixed nitrogen species (NO, HCN, and NH_3) were found to be very difficult with a remote GC/MS. Adsorption of HCN and NH_3 on container walls and oxidation of NO to NO_2 during transport were found to be major barriers to achieving reproducible GC/MS data.

Quantitative NO data was taken from an on-line chemiluminescence (Thermoelectron) analyzer. HCN and NH_3 were captured in a 0.1N HNO_3 aqueous solution and quantified using specific ion electrodes (Orion Research). $Pb(NO_3)_2$ was used to precipitate sulfides prior to HCN analysis. The on-line quantitative analysis also included O_2, CO_2 and CO. Quantitative analysis of N_2 was performed by GC/MS.

Qualitative analysis or separation of nitrogenous species isotopes was performed by GC/MS. Samples of the reactor effluent were captured in 300 cm^3 stainless steel containers. To eliminate contamination from past runs the containers were heated under vacuum between runs to remove HCN and NH_3 adsorbed onto the walls.

Two chromatographic columns were used for separation of the nitrogen compounds. N_2 and NO were effectively separated from other fixed gases on a 20 ft. x 1/8 in. S.S. Hayesep D_B column (Hayes Separations) at 25 °C isothermal. Separation of NH_3 and HCN was accomplished using an 8-ft. x 1/8-in. S.S. Hayesep C column operated at 80 °C for NH_3 and 120 °C for HCN. Due to active sites on the column, low concentrations of these species (less than 200 ppm) required several saturation injections and isothermal conditions to give quantifiable mass peaks. Lower

concentrations of NH_3 and HCN (less than 75 ppm) were analyzed by "loading" the column with repeated injection onto a cold column (25 °C). The oven temperature was then rapidly raised to the desired operating temperature to facilitate elution. This procedure was repeated until the isotope distribution of the HCN and NH_3 stabilized, signifying that active sites were filled with species from the current sample.

GC/MS samples were injected via evacuated and heated static injection loops. For fixed gas analysis, a 10 cm^3 S.S. loop was used. For HCN and NH_3 analysis a 40 cm^3 S.S. loop was used to help overcome low concentrations and active column sites.

Results

Reburning experiments were conducted using a Pittsburgh #8 bituminous coal and a Zap, North Dakota lignite with properties shown in Table 1. These coals were taken as representative of coals known to produce primarily HCN (bituminous) or NH_3 (lignite) from fuel nitrogen in pyrolysis or fuel-rich combustion.

The total fixed nitrogen (TFN) distributions for reburning with these coals are shown as cumulative concentrations in Figures 1 and 2. Analysis of char samples collected showed no perceptible change in nitrogen content with stoichiometry. Therefore average char data were used to calculate the gas-phase equivalent nitrogen bound in the char as shown in Figures 1 and 2. On average, lignite char contained 50% of the nitrogen contained in the coal whereas bituminous char contained 58% of the original nitrogen. A detailed discussion of the gas-phase speciation is given elsewhere (Burch, et al., 1990). For the present purposes it is important to note that

the gas-phase TFN for bituminous coal was dominated by HCN while the lignite TFN was dominated by NH_3.

The product distributions of N^{15} atoms for lignite and bituminous reburning are shown in Figures 3 and 4 respectively. The recovery of N^{15} atoms at all conditions was excellent [1000 ppm (± 7%)] except for bituminous coal at SR = 0.7. The relatively low recovery at SR = 0.7 was probably due to experimental error but could have resulted from loss of N^{15} in heavy nitrogenous species not measured. Concentrations of HCN for lignite and NH_3 for bituminous were too low for GC/MS analysis. The contributions of these species to N^{15} recovery have been estimated by assuming the isotope ratios in NH_3 and HCN were equal. The maximum error introduced by this assumption is less than 1% for lignite and less than 4% for bituminous coal.

For lignite, much of the TFN^{15} was found to be $N^{15}H_3$ demonstrating an accelerated conversion of fixed-nitrogen species to NH_3. Further discussion of the phenomena is given elsewhere (Burch et al., 1990). Note that in the neighborhood of the optimum reburning stoichiometry, 60% to 70% of the N^{15} atoms were found in $N^{15}N^{15}$. This seems to indicate that much of the NO reduction takes place without interacting with fuel-bound nitrogen.

The cumulative N^{14} atom distributions are shown in Figures 5 (lignite) and 6 (bituminous). The calculated N^{14} feed as coal nitrogen is shown as a reference. Again the N^{14} recovery was quite good, being within 100 ppm for all stoichiometries. The

observed error can be attributed to a number of factors including errors in gas analysis, coal and char analysis, char collection method, and coal feed rate.

In spite of the radically different coals used and the diverse distributions of gas-phase nitrogen compounds, the fraction of total gas-phase nitrogen atoms as N^{15} was very much the same for both coals at any given stoichiometry. This is demonstrated in Figure 7. Although purely coincidental, this feature makes the overall gas-phase N^{15}/N^{14} ratio a convenient normalizing factor for comparing the two coals.

Using the normalizing factor, the gas-phase behavior of both coals was shown to be very similar as shown in Figure 8. Under fuel-rich conditions, lignites typically produce large quantities of NH_3 whereas bituminous coals produce mostly HCN. The strong correlation of HCN for bituminous with NH_3 for lignite (shown in Figure 8), adds to the substantial evidence that HCN is a precursor to NH_3 in lignite reburning. Bose, et al. (1988) alluded to this when HCN was observed in the bulk gas phase before NH_3 while reburning with a German brown coal.

Figure 8 exhibits several interesting features. First, NO was much richer in N^{15} atoms than was the overall gas phase. This indicates that very little of the intermediate nitrogen species recycled to form NO. As would be expected, leaner stoichiometries promoted recycling while richer stoichiometries retarded the process.

Low levels of N^{14} atoms as NO indicate the delay of nitrogen evolution from the coals until after significant combustible species have evolved. This is consistent with the findings of Pohl and Sarofim (1977) and Blair, et al. (1977). Further

evidence of delayed nitrogen release from the coals is given by the high N^{14} atom content of HCN and NH_3.

The curve for N_2 in Figure 8 also gives some insight into the reburning process. At stoichiometries richer than SR=0.8, the N^{15}/N^{14} ratio for N_2 was approximately the same as for the overall gas phase. However, at leaner stoichiometries, N_2 became progressively richer in N^{14} atoms. Data from Figures 3 and 4 indicate that very little of the original $N^{15}O$ was reduced in lean stoichiometries. Thus, N^{14}-rich N_2 at these stoichiometries implies an N_2 production mechanism that involves mostly intermediate species such as NH_3, HCN or their derivatives.

The dominant N_2 production mechanism proposed by Miller and Bowman (1989) for reburning was

$$N + NO \rightarrow N_2 + O$$

where N atoms were derived from HCN primarily by the sequence

$$HCN + O \rightarrow NCO + H$$
$$NCO + H \rightarrow NH + CO$$
$$NH + H \rightarrow N + H_2.$$

However, the isotope distributions as $N^{14}N^{14}$, $N^{14}N^{15}$, and $N^{15}N^{15}$ as shown in Figures 9 through 11 were inconsistent with this mechanism.

Using the experimentally determined N^{15}/N^{14} ratios for NO and HCN (or NH_3), and the mechanism of Miller and Bowman, the product probabilities for the three N_2 isotopes were calculated. As shown in Figure 9, the N + NO mechanism significantly underpredicted $N^{14}N^{14}$. In contrast, $N^{14}N^{15}$ and $N^{15}N^{15}$ were slightly overpredicted at most stoichiometries as shown in Figures 10 and 11.

An alternate mechanism was proposed by Miller, et al. (1983) for N_2 production from non - NO reaction paths. The sequence was

$$NH + NH_2 \rightarrow N_2H_2 + H$$

$$N_2H_2 + M \rightarrow NNH + H + M$$

$$N_2H_2 + H \rightarrow NNH + H_2$$

$$NNH + M \rightarrow N_2 + H + M.$$

Probability analysis based on this mechanism predicted too little $N^{15}N^{15}$ and too much $N^{14}N^{14}$. Both mechanisms predicted essentially the same level of $N^{14}N^{15}$. Thus, neither mechanism alone can account for the experimental observations. In fact, no combination of the mechanisms would accurately predict all three isotopes of N_2.

This dilemma is resolved by considering delayed nitrogen release from the coals along with the mechanisms described above. In this scenario, the isotope composition of each primary reactant (i.e., NO, HCN, and NH_3) changes with time. Early in the reaction sequence very little N^{14} has evolved from the coal so NO, HCN, and NH_3 would be rich in the N^{15} isotope. Thus N_2 production would initially include

mostly $N^{15}N^{15}$ by either mechanism. Miller, et al. (1983) suggested that the non - NO mechanism was more important in rich stoichiometries so N_2 production in the relatively lean early stages of devolatilization is probably by the N + NO mechanism.

As devolatilization progresses, the gas-phase stoichiometry becomes richer and more of the N_2 production occurs through the non - NO mechanism. Also, the HCN and NH_3 contain progressively more of the N^{14} isotope. The $N^{14}O$ isotope also increases but never exceeds 10% of the total NO. In the latter stages of devolatilization, most of the N_2 production occurs through the non - NO mechanism with reactants rich in the N^{14} isotope.

Using the above scenario and a very simplified model in which coal devolatilization and N_2 production take place in three discrete steps, the isotope distributions for diatomic nitrogen were duplicated almost exactly. Although not conclusive, the results of this model were consistent with both delayed nitrogen devolatilization and shifting of the dominant N_2 producing mechanism with stoichiometry.

Limited knowledge of the temporal changes in isotope concentration for reactant species prevent exact modelling of which N_2 production paths dominate. However, one can reasonably conclude that the percentage of N^{15} isotopes as either NO, HCN, or NH_3 declines with time. Thus, upper bounds for the fraction of N_2 formed by the N + NO reaction path can be established by considering the fraction of $N^{14}N^{14}$ that must be formed together with the final isotope distributions measured for NO, HCN, and NH_3. This analysis shows that a maximum of 56% of the N_2 was

formed by the N + NO mechanism at SR = 0.9. At SR = 0.8 only 49% could have been formed by the N + NO reaction and at SR = 0.7 NO more than 40%.

These estimates are extreme upper bounds since the maximum concentration of N^{14} isotopes in each reactant was assumed. Thus, non - NO mechanisms could have been responsible for even more of the N_2 production.

Conclusions

The lignite produced the lowest fixed-nitrogen levels whether char nitrogen was included or not. Although N_2 production for the lignite was higher and fixed-nitrogen speciation decidedly different, the nitrogen reaction pathways seem to be consistent with those of the bituminous coal. For each nitrogen species, the isotope distribution versus stoichiometry was independent of coal type.

Delayed nitrogen release was evident from both coals. As expected, fixed nitrogen originating as fuel nitrogen was dominated by NH_3 for the lignite and HCN for the bituminous.

Analysis of the N_2 isotope distribution showed that more than half of the N_2 production occurred through mechanism(s) other than N + NO. Surviving NO levels for lignite reached extremely low levels (< 1 ppm) in richer stoichiometries. These low levels are probably due to contribution from heterogeneous reactions.

Surprisingly, there is little evidence of recycling of intermediates such as NH_3 and HCN to form NO. The N^{14} isotope contribution to NO ranged from 5% at SR

= 0.7 to 10% at SR = 0.9. However, recycling would be most likely to occur early in the process, perhaps before significant nitrogen is released from the coal.

Although verification is needed, fuel-bound nitrogen from coal does not appear to raise gas-phase, fixed-nitrogen levels significantly above those of other fuels. In fact, kinetic pathways unique to coal (particularly lignite) reburning seem to lower fixed-nitrogen levels. A better understanding of these mechanisms could improve reburning technology.

Time resolved studies of gas-phase nitrogen speciation and isotope distributions are needed to determine the extent of nitrogen release delay and isolate N_2 production mechanisms.

Acknowledgements

This work was funded by the U.S. Department of Energy, Pittsburgh Energy Technology Center under Contract No. DE-AC22-88PC88859. The authors would like to acknowledge the assistance of Bill Hayes (Hayes Separation) in the GC/MS analysis of nitrogenous species.

References

Blair, D.W., J.O.L. Wendt, and W. Bartok, "Evolution of Nitrogen and Other Species During Controlled Pyrolysis of Coal", Sixteenth Symposium (International) on Combustion, p. 475, The Combustion Institute, 1977.

Bose, A.C., K.M. Dannecker, and J.O.L. Wendt, "Coal Composition Effects on Mechanisms Governing the Destruction of NO and Other Nitrogenous Species During Fuel-Rich Combustion", Energy and Fuels, Vol. 2, No. 3, 1988.

Burch, T.E., F.R. Tillman, W.Y. Chen, T.W. Lester, R.B. Conway, and A.M. Sterling, "Partitioning of Nitrogenous Species in the Fuel Rich Stage of Reburning", submitted to Combustion and Flame, May, 1990.

Chen, S.L., M.P. Heap, D.W. Pershing, and G.B. Martin, "Influence of Coal Composition on the Fate of Volatile and Char Nitrogen During Combustion", Nineteenth Symposium (International) on Combustion, p. 1271, The Combustion Institute, 1982.

Glass, J.W. and J.O.L. Wendt, "Mechanisms Governing the Destruction of Nitrogenous Species During the Fuel Rich Combustion of Pulverized Coal", Nineteenth Symposium (International) on Combustion, p. 1243, The Combustion Institute, 1982.

Miller, J.A., M.D. Smooke, R.M. Green, and R.J. Kee, "Kinetic Modeling of the Oxidation of Ammonia in Flames", Combustion Science and Technology, Vol. 34, p. 149, 1983. Miller, J.A., and C.T. Bowman, "Mechanism and Modeling of Nitrogen Chemistry in Combustion", Progress Energy Combustion Science, Vol. 15, No. 4, p. 287, 1989.

Pohl, J.H. and A.F. Sarofim, "Devolatilization and Oxidation of Coal Nitrogen", Sixteenth Symposium (International) on Combustion, p. 491, The Combustion Institute, 1977.

Takahashi, Y., M. Sakai, T. Kunimoto, S. Ohme, H. Haneda, T. Kawamura, and S.Kaneko, "Development of "MACT" In-Furnace NOx Removal Process for Steam Generators", Proc. 1982 Join Symposium Stationary NOx Control, Vol. 1, EPRI Report No. CS-3182, July, 1983.

Wendt, J.O.L., C.V. Sternling, and M.A. Matovich, "Reduction of Sulfur Trioxide and Nitrogen Oxides by Secondary Fuel Injection", Fourteenth Symposium (International) on Combustion, p. 897, The Combustion Institute, 1973.

Table 1. Analysis of Coals

	Pittsburgh #8, Bituminous	North Dakota Lignite (PSOC 1507)
Moisture*	2.02	33.57
Carbon	70.48	62.61
Hydrogen	4.66	4.41
Oxygen (Diff)	8.53	18.23
Nitrogen	1.44	0.83
Sulfur	3.35	1.43
Ash	11.54	12.49
Vol. Matter	33.25	40.77
Fixed Carbon	55.21	46.75

*Moisture is reported on an as received basis all other results are on a dry basis.

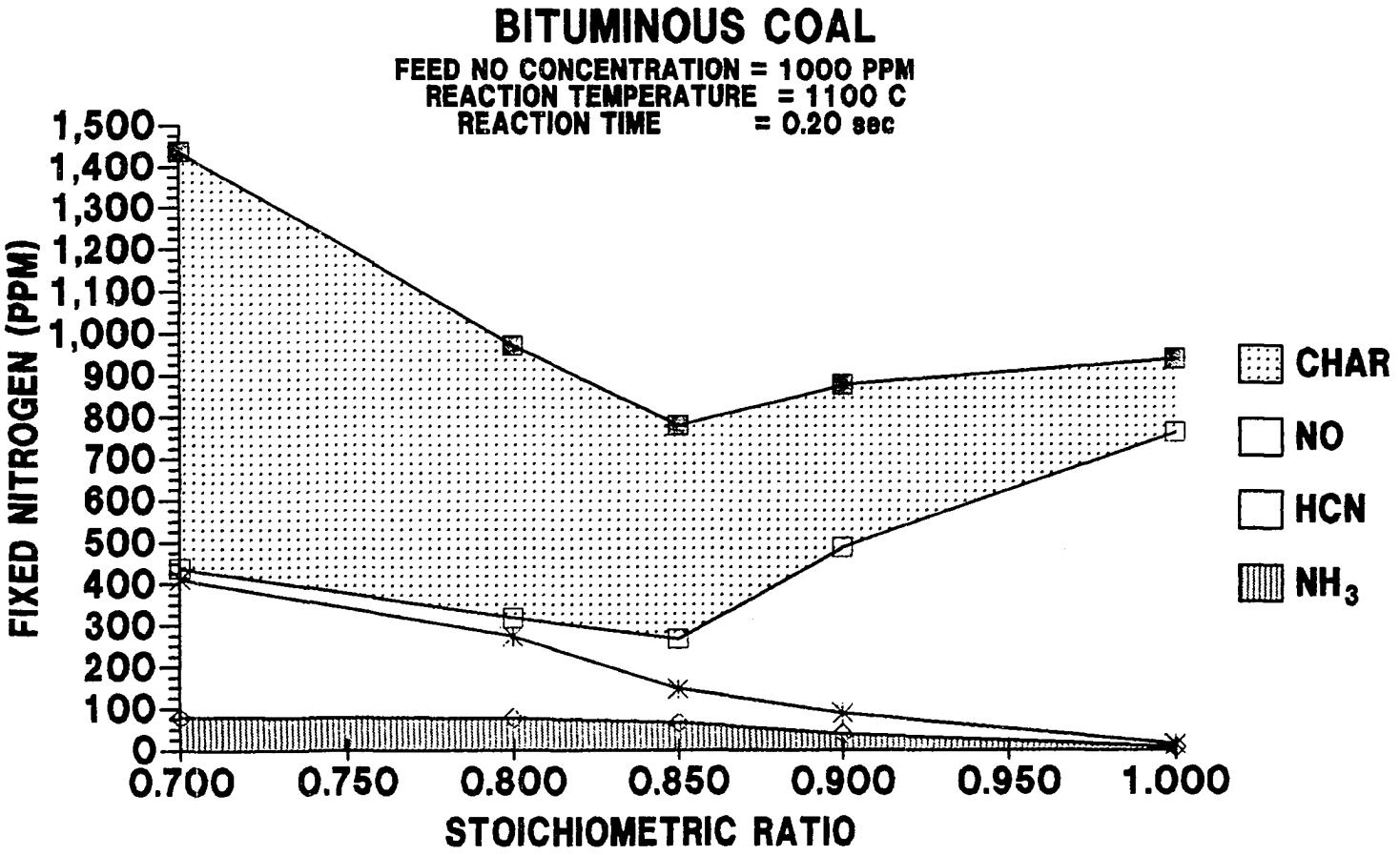

Figure 1. Cumulative total fixed nitrogen for reburning with Pittsburgh #8 bituminous coal.

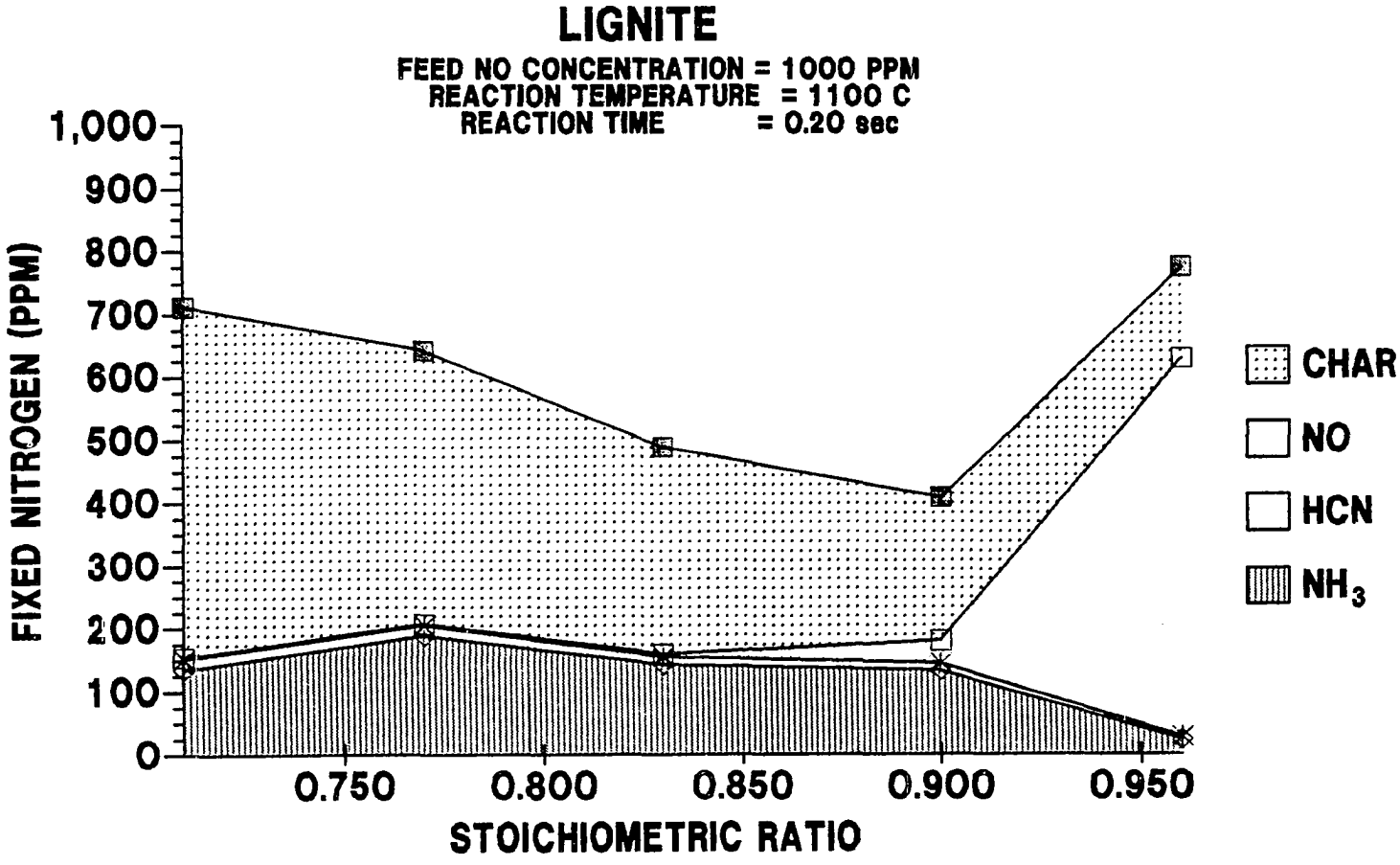

Figure 2. Cumulative total fixed nitrogen for reburning with Zap, North Dakota lignite.

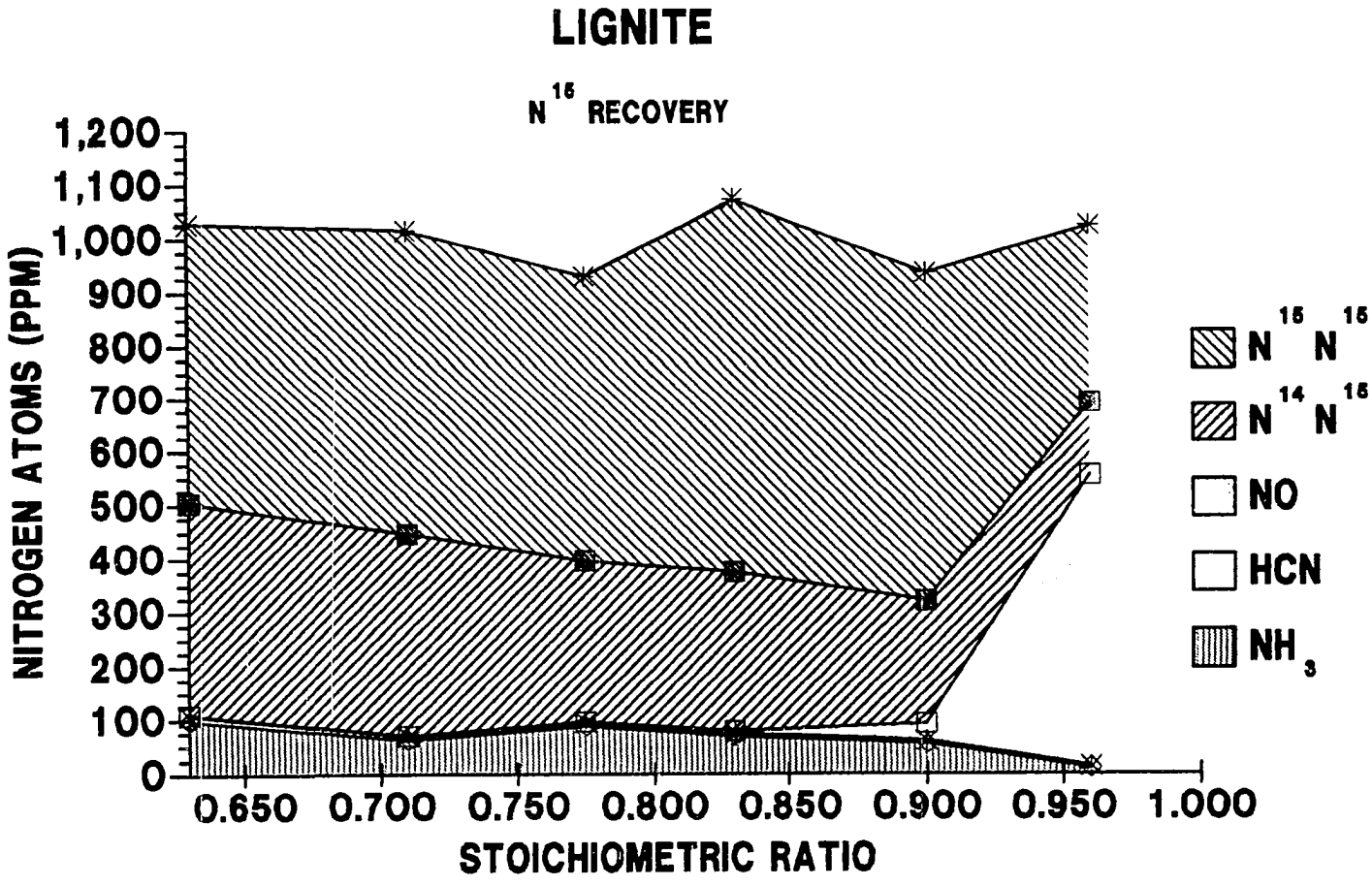

Figure 3. Partitioning of N^{15} atoms for reburning with Zap, North Dakota lignite shown as cumulative values.

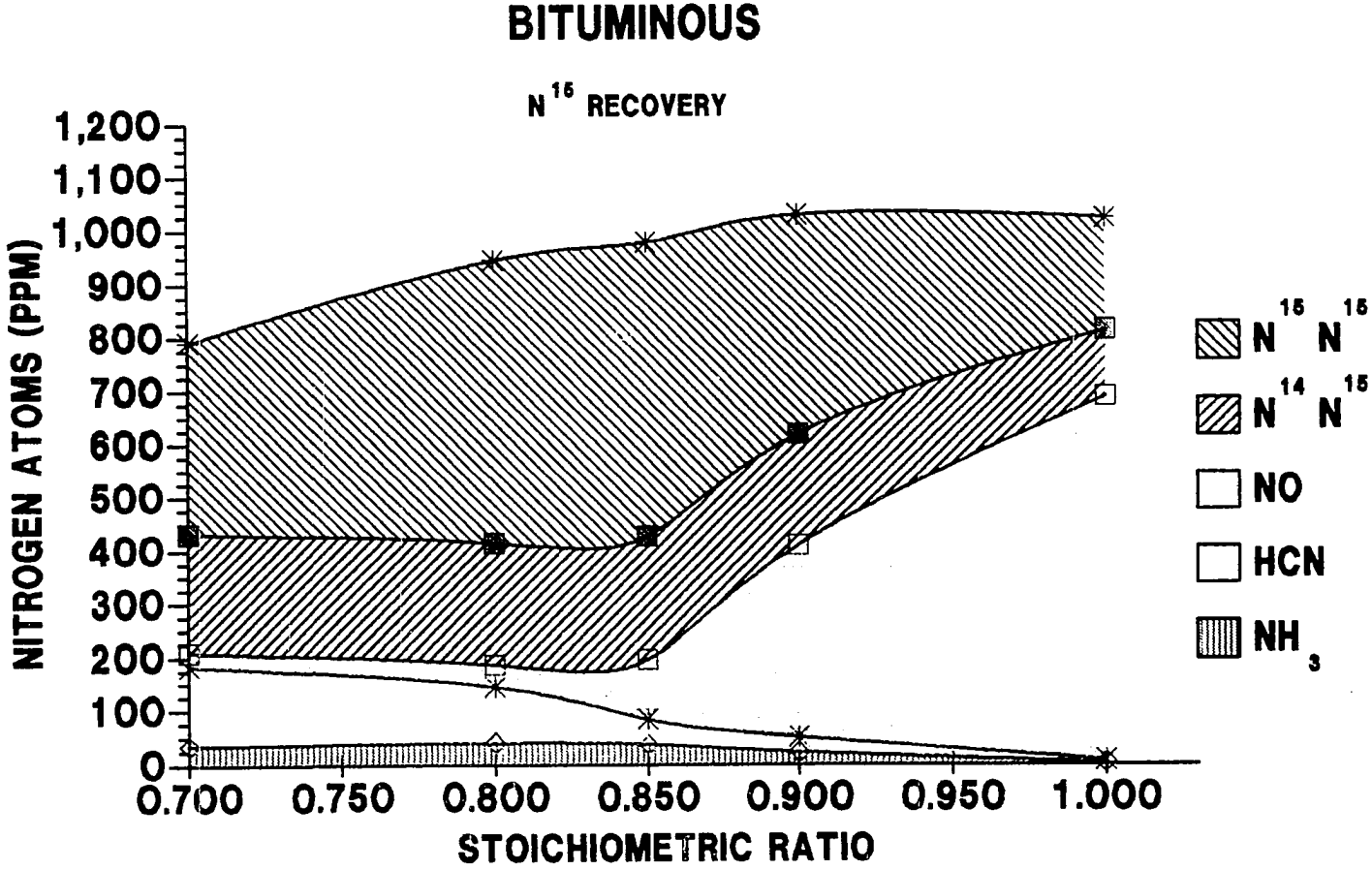

Figure 4. Partitioning of N^{15} atoms for reburning with Pittsburgh #8 bituminous coal shown as cumulative values.

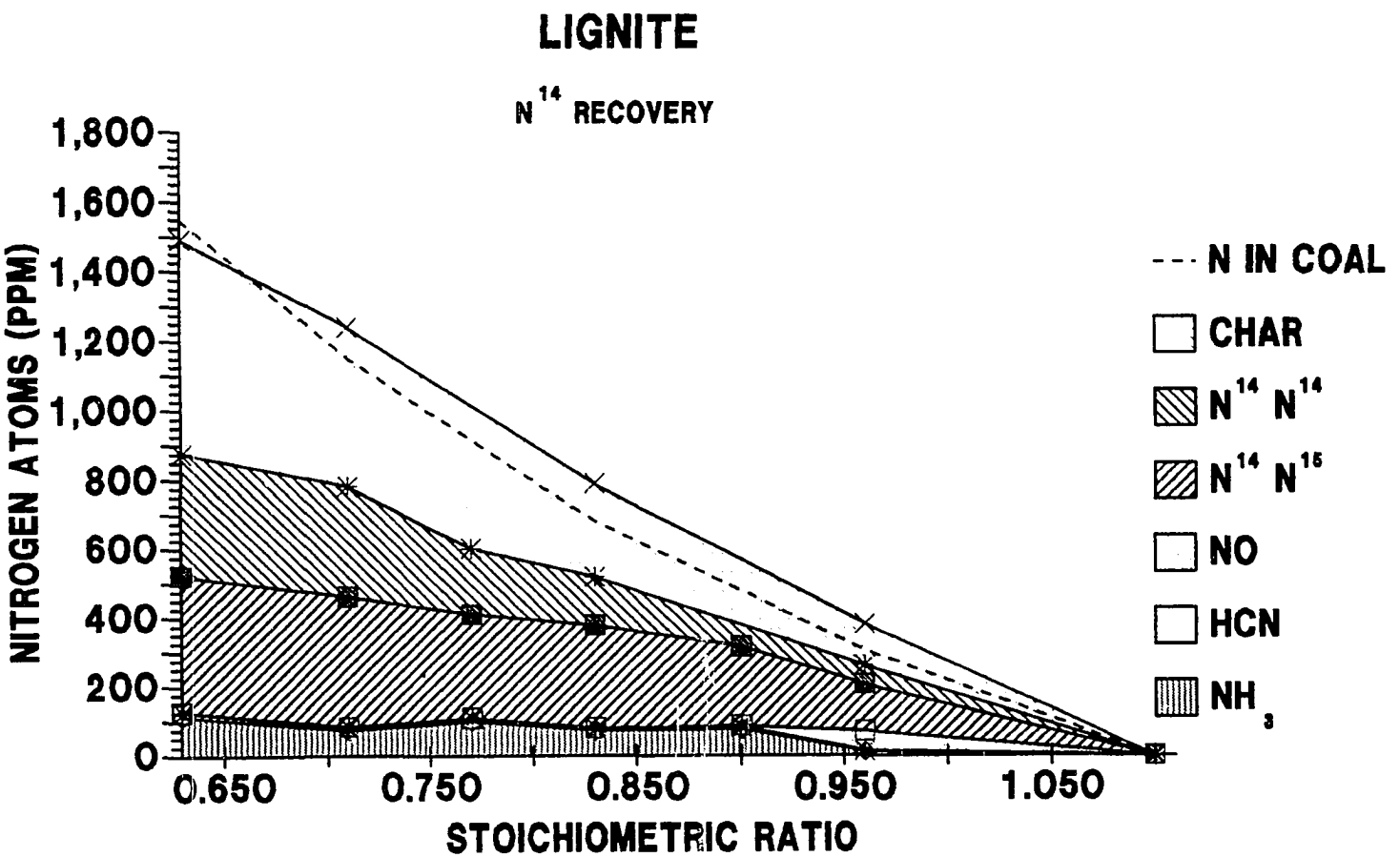

Figure 5. Partitioning of N^{14} atoms for reburning with Zap, North Dakota lignite shown as cumulative values. The calculated fuel nitrogen input from the lignite is designated by - - - - -.

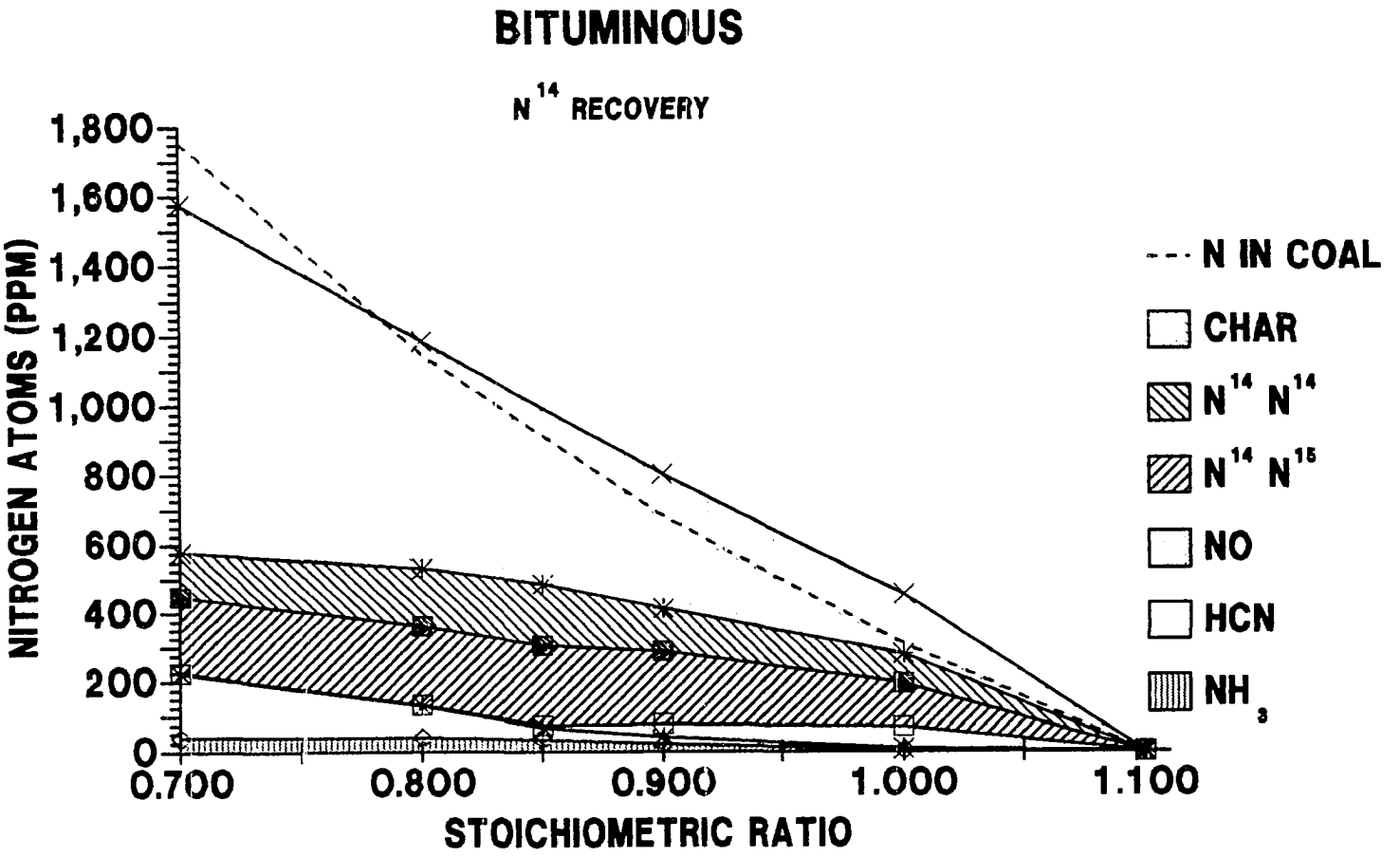

Figure 6. Partitioning of N^{14} atoms for reburning with Pittsburgh #8 bituminous coal shown as cumulative values. The calculated fuel nitrogen input from the coal is designated by - - - - -.

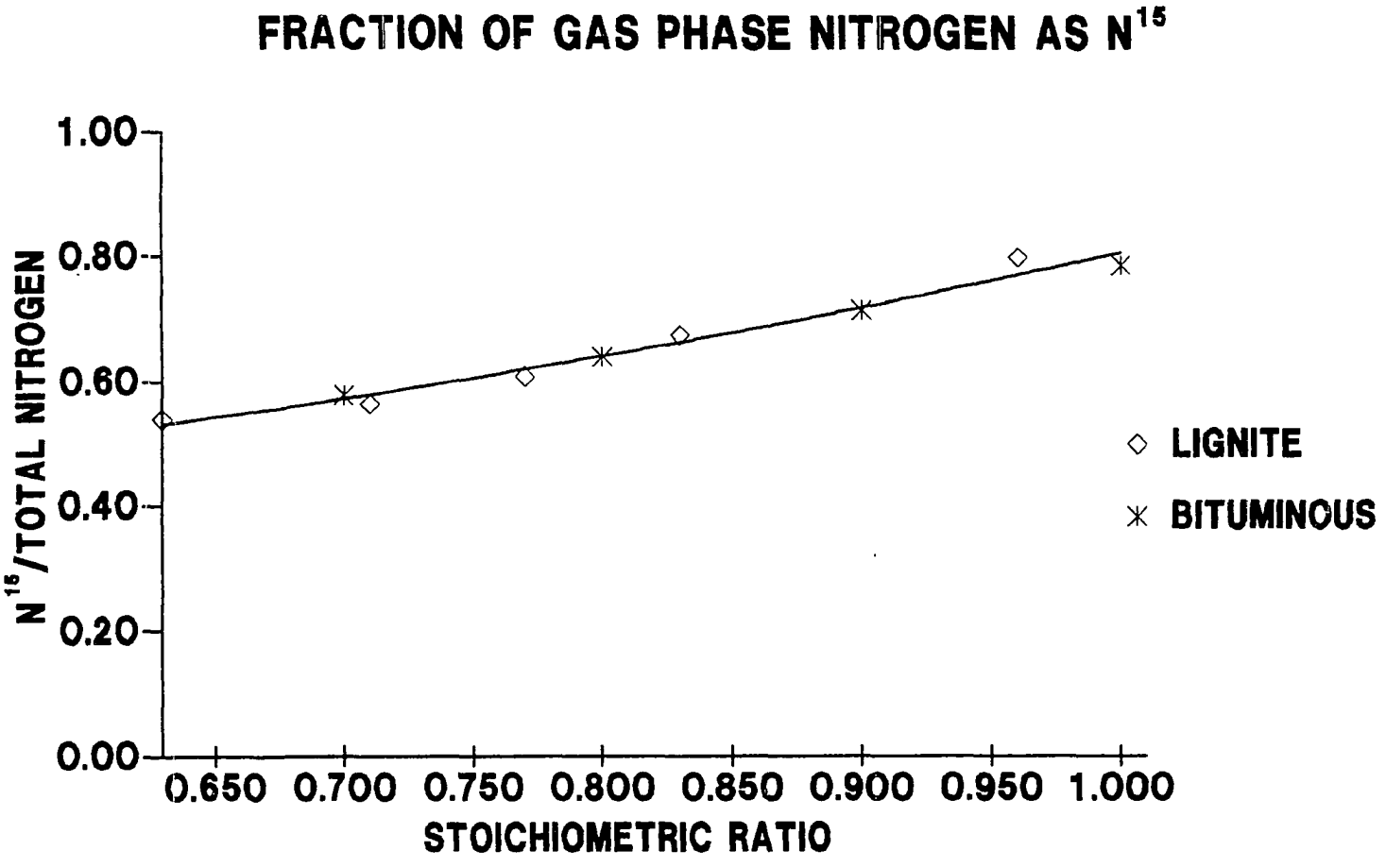

Figure 7. Distribution of N^{15} and N^{14} isotopes in the total gas-phase nitrogen for lignite and bituminous coal.

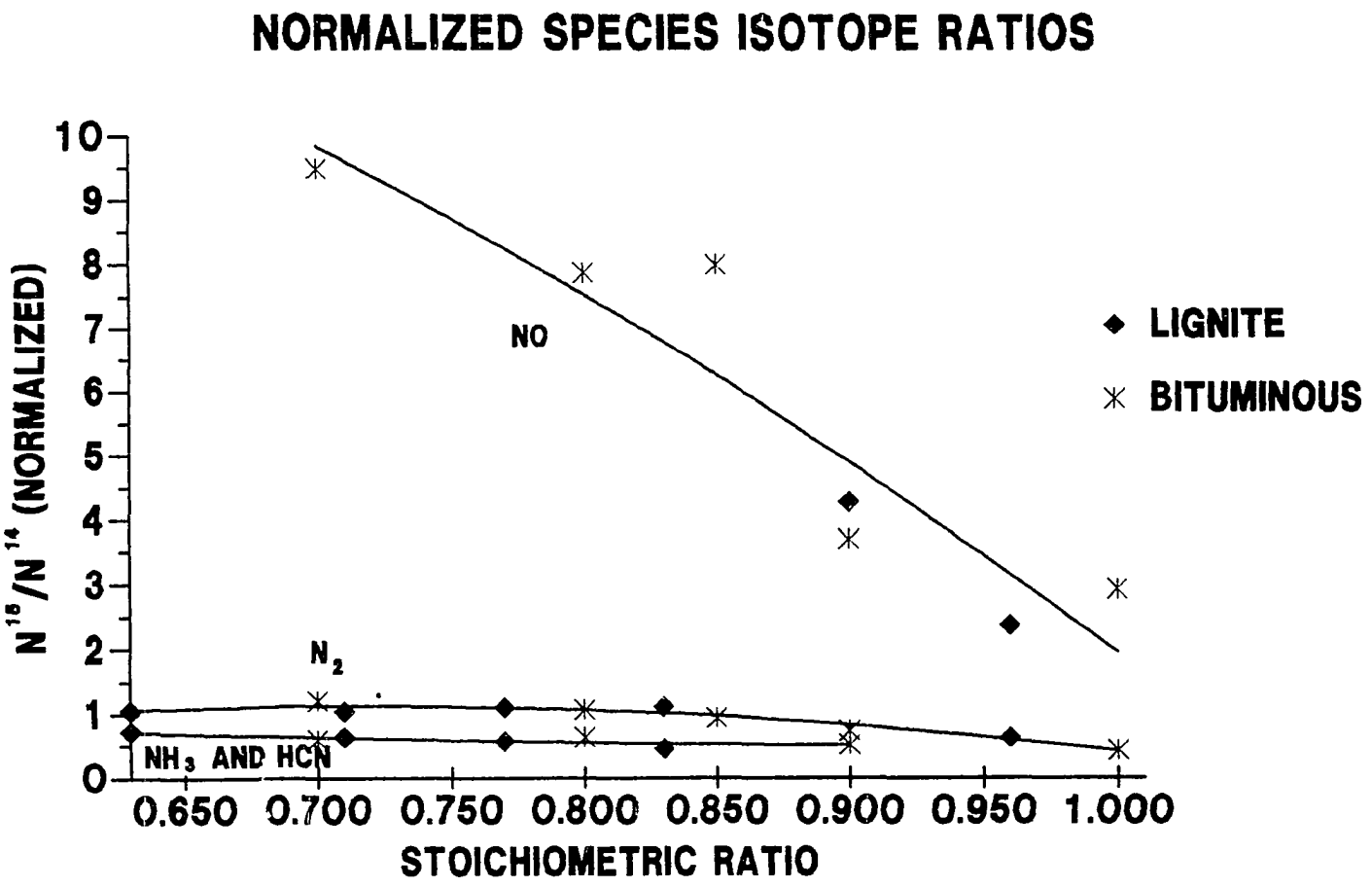

Figure 8. Measured species isotope ratios (N^{15}/N^{14}) for NO, N_2, NH_3, and HCN. The ordinate is normalized by the N^{15}/N^{14} ratio for the total gas-phase nitrogen. Note that NH_3 data are for lignite only and HCN data are for bituminous only.

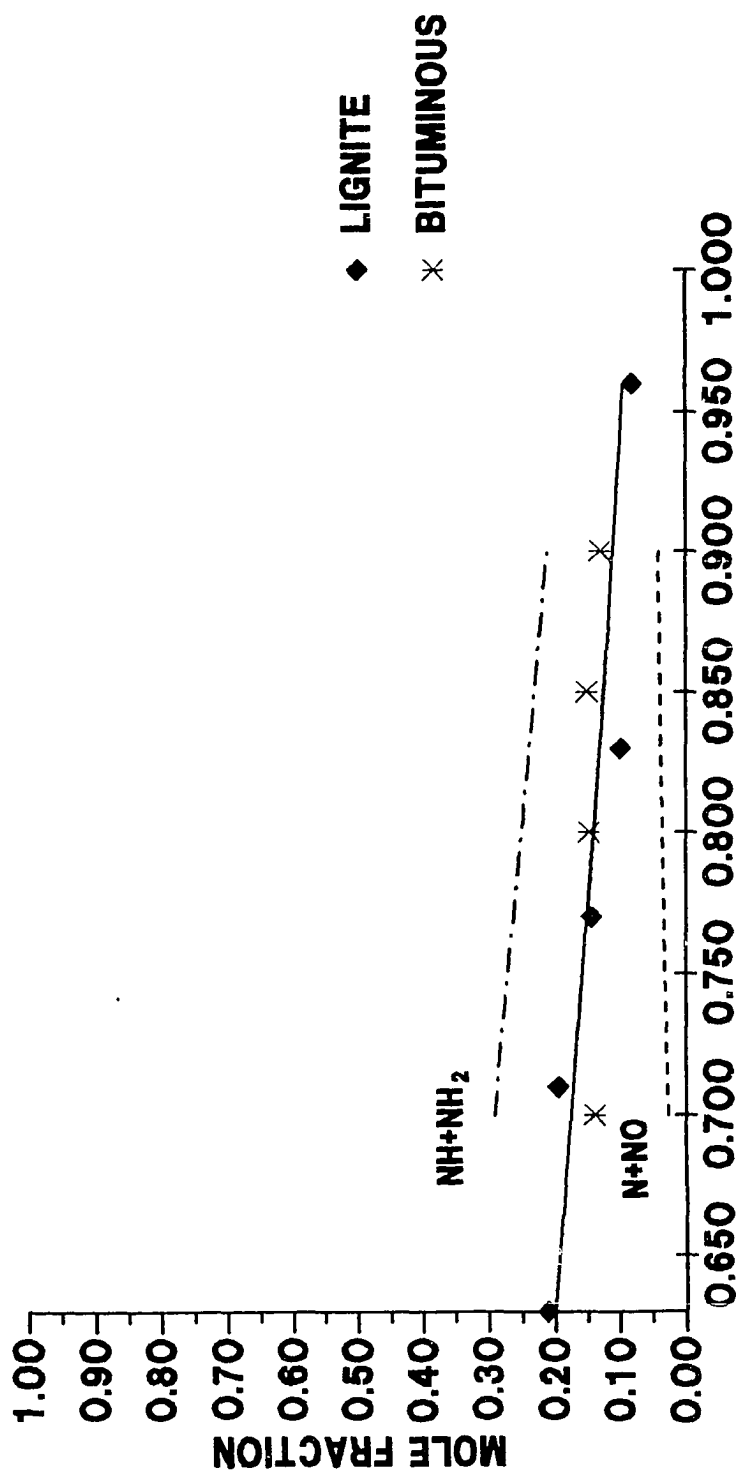

Figure 9. Fraction of diatomic nitrogen found as $N^{14}N^{14}$.

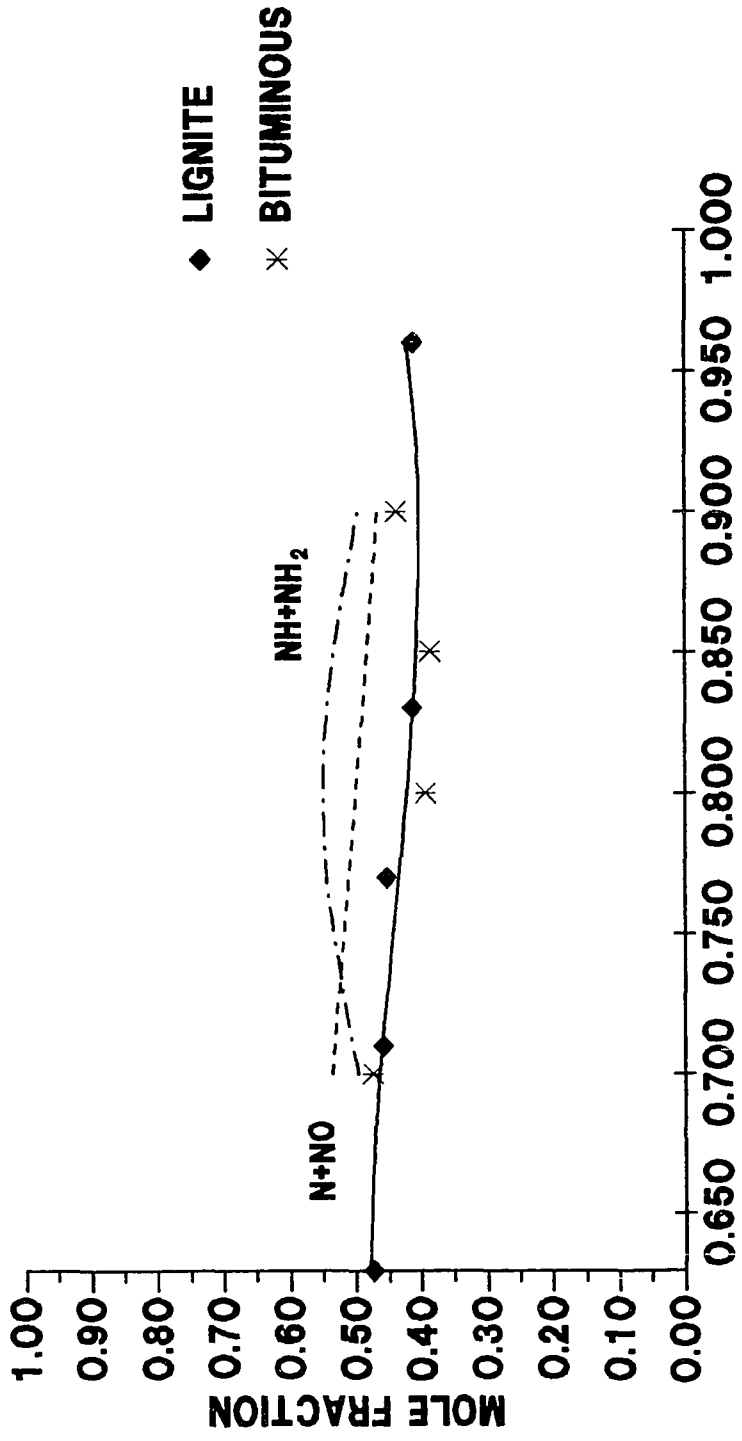

Figure 10. Fraction of diatomic nitrogen found as $N^{14}N^{15}$.

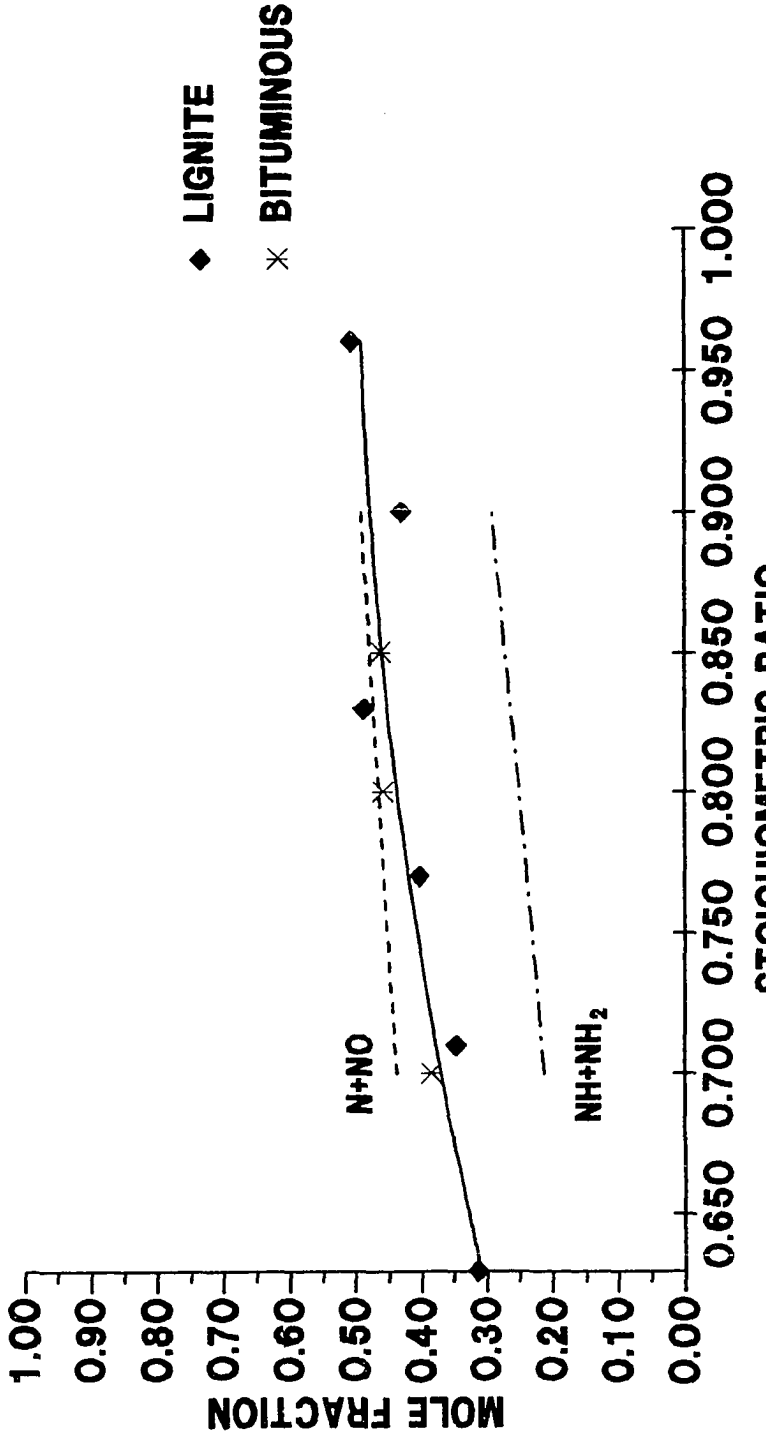

Figure 11. Fraction of diatomic nitrogen found as $N^{15}N^{15}$.

CHAPTER V

Conclusions and Recommendations

The reburning characteristics of five fuels have been studied under simulated reburning conditions. The facility used to study these fuels has been described, including a novel coal entrainment device suitable for stable coal feed at low delivery rates. A GC/MS method has been developed to analyze all major stable nitrogenous species except NO_2. Stable nitrogen species mole fraction data have been presented for each of the five fuels at stoichiometric ratios ranging from 0.7 to 1.0. Fuel nitrogen and NO interaction for coal reburning has been studied using isotope labelling and GC/MS.

A number of conclusions can be drawn from the data presented. Although most of the conclusions drawn have application to large scale reburning, the idealized environment of the flow reactor eliminates important scaling variables such as mixing effects, turbulence, and thermal history. Thus, extrapolation of these conclusions to full scale reburning requires careful consideration of scaling effects. These conclusions follow.

*Fuel type has a significant impact on the reburning TFN speciation. This is important because TFN speciation is indicative of which kinetic barriers limit reburning effectiveness. Thus, by direct inference, the

fuel type impacts the kinetic barriers in reburning. This conclusion is valid even when only homogeneous gas-phase reactions are considered.

*Lignite reburning introduces additional kinetic pathways through direct heterogeneous reduction of NO to N_2. The experiments with lignite char have shown that this pathway can be significant in fuel-rich environments.

*Lignite reburning accelerates certain reactions by catalyzing the conversion of HCN to NH_3. The lignite ash acts as the catalyst for this reaction. Conversion of HCN to NH_3 is not quantitative so NH_3 is probably not the primary product of the reaction. Instead, another less stable compound is likely produced which then undergoes further reaction to form NH_3 or N_2. In addition to directly increased production of N_2, this catalyzed reaction has a secondary reburning benefit. In the burnout stage, the conversion efficiency of NH_3 to NO is lower than for HCN thus producing even more N_2.

*Nitrogen evolution from the coals is delayed sufficiently to allow substantial conversion of NO to N_2 before fuel nitrogen appears in the gas phase. Consequently, the interaction of fuel nitrogen with NO is limited to the temporal overlap of these species in a reactive environment.

*Much of the N_2 production occurs through non-NO pathways with coal. This is contrasted with the N+NO reaction thought to dominate

N_2 production with methane reburning. The data indicate that char or ash reactions may be enhancing N_2 production through non-NO pathways.

*In coal reburning, there is little recycling of intermediate species to form NO after fuel nitrogen evolves into the gas phase. This is important because it demonstrates the relative irreversibility of reducing NO to HCN in coal reburning. This simplifies the analysis of coal reburning by allowing only sequential reactions to be considered.

*In optimal lignite reburning, more than 90% of the original NO is converted to N_2. The TFN is boosted by fuel nitrogen to over 200 ppm in the gas phase, and to over 400 ppm when char nitrogen is included. However, when reasonable burnout conversions to NO are assumed, lignite appears competitive with methane as a reburning fuel.

The findings of this research have shed some light on the mechanisms important in reburning. However, there is still much room for improvement in the manipulation of these mechanisms to further the approach to equilibrium TFN concentrations. Many of the findings presented here raise important questions that define new research with the potential to significantly impact reburning technology.

The methane, hexane, and benzene results indicate that there may be an optimum H/C ratio and structure for reburning fuels. In the absence of suitable oxidation mechanisms for modelling of heavier fuels, experimental trials are needed

to identify fuel characteristics which are important in the homogeneous reduction of NO to N_2. Fuel mixtures must also be considered since different kinetic barriers seem to dominate with different reburning fuels.

The most promising research areas indicated by this work involve the phenomena associated with lignite reburning. The reactive nature of lignite char and the catalytic properties of lignite ash seem to offer the promise of significant improvements in reburning efficiency through enhancement by char or ash addition. The preliminary experiment of adding lignite ash to methane reburning reduced TFN levels by 40%, indicating the potential of this approach.

The catalytic action of lignite ash gives reason to believe that reburning with gas might be more effective for lignite primary flames than for bituminous. With lignite primary flames, the ash should carry through to the reburning stage and enhance the N_2 production. If this proves to be true, then seeding of bituminous primary flames with lignite might be fruitful. However, more information about the catalytic nature of lignite ash is needed to determine the conditions needed to drive the reaction. Possible poisoning of the catalyst, which might occur in the primary flame, and the thermal stability of this catalyst are also of concern.

The highly active lignite char is of interest due to its demonstrated ability to directly convert NO to N_2. The possibility of ash catalyzation in this reaction must also be considered. If the heterogeneous NO reduction benefits of lignite char can be duplicated without introducing additional fuel nitrogen, the entire nature of reburning might be altered. At the present time, reburning technology depends entirely on

homogeneous gas-phase reactions for effectiveness. If highly reactive char could be added, the combined homogeneous and heterogeneous effects could produce significantly lower TFN levels. If the heterogeneous effects prove strong enough, the optimum stoichiometric conditions might be expected to shift toward leaner conditions, producing fewer intermediates such as HCN and NH_3. This would allow less fuel to be introduced in the reburning stage, reducing the impact of reburning on furnace heat transfer.

Finally, in regards to the direct application of coal reburning, the effect of delayed nitrogen evolution from coal needs to be explored more fully. Also, the data presented here indicate that the dominant N_2 production mechanism may change with reaction time during coal reburning. Both of these interests would be well served by time resolved labelled isotope studies.

References

1. Dyer, D.F., and Maples, G., "Boiler Efficiency Improvement", Boiler Efficiency Institute, Auburn, Alabama, 1981.

2. Sawyer, R.F., Eighteenth Symposium (International) on Combustion, p. 1, The Combustion Institute, 1981.

3. Levy, A., Nineteenth Symposium (International) on Combustion, p. 1223, The Combustion Institute, 1982.

4. American Society of Testing and Materials, Designation ASTM D-388-64T.

5. "Steam/Its Generation and Use", The Babcock and Wilcox Company, New York, New York, 1972.

6. Haider, G., Micronized Coal Testing (Phase 1), Alliance Research Center Report 5277, Babcock and Wilcox, Alliance, Ohio, 1982.

7. Seeker, W.R., "The Kinetics of Ignition and Particle Burnout of Coal Dust Suspensions Under Rapid Heating Conditions", Ph.D. Dissertation, Kansas State University, 1979.

8. DeSoete, G.G., "Mechanisms of Nitric Oxide Reduction of Solid Particles; Trials on Fly Ashes and Study of Reactions Involving HCN", Report on E.E.R.C. Subcontract No. 8318-6, (Internal Report, Institut Francais du Petrole, REF No. 28666).

9. Mahajan, O.P., Fuel, 64, p. 973, 1985.

10. Miller, J.A., and Fisk, G.A., "Combustion Chemistry", Special Report, Chemical and Engineering News, August 31, 1987.

11. Fenimore, C.P., Thirteenth Symposium (International) on Combustion, p. 373, The Combustion Institute, 1971.

12. Morley, C., Eighteenth Symposium (International) on Combustion, p. 23, The Combustion Institute, 1981.

13. Fenimore, C.P., Seventeenth Symposium (International) on Combustion, p. 661, The Combustion Institute, 1979.

14. Haynes, B.S., Combustion and Flame, 28, p. 113, 1977.

15. Haynes, B.S., Combustion and Flame, 28, p. 81, 1977.

16. Morley, C., Combustion and Flame, 27, p. 189, 1976.

17. Fenimore, C.P., Combustion and Flame, 26, p. 249, 1976.

18. Haynes, B.S., Iverach, D. and Kirov, N.Y., Fifteenth Symposium (International) on Combustion, p. 1103, The Combustion Institute, 1975.

19. DeSoete, G.G., Fifteenth Symposium (International) on Combustion, p. 1093, The Combustion Institute, 1975.

20. Fenimore, C.P., Combustion and Flame, 19, p. 289, 1972.

21. Song, Y.H., Blair, D.W., Siminski, V.J., and Bartok, W., Eighteenth Symposium (International) on Combustion, p. 53, The Combustion Institute, 1981.

22. Fenimore, C.P., Combustion and Flame, 25, p. 85, 1975.

23. Miller, J.A., Smooke, M.D., Green, R.M., and Kee, R.J., Combustion Science and Technology, 34, p. 149, 1983.

24. Perry, R.A., Journal of Chemical Physics, 12, p. 5485, 1985.

25. Albers, E.A., Hoyermann, K., Schacke, H., Schmatjko, K.J., Wagner, H. Gg., and Wolfrum, J., Fifteenth Symposium (International) on Combustion, p. 765, The Combustion Institute, 1975.

26. Louge, M.Y., and Hanson, R.K., Combustion and Flame, 58, p. 291, 1984.

27. Myerson, A.L., Fifteenth Symposium (International) on Combustion, p. 1085, The Combustion Institute, 1975.

28. Muzio, L.J., Arand, J.K., and Teixeira, D.P., Sixteenth Symposium (International) on Combustion, p. 199, The Combustion Institute, 1977.

29. DeSoete, G.G., "Mechanisms of NO Reduction on Solid Particles", EPA Workshop on Fundamental Combustion Research Applied to Pollution Control, Newport Beach, CA, January 23-25, 1980.

30. Martin, F.J., and Dederick, P.K., Sixteenth Symposium (International) on Combustion, p. 191, The Combustion Institute, 1977.

31. Turner, D.W., Andrews, R.L., and Siegmund, C.W., Combustion, 21, 1972.

32. Gibbs, B.M., Pereira, F.J., and Beer, J.M., Sixteenth Symposium (International) on Combustion, p. 289, The Combustion Institute, 1977.

33. Takagi, T., Tatsumi, T., and Ogsawara, M., Combustion and Flame, 35, p. 17, 1979.

34. Lyon, R.K., U.S. Patent No. 3,900,554, August 1975.

35. Lyon, R.K., International Journal of Chemical Kinetics, 8, p. 315, 1976.

36. Lyon, R.K., and Benn, D.J., Seventeenth Symposium (International) on Combustion, p. 601, The Combustion Institute, 1979.

37. Seery, D.J., and Zabielski, M.F., Combustion and Flame, 28, p. 93, 1977.

38. Miller, J.A., Branch, M.L., and Kee, R.K., Combustion and Flame, 43, p. 81, 1981.

39. Jones, G.D., "Selective Catalytic Reduction and NO_x Control in Japan, A Status Report", EPA-600/7-81-030, January 1981.

40. Perry, R.A., and Siebers, D.L., "Rapid Reduction of Nitrogen Oxides in Exhaust Gas Streams", Sandia Combustion Research Annual Report, p. 3-1, 1986.

41. DeSoete, G.G., "Mechanisms of Nitric Oxide Reduction on Solid Particles; Comparative Study on Coal and Char Particles", Report on EERC Subcontract No. 8218-6, (Internal Report, Institut Francais du Petrole, Ref. No. 28136), 1978.

42. Edwards, H.W., AICHE Symposium Series, No. 126, 68, p. 91, 1972.

43. DeSoete, G.G., "Mechanisms of Nitric Oxide Reduction On Solid Particles", Final Report EERC Subcontract No. 8318-6, 1979.

44. Tucker, J.R., "The Reduction of Nitric Oxide on Activated Carbon at Elevated Temperatures", Ph.D. Thesis, Clemson University, 1972.

45. Levy, J.M., Chan, L.K., Sarofim, A.F., and Beer, J.M., Eighteenth Symposium (International) on Combustion, p. 111, The Combustion Institute, 1981.

46. Merryman, E.L., Miller, S.E., and Levy, A., Combustion Science and Technology, 20, p. 161, 1979.

47. Furasawa, T., Kunii, O., Oguma, A., and Yamada, N., Proceedings of the Society of Chemical Engineers, Japan, 6, p. 562, 1978.

48. Walsh, P.M., Chaung, T.Z., Dutta, A., Beer, J.M. and Sarofim, A.F., Nineteenth Symposium (International) on Combustion, p. 1281, The Combustion Institute, 1982.

49. Hammons, G.A., and Skopp, A., "NO_x Formation and Control in Fluidized Bed Coal Combustion Processes", ASME Paper No. 71-WA/APC-3, Winter Annual Meeting, Washington, DC, November 28, 1971.

50. Haynes, B.S., and Kirov, N.Y., Combustion and Flame, 23, p. 277, 1974.

51. Heap, M.P., Lowes, T.M., and Walmsley, R., Combustion Institute European Symposium, F.J. Weinberg Ed., Academic Press, New York, p. 493, 1973.

52. Pershing, D.W., and Wendt, J.O.L., Sixteenth Symposium (International) on Combustion, p. 389, The Combustion Institute, 1977.

53. Sarofim, A.F. and Flagon, R.C., "Nitrogen Oxide Control Techniques", Air Quality and Stationary Source Emission Control, A Report by the Commission on Natural Resources, National Academy of Sciences. National Academy of Engineering, National Research Council, Serial No. 94-4 U.S. Government Printing Office, March 1975.

54. Okazaki, K., Shishido, H., Nishikawa, T. and Ohtake, K., Twentieth Symposium (International) on Combustion, p. 1381, The Combustion Institute, 1984.

55. Chen, S.L., Heap, M.P., Pershing, D.W., and Martin, G.B., Nineteenth Symposium (International) on Combustion, p. 1271, The Combustion Institute, 1982.

56. Song, Y.H., Pohl, J.H., Beer, J.M., and Sarofim, A.F., Combustion Science and Technology, 28, p. 31, 1982.

57. Peck, R.E., Midkiff, K.C., and Altenkirch, R.A., Twentieth Symposium (International) on Combustion, p. 1373, The Combustion Institute, 1984.

58. Harding, N.S., Smoot, L.D., Hedman, P.O., American Institute of Chemical Engineers Journal, 28, No. 4, p. 573, 1982.

59. Seeker, W.R., Samuelsen, G.S., Heap, M.P., and Trolinger, J.D., Eighteenth Symposium (International) on Combustion, p. 213, The Combustion Institute, 1981.

60. Morris, T.A., "Micronized Coal Testing (Phase 2)", Alliance Research Center Report RDD:83:4871-05-02:01, Babcock and Wilcox, Alliance, Ohio, 1983.

61. Briceland, C.L., Khinkis, M.J., and Waibel, R.T., "Combustion Characteristics of Fine Ground Coal", International Symposium on Combustion Diagnostics, Paper No. 10, American Flame Research Committee, 1983.

62. Rees, D.P. Smoot, L.D., and Hedman, P.O., Eighteenth Symposium (International) on Combustion, p. 1305, The Combustion Institute, 1981.

63. Suuberg, E.M., Peters, W.A., and Howard, J.B., Seventeenth Symposium (International) on Combustion, p. 117, The Combustion Institute, 1979.

64. Solomon, P.R., Hamblen, D.G., Carangeco, R.M., and Krause, J.L., Nineteenth Symposium (International) on Combustion, p. 1139, The Combustion Institute, 1982.

65. Kobayashi, H., Howard, J.B., and Sarofim, A.F., Sixteenth Symposium (International) on Combustion, p. 411, The Combustion Institute, 1977.

66. Anthony, D.B., Howard, J.B., Hottel, H.C., and Meissner, H.P., Fifteenth Symposium (International) on Combustion, p. 1303, The Combustion Institute, 1975.

67. Freihaut, J.D., Zabielski, M.F., and Seery, D.J., Nineteenth Symposium (International) on Combustion, p. 1154, The Combustion Institute, 1982.

68. Solomon, P.R., and Colket, M.B., Seventeenth Symposium (International) on Combustion, p. 131, The Combustion Institute, 1979.

69. Pohl, J.H., and Sarofim, A.F., Sixteenth Symposium (International) on Combustion, p. 491, The Combustion Institute, 1977.

70. Blair, D.W., Wendt, J.O.L., and Bartok, W., Sixteenth Symposium (International) on Combustion, p. 475, The Combustion Institute, 1977.

71. Song, Y.H., Beer, J.M., and Sarofim, A.F., Combustion Science and Technology, 28, p. 177, 1982.

72. Mrazikova, J., Sindler, S., Veverka, L., and Macak, J., Fuel, 65, p. 342, 1986.

73. Gay, R.L., Axworthy, A.E., Dayan, V.H., and Recht, H.L., "Volatility of Fuel Nitrogen", Final Report, Energy and Environmental Research Corporation Contract EER-8218-4, Santa Ana, California, 1979.

74. Wendt, J.O.L., Sternling, C.V., and Matovich, M.A., Fourteenth Symposium (International) on Combustion, The Combustion Institute, 1973, p. 897.

75. Takahashi, Y., et al., Proc. 1982 Joint Symposium Stationary Combustion NO_x Control, Vol. 1, "EPRI Report NO CS-3182, July, 1983.

76. Mulholland, J.A., and Lanier, W.S., "Application of Reburning For NO_x Control to a Firetube Package Boiler", EPA-600/D-84-170, US EPA, June, 1984.

77. Greene, G.C., and Weaver, R.E.C., Proceedings of the Joint VTG-AIChE Meeting, Munchen BRD, September 17-20, 1974, Vol. IV, p. 5-11.

78. Overmoe, B.J., McCarthy, J.M., Chen, S.L., Seeker, W.R., Silcox, G.D., and Pershing, D.W., Proceedings: 1985 Symposium Stationary Combustion NO_x Control, Vol 1. Utility Boiler Application, EPRI CS-4360, Jan., 1986.

79. Mulholland, J.A., and Hall, R.E., Proceedings 1985 Symposium Stationary Combustion NO_x Control, Vol. 1. Utility Boiler Application, EPRI CS-4360, Jan., 1986.

80. Chen, S.L., Clark, W.C., Heap, M.P., Pershing, D.W., and Seeker, W.R., Proceedings EPRI/EPA Symposium Stationary Combustion NO_x Control, EPRI Report CS-3182, July, 1983.

81. England, G.C., et al., Eighteenth Symposium (International) On Combustion, The Combustion Institute, 1981, p. 163.

82. Johnson, S.A., et al., Proceedings: Second NO_x Control Technology Seminar, EPRI FP 1109-SR, July 1979.

83. Greene, S.B., Chen, S.L., Pershing, D.W., Heap, M.P. and Seeker, W.R., Amer. Soc. Mech. Eng., 84-JPGC-APC-9.

84. Glarborg, P., Miller, J.A., and Kee, R.J., Combustion and Flame, 65, p. 177, 1986.

85. Miller, J.A. and C.J. Bowman, "Mechanism and Modelling of Nitrogen Chemistry in Combustion", Prog. Energy Combustion Science, 15, p. 287, 1989.

86. Chen, J.K., W.Y. Chen and REC Weaver, "Nitric Oxide Emission Under Reburning Conditions: Equilibrium Concentration", Spring National Meeting AICHE, Houston, Texas, Paper No. 76c, April 1987.

87. Chen, S.L., J.C. Kremlich, W.R. Seeker, and D.W. Pershing, "Optimization of Reburning For Advanced NO_x Control On Coal-Fired Boilers", Journal Air Waste Management Association, 39, p. 1375, October 1989.

88. Sellars, J.R., M. Tribus, and J.S. Klein, "Heat Transfer To Laminar Flow in a Round Tube or Flat Conduit - Gratz Problem Extended", Trans. ASME, 78, p. 441, 1956.

APPENDIX I

GC/MS Method for Nitrogen Species

In order to perform nitrogen source tracing for coal reburning experiments isotopically labelled $N^{15}O$ was used. Separation of the Nitrogen isotopes then required the development of a GC/MS method to allow analysis of the stable nitrogen species. As a minimum, analysis of N_2, NO, HCN and NH_3 was required. NO_2 and N_2O generally constitute only a minor fraction of the total nitrogen but analysis of these species was desired for completeness. In addition to separating the nitrogen species from each other, separation from other major products of fuel-rich combustion was necessary.

An extensive literature search was performed in an effort to identify an existing GC method suitable for this analysis. The search concentrated on GC methods for the more difficult nitrogenous species. Although several methods were found for each of the individual species, no coherent method suitable for the combination of species could be found. In fact, most of the methods reported utilized highly customized columns containing exotic materials to enhance the sensitivity for a specific gas. Also, detection limits were typically 400 ppm or higher. Major chromatographic supply companies and several industrial experts were also contacted, but no existing method using commonly available chromatographic supplies was identified. Much of the problem with analyzing the nitrogenous species centers around the strongly polar and reactive nature of these compounds. NH_3 is a base and tends to adsorb strongly on most surfaces. HCN, on the other hand, is acidic, but exhibits similar absorption characteristics. Thus column materials exhibiting basic behavior eliminate the possibility of HCN analysis while acidic column materials prevent NH_3 analysis. NO_2

is both strongly adsorbed and very unstable, reacting with many common column packings. Greene and Pust[1] reported the conversion of NO_2 to NO by reaction with water on a molecular sieve 5A column. Also, Trowell[2] found that NO_2 reacts with porous polymer packings to form H_2O, NO, and nitrated aromatic rings of the polymer.

In addition to reactions on the column packing, contamination of sample loops, valves and transfer lines with weak acid or base sites also subverts HCN and NH_3 analysis. This problem was identified in the GC/MS used for this work by injecting NH_3 or HCN without a column and comparing the mass spectrometer response to that of N_2 injected in the same manner. The HCN and NH_3 peaks showed excessive tailing indicative of system contamination. Efforts to neutralize the system with various washing techniques were not successful. The problem was solved by replacing the entire injection system and all transfer lines with new acetone-rinsed materials. All transfer lines were stainless steel, except those downstream of the column, where glass-lined stainless steel lines were used.

A suitable chromatographic technique was developed by working in conjunction with Hayes Separations, a company specializing in porous polymer column packings. Two columns were necessary to give complete separation. The Hayesep C column provided separation of CO_2, N_2O, NH_3, H_2O, HCN and C_2 through C_6 hydrocarbons. The second column, a Hayesep D_B provided separation of N_2, O_2, CO, NO, Ar, and CH_4.

The GC arrangement used originally is shown in Figure AI-1. In this setup, the Hayesep C column was maintained at 35 °C for four minutes followed by a

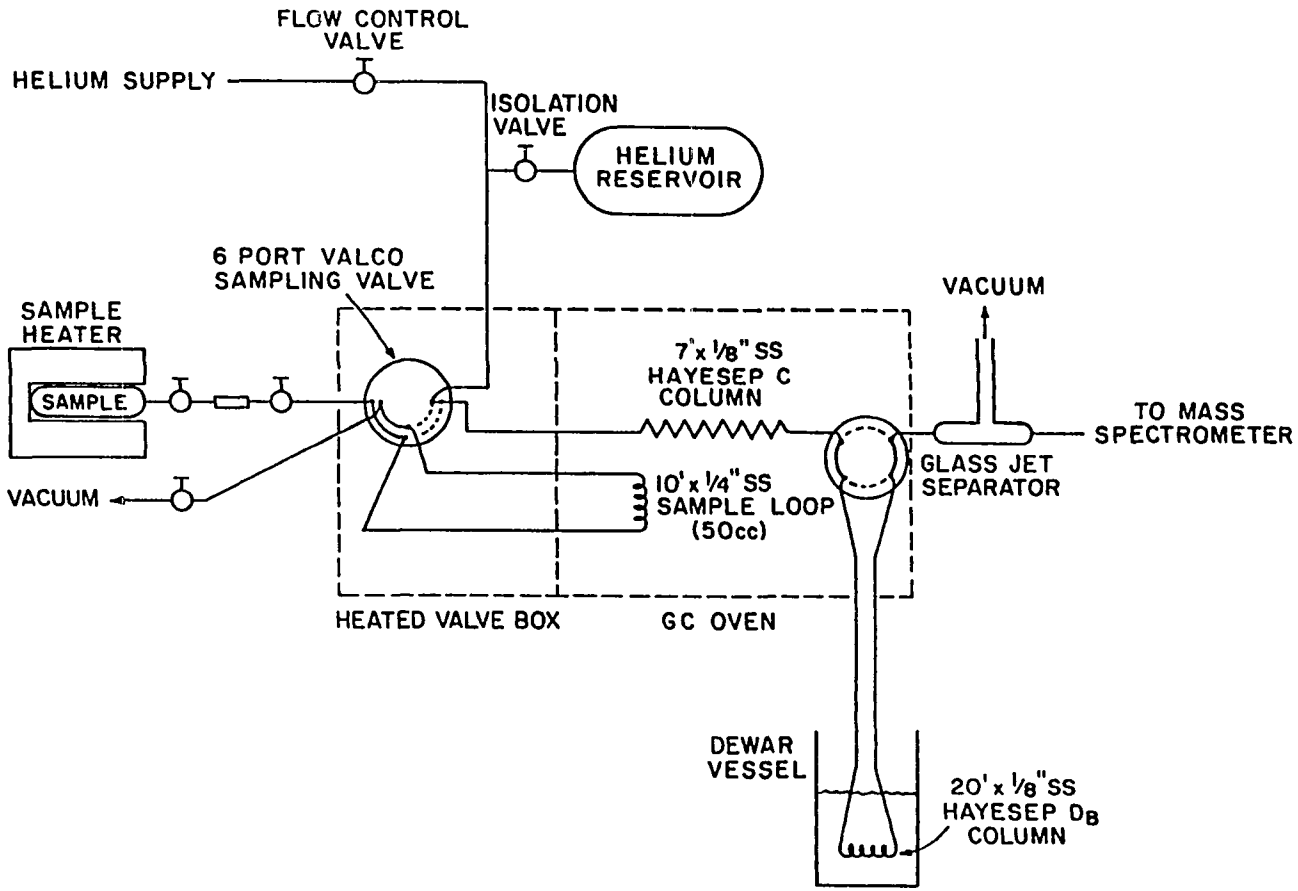

Figure AI-1. GC/MS setup for analysis of fuel-rich combustion products including nitrogenous species.

temperature ramp to 200 °C at a rate of 35 °C per minute. The Hayesep D_B column was held at -30 °C in a bath containing a mixture of Methanol and water cooled by dry ice. A sample chromatogram using this setup is shown in Figure AI-2.

The sample flow was directed through both columns in series when the sample was injected. After 180 seconds the 4-port Valco valve was switched to allow CO_2, N_2O and all hydrocarbons except CH_4 to pass directly from the Hayesep C column to the mass spectrometer. Meanwhile, the other species which elute from the Hayesep C column as a "fixed gas" peak were trapped in the Hayesep D_B column. After the C_6 hydrocarbon eluted (about 800 seconds) from the Hayesep C, the 4-port valve was switched back to flow the carrier gas through the Hayesep D_B to complete the analysis. The complete chromatogram took approximately 30 minutes. The helium carrier gas was maintained at approximately 80 psig at the inlet to the Hayesep C for the entire run.

This method was initially intended to include both NH_3 and HCN along with the aforementioned species. Although HCN and NH_3 can be analyzed using the Hayesep C column the required conditions are different. The column and transfer lines contain some mildly active sites in spite of all efforts to eliminate them. Therefore the analysis of HCN and NH_3 requires saturation of these sites to minimize peak loss and tailing. Saturation is achieved by repeated injections of high concentrations of HCN and NH_3 (ca. 1%). When the active sites become saturated, the detector response becomes constant for successive injections. The column must remain isothermal after saturation and during the run to prevent exposure of new active sites.

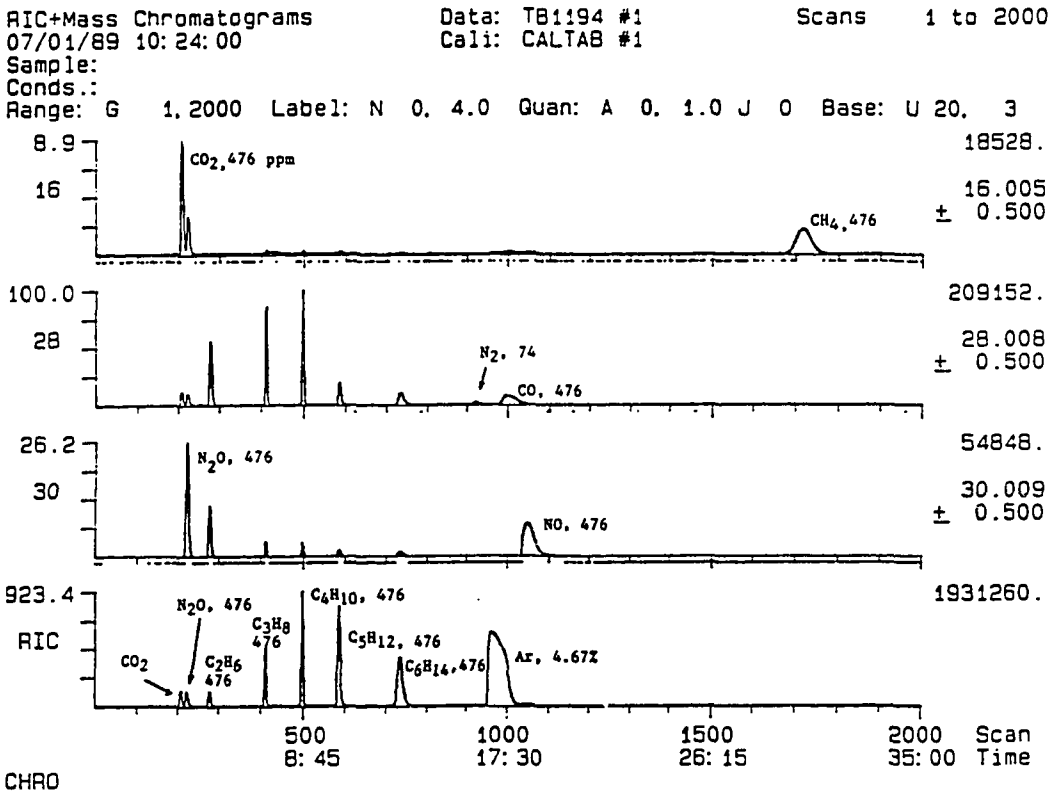

Figure AI-2. Sample mass chromatogram for a gas mixture containing species of interest in reburning.

A sample chromatogram for the analysis of HCN and NH_3 is shown in Figure AI-3. This chromatogram was produced using only the Hayesep C column at 80 °C and a column head pressure of 40 psig. Although reasonable mass peaks are shown for NH_3 and HCN, reproducibility at such low concentrations was non-existent. Even under the most carefully controlled conditions the quantitative analysis of HCN and NH_3 proved to be almost impossible at concentrations below 100 ppm. The grab sample technique necessitated in this work amplified the problems to the point that quantitative analysis by GC/MS was discarded in favor of specific ion probes.

The GC/MS method actually used in the experimental work differed somewhat from those outlined above. The light gases (N_2, NO, and N_2O) were analyzed on the Hayesep D_B column maintained at room temperature. Since argon was not present in the reactor effluent, the higher column temperature gave good separation and a shorter analysis time. HCN was analyzed using the Hayesep C column at 120 °C to produce a sharper peak. Also, the NH_3 analysis temperature was reduced to 60 °C to give better separation from the large CO_2 peak.

Sources:

1. Greene, S.A. and H. Pusjt, Anal. Chem., 30, 1039 (1958)
2. Trowell, J.M., J Chromatog. Sci., 9, 253 (1971)

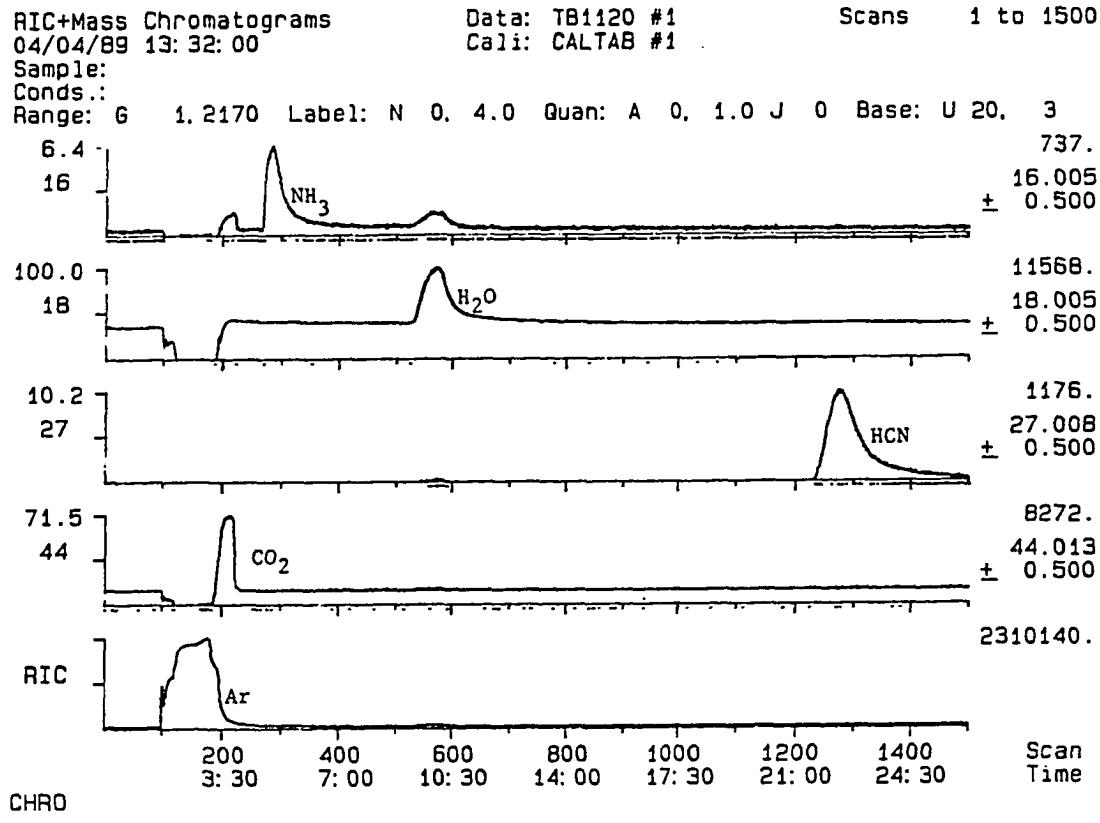

Figure AI-3. Sample mass chromatogram for 5 ppm each of HCN and NH_3 on a Hayesep C column operated at 80°C and a column head pressure of 40 psig.

APPENDIX II

Reactor Wall and Gas Temperature Profiles

The gas temperature profile in the flow reactor is of primary interest in defining the reburning conditions. Both the maximum temperature and residence time at that temperature are important for comparing the data obtained here with data and numerical calculations of other authors. Heating and cooling rates may also be important in determining the final TFN speciation.

The initial attempt at measuring the gas temperature profile consisted of making centerline traverses of the reactor length using a sheathed 0.125 in. diameter type K thermocouple. However, the low gas velocity (ca. 1 ft/s) and high wall radiation to the relatively large thermocouple made data obtained by this method suspect. Heat transfer estimates for the thermocouple indicated that measured temperatures probably represented the wall temperature better than the gas temperature. Also, measurements made in this fashion do not account for radial temperature variations inherent in a wall heated conduit.

A better estimate of the gas temperature was obtained by measuring the wall temperature profile and calculating the gas temperature profile from heat transfer considerations. The wall temperature profile was obtained by modifying one of the ceramic reactor tubes to accept wall mounted thermocouples. The modified tube was constructed by drilling through the ceramic wall and cementing Type K thermocouples into place. Seven thermocouples were positioned in a spiral pattern along the heated length of the reactor tube. The thermocouple leads were strung along the outside of the tube surface to the reactor inlet. Wall temperature measurements made with this

method matched (within 10 °C) those obtained with the centerline thermocouple traverse.

The gas temperature profile was calculated by assuming conduction heat transfer into a fully developed laminar flow. The equation for heat conduction to the fluid at the wall for an arbitrary wall temperature profile is given as

$$\dot{q}_0''(x^+) = -\frac{k}{r_0}\left[\int_0^{x^+} \Theta_{r^+}(x^+-\xi,1)\,\frac{dT_0}{d\xi}\,d\xi + \sum_{i=1}^{k} \Theta_{r^+}(x^+-\xi_i,1)\,\Delta T_{0,i}\right]$$

where

x = Distance from entrance to heated length

r_o = Inside diameter of the conduit

$x^+ = (x/r_o)/(Re\ Pr)$

$r^+ = r/r_o$

ξ = A dummy integration variable

$\Theta = (T_0 - T)/(T_0 - T_e)$

and

k = the thermal conductivity of the gas.

The subscript $_0$ indicates values at the wall and $_e$ indicates free stream values at the entrance.

This equation is for a fully developed velocity profile which is valid if x/D at the entrance to the heated zone is such that x/D > Re/20. The geometry of the flow reactor is such that x/D = 4 and Re = 60 (Re/20 = 3). Thus the assumption of a fully developed velocity profile is valid.

The wall temperature profile is accurately approximated by

$$\Theta_w = \frac{(T_0 - T_{0,e})}{(T_{0,max} - T_{0,e})} = 1 - e^{-\frac{x}{RC1}}$$

from the entrance to the point of maximum temperature and by

$$\Theta_w = \frac{(T_{0,max} - T_0)}{(T_{0,max} - T_{0,exit})} = 1 - e^{-\frac{x_{exit} - x}{RC2}}$$

from the maximum wall temperature to the exit of the heated length. RC1 and RC2 are constants which are determined by curve fitting the wall temperature data.

Details of the solution are given by Sellars et al.[1] and by Kays and Crawford[2]. The solution proceeds generally as follows. Equation 1 is evaluated to give the wall heat flux as a function of distance along the wall. The wall heat flux is then integrated with respect to x^+ to give the total heat transferred to the fluid. The mean fluid temperature is then extracted by performing an energy balance on the fluid which yields

$$\dot{q} = \pi r_0^2 \rho v c (T_{mean} - T_e)$$

The solution from the entrance to the point of maximum wall temperature is exact based on the curve fitted wall temperature profile. However, to mesh the rising wall temperature solution to the declining wall temperature solution, the gas temperature calculated at the interface is assumed to be uniform across the cross section. This assumption causes wall heat fluxes calculated downstream of the maximum wall temperature to be somewhat higher than those actually existing. However, this effect is short-lived since the calculated thermal boundary layer redevelops quickly. Also, the radial temperature gradients are small in this region so the error introduced is small.

The solution for the mean gas temperature from the entrance of the heated length to the point of maximum wall temperature is given by the following expression.

$$T_{mean} - T_e = -\frac{8RePrD}{2RCI}(T_{0,xI} - T_{0,e}) \left[\sum \frac{G_n}{\left(\lambda_n^2 - \frac{RePrD}{2RCI}\right)\left(\frac{RePrD}{2RCI}\right)} \exp\left(-\frac{RePrD}{2RCI}x^+\right) \right.$$

$$-\sum \frac{G_n}{\left(\lambda_n^2 - \frac{RePrD}{2RCI}\right)\left(\frac{RePrD}{2RCI}\right)} - \sum \frac{G_n}{\left(\lambda_n^2 - \frac{RePrD}{2RCI}\right)\lambda_n^2} \exp(-\lambda_n^2 x^+)$$

$$\left. + \sum \frac{G_n}{\left(\lambda_n^2 - \frac{RePrD}{2RCI}\right)\lambda_n^2} \right]$$

The solution from the point of maximum temperature to the furnace exit is given by;

$$T_{mean}-T_{mean,x1} =$$

$$-\frac{8RePrD}{2RC2}(T_{0,x1^+}-T_{0,exit})\left\{\sum\frac{G_n}{\left(\lambda_n^2+\frac{RePrD}{2RC2}\right)\frac{RePrD}{2RC2}}\exp\left[-\frac{RePrD}{2RC2}(x^+-x1^+)\right]\right.$$

$$-\sum\frac{G_n}{\left(\lambda_n^2+\frac{RePrD}{2RC2}\right)\frac{RePrD}{2RC2}}\exp[-\lambda_n^2(x^+-x1^+)]$$

$$+\sum\frac{G_n}{\left(\lambda_n^2+\frac{RePrD}{2RC2}\right)\lambda_n^2}\exp\left[-\lambda_n^2(x^+-x1^+)-\frac{RePrD}{2RC2}(x2^+-x1^+)\right]$$

$$\left.-\sum\frac{G_n}{\left(\lambda_n^2+\frac{RePrD}{2RC2}\right)\lambda_n^2}\exp\left[-\frac{RePrD}{2RC2}(x2^+-x1^+)\right]\right\}$$

$$+(T_{0,x1}-T_{mean,x1})\left\{\sum\frac{G_n}{\lambda_n^2}\exp[-\lambda_n^2(x^+-x1^+)]-\frac{1}{8}\right\}$$

Where the subscript $x1^+$ denotes conditions at the location of the maximum wall temperature and $x2^+$ denotes conditions at the furnace exit.

The infinite series solution functions λ_n and G_n are tabulated by Kays and Crawford.

To evaluate the solutions to these equations the weighted average properties based on gas composition and temperature in the furnace were used. Based on these

calculations Re = 34.7 and Pr = 0.73. The wall temperature curve fit constants were found to be RC1 = 1.5 and RC2 = 1.5. The solutions for the gas temperature profile were evaluated using a computer code. A listing of this code and the output for the conditions listed above are given in the following pages. The measured wall temperature and the calculated gas temperature profiles are shown graphically in Figure AII-1.

Sources:

1. Sellars, J.R., M. Tribus, and J.S. Klein, "Heat Transfer to Laminar Flow in a Round Tube or Flat Conduit-Grate Problem Extended", Trans. ASME, Vol. 78, p. 441, 1956.

2. Kays, W.M., and M.E. Crawford, "Convective Heat and Mass Transfer", Second Edition, McGraw Hill, New York, pp 106-126, 1980.

```
$JOB
C
C   COMMENTS:
C     THIS PROGRAM IS DESIGNED FOR CALCULATING THE GAS TEMPERATURE
C     PROFILE IN A TUBULAR FURNACE WITH VARYING WALL TEMPERATURE.
C     THE WALL TEMPERATURE VARIATIONS ARE ASSUMED TO BE OF THE FORM.
C
C     THETA N= (TW(MAX)-TW)/(TW(MAX)-TW(X0))=1-EXP(-(X-X0)/RC1)
C                                                          X0<X<X1
C     THETA W= (TW(MAX)-TW)/(TW(MAX)-TW(X2))=1-EXP(-(X2-X)/RC2)
C                                                          X1<X<X2
C     THE PROGRAM INPURS ARE DEFINED AS:
C       RE   =   REYNOLDS NUMBER, RHO * V * D / MU
C       PR   =   PRANDTL NUMBER, MU * CP / K
C       D    =   INTERNAL DIAMETER OF THE FURNACE
C       RC1  =   DECAY CONSTANT FOR THE WALL
C       RC2  =   DECAY CONSTANT FOR THE WALL TEMPERATURE PROFILE AFTER
C                 THE MAXIMUM TEMPERATURE.
C       TDIF1 = THE DIFFERENCE BETWEEN THE MAXIMUM WALL TEMPERATURE
C               AND THE ASSUMED WALL TEMPERAURE AT X0.
C       TDIF2 = THE DIFFERENCE BETWEEN THE MAXIMUM WALL TEMPERATURE
C               AND THE ASSUMED WALL TEMPERATURE AT X2.
C       X0     = THE LOCATION OF THE ASSUMED INITIAL WALL TEMPERATURE
C               RELATIVE TO THE TOP OF THE HEATED SECTION OF THE
C               FURNACE (USUALLY A NEGATIVE NUMBER)
C       X1     = THE LOCATION OF THE MAXUMUM WALL TEMPERATURE RELATIVE
C               TO THE HEATED SECTION OF THE FURNACE.
C       X2     = THE LOCATION OF THE ASSUMED FINAL WALL TEMPERATURE
C               RELATIVE TO THE TOP OF THE HEATED SECTION OF THE
C               FURNACE.
C       TMEAN0= THE ASSUMED MEAN GAS TEMPERATURE AT X0.  THIS VALUE IS
C               THE WALL TEMPERATURE AT X0.
C       TWMAX = THE MAXIMUM WALL TEMPERATURE IN THE HEATED SECTION OF
C               FURNACE.
C
C234567
      REAL RE, PR, D, RC1, RC2, TDIF1, TDIF2, X0, X1, X2, TMEAN0,
     +     TWMAX, LAMDA(50), G(50), X, PARM1, PARM2, SUM1, SUM2,
     +     SUM3, XPLUS, TEMP, TMEANX, X1PLUS, X2PLUS, TMX1, A, SUM4,
     +     SUM5, TEMP1, XFLOWO, EX
C
      INTEGER I, K
C
      READ, RE, PR, D
      READ, RC1, RC2, TDIF1
      READ, TDIF2, X0, X1
      READ, X2, TMEAN0, TWMAX
C
      PRINT, ' '
      PRINT, ' '
      PRINT, ' '
      PRINT, 'RE =',RE
      PRINT, 'PR =',PR
      PRINT, 'D  =',D
      PRINT, 'RC1 =',RC1
```

```
      PRINT, 'RC2 =',RC2
      PRINT, 'TDIF1 =',TDIF1
      PRINT, 'TDIF2 =',TDIF2
      PRINT, 'X0 =',X0
      PRINT, 'X1 =',X1
      PRINT, 'X2 =',X2
      PRINT, 'TMEAN0 =',TMEAN0
      PRINT, 'TWMAX  =',TWMAX
C
C
      X1 = X1 - X0
      X2 = X2 - X0
      X  = -X0
      LAMDA(1) = 7.312
      LAMDA(2) = 44.62
      G(1)     = 0.749
      G(2)     = 0.549
      PARM1    = (RE * PR * D)/(2.0 * RC1)
      PARM2    = (RE * PR * D)/(2.0 * RC2)
C
      DO 10 I = 3, 41
        K = I -1
        LAMDA(I) = 4.0 * K + (8.0/3.0)
        G(I)     = 1.01276/(LAMDA(I)**(1.0/3.0))
        LAMDA(I) = LAMDA(I)**2
 10   CONTINUE
C
      WHILE (X .LE. X1)  DO
        SUM1 = 0.0
        SUM2 = 0.0
        SUM3 = 0.0
        XPLUS = (2.0 * X)/(RE * PR * D)
        DO 30 I = 1,41
          K= I
          SUM1 = SUM1 + G(K)/((LAMDA(K) - PARM1) * PARM1)
          TEMP = G(K)/((LAMDA(K) - PARM1) * LAMDA(K))
C
C
          IF ((-LAMDA(K) * XPLUS) .LT. -160) THEN
              XFLOWO = 0.0
          ELSE
              XFLOWO = EXP(-LAMDA(K) * XPLUS)
          ENDIF
C
          SUM2 = SUM2 + TEMP * XFLOWO
          SUM3 = SUM3 + TEMP
 30     CONTINUE
        TMEANX = TMEAN0 - 8.0 * PARM1 * TDIF1 * (SUM1 * (EXP(-PARM1 *
     +    XPLUS) - 1) - SUM2 + SUM3)
        PRINT, ' '
        PRINT, 'X =', X
        PRINT, 'TMEANX = ', TMEANX
C
        X = X + 1.0
        END WHILE
```

```
      X = X - 1.0
C
C
      X1PLUS = (2.0 * X1)/(RE * PR * D)
      X2PLUS = (2.0 * X2)/(RE * PR * D)
      TMX1   = TMEANX
      A      = TWMAX - TMX1
C
C
      WHILE (X .NE. X2)  DO
        SUM1 = 0.0
        SUM2 = 0.0
        SUM3 = 0.0
        SUM4 = 0.0
        SUM5 = 0.0
        XPLUS = (2.0 * X)/(RE * PR * D)
        DO 60 I = 1, 41
          K = I
          SUM1 = SUM1 + G(K)/((LAMDA(K) + PARM2) * PARM2)
          SUM2 = SUM1
          TEMP1 = G(K)/((LAMDA(K) + PARM2) * LAMDA(K))
C
C
          EX = (-LAMDA(K) * (XPLUS - X1PLUS) - PARM2 * (X2PLUS -
     +      X1PLUS))
          IF (EX .LT. -160) THEN
             XFLOWO = 0.0
          ELSE
             XFLOWO = EXP(EX)
          ENDIF
C
          SUM3 = SUM3 + TEMP1 * XFLOWO
          SUM4 = SUM4 + TEMP1
C
C
          EX = -LAMDA(K) * (XPLUS - X1PLUS)
          IF (EX .LT. -160) THEN
              XFLOWO = 0.0
          ELSE
              XFLOWO = EXP(EX)
          ENDIF
C
          SUM5 = SUM5 + G(K)/LAMDA(K) * XFLOWO
 60     CONTINUE
C
        TMEANX = TMX1 - 8.0 * PARM2 * TDIF2 * (SUM1 * EXP(-PARM2 *
     +         (X2PLUS - XPLUS)) - SUM2 * EXP(-PARM2 * ( X2PLUS -
     +         X1PLUS)) + SUM3 + SUM4 * EXP(-PARM2 * (X2PLUS - X1PLUS)))
     +         -  8.0 * A * (SUM5 - 1.0/8.0)
        PRINT, ' '
        PRINT, 'X = ',X
        PRINT, 'TMEANX =',TMEANX
C
        X = X + 1.0
        IF ((X2 - X) .LT. 0) THEN
```

```
    X = X2
  ENDIF
ENDWHILE
STOP
END
```

```
RE =          34.6999900
PR =           0.7300000
D  =           0.7500000
RC1 =          1.5000000
RC2 =          1.5000000
TDIF1 =     1009.0000000
TDIF2 =     1009.0000000
X0 =          -1.3500000
X1 =           6.0000000
X2 =          14.3500000
TMEAN0 =     100.0000000
TWMAX  =    1109.0000000

X =           1.3500000
TMEANX =      408.1904000

X =           2.3500000
TMEANX =      653.7253000

X =           3.3500000
TMEANX =      830.8791000

X =           4.3500000
TMEANX =      945.4809000

X =           5.3500000
TMEANX =     1015.2750000

X =           6.3500000
TMEANX =     1056.1820000

X =           7.3500000
TMEANX =     1079.5330000

X =           7.3500000
TMEANX =     1076.5040000

X =           8.3500000
TMEANX =     1093.3770000

X =           9.3500000
TMEANX =     1095.4680000

X =          10.3500000
TMEANX =     1090.0360000

X =          11.3500000
TMEANX =     1075.0750000

X =          12.3500000
TMEANX =     1043.9090000

X =          13.3500000
TMEANX =      982.2653000

X =          14.3500000
TMEANX =      861.7656000
```

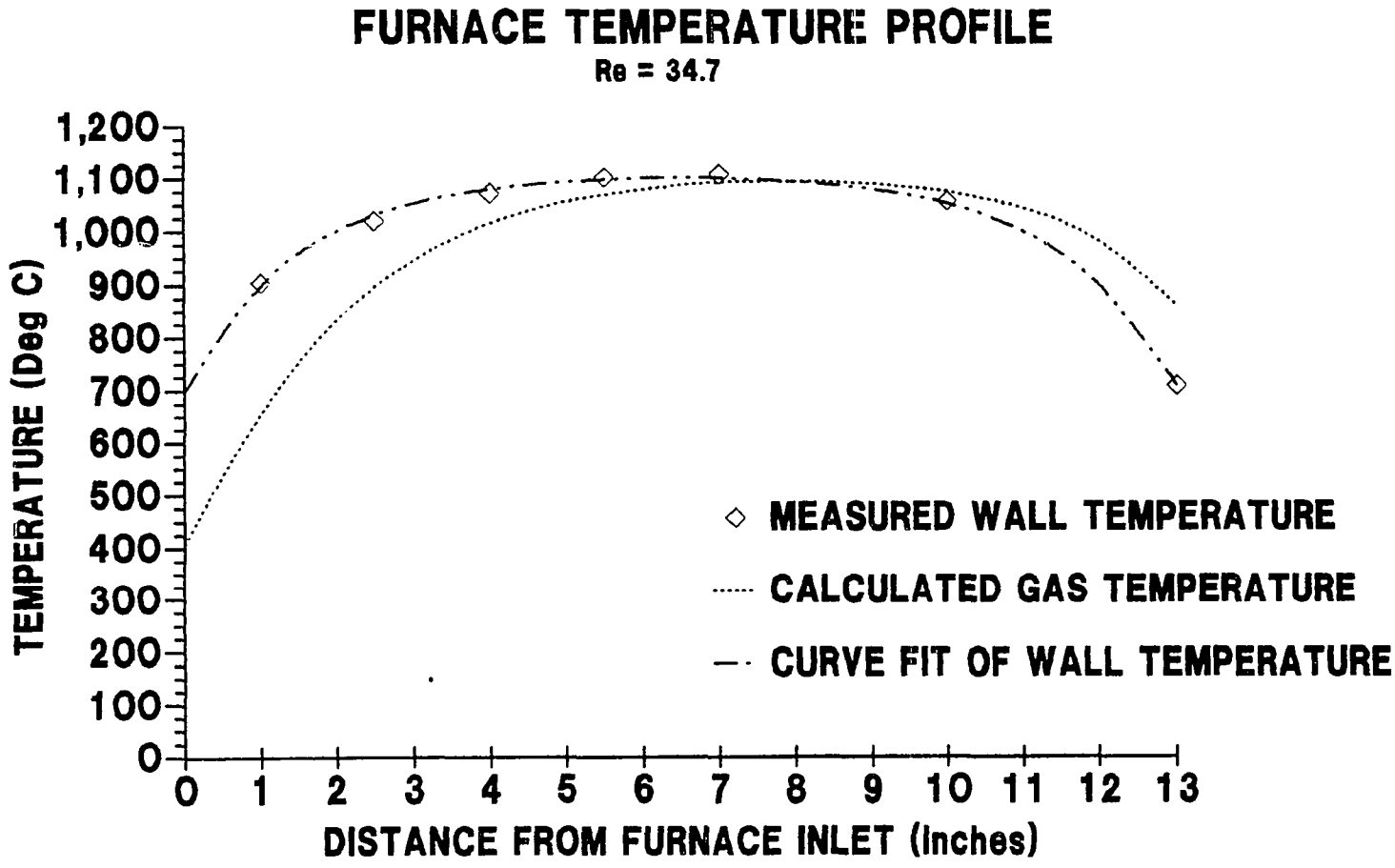

Figure AII-1. Measured reactor wall temperature and calculated gas temperature profiles.

APPENDIX III

Data Reduction Techniques

Isotope Separation

The nitrogen source tracing used in coal reburning studies with isotopically labelled $N^{15}O$ required separation of the various nitrogen species isotopes. This was accomplished by assuming superposition of isotope mass spectra.

For NO and N_2 the isotope separation was simplified because these species produce primarily molecular ions with a single positive charge. Also, ions resulting from fragmentation of these species were separated from the molecular ions by at least 14 mass units allowing the molecular ions alone to be used for isotope separation. Thus for NO and N_2 source tracing, knowledge of the natural abundance of the stable isotopes of atomic nitrogen and oxygen is all that is required.

The natural abundances of atomic nitrogen isotopes are given as N^{14} (99.64%) and N^{15} (0.36%). Thus, the natural abundances of diatomic nitrogen isotopes are calculated to be N_2^{28} (99.28%), N_2^{29}(0.72%), and N_2^{30}(0.001%).

In the experimental work conducted here, the measured abundance of all three isotopes are approximately equal. Therefore, the natural abundances of N_2^{29} and N_2^{30} are assumed to be negligible. With this simplified approach the N_2^{28} is assumed to be the combination of two fuel nitrogen atoms while N_2^{30} is taken to be formed by the combination of two nitrogen atoms originating as $N^{15}O$. The N_2^{29} is assumed to be the combination of one fuel nitrogen atom with one nitrogen atom from $N^{15}O$. The maximum error from the simplifications outlined above is less than 1%.

For NO source tracing the analysis is similar except that the natural abundance of atomic oxygen isotopes must also be considered. The stable isotopes of oxygen are

O^{16}(99.76%), O^{17}(0.04%), and O^{18}(0.20%). Thus the naturally occurring isotopes of NO are NO^{30}(99.40%), NO^{31}(0.40%), NO^{32}(0.20%), and NO^{33} (0.001%). Again, assuming naturally occurring NO to be entirely NO^{30} gives iess than 1% error.

Nitrogen source tracing for HCN and NH_3 is complicated by the fact that fragmentation by the removal of hydrogen atoms produces significant mass peaks separated from the molecular ions by only one mass unit. For example, a typical mass spectrum for natural abundance HCN gives normalized peak areas of 100 for mass 27, 1.5 for mass 28, and 20.2 for mass 26. The normalized peak areas for HCN^{15} would be the same except for a shift of one mass unit. Thus the two largest peaks would be at mass 27 and mass 28 but each would contain a contribution from HCN^{14} as well as HCN^{15}. The peak areas are defined by

$$A_{27} = HCN^{14} + .202\ HCN^{15}$$

and,

$$A_{28} = HCN^{15} + .015\ HCN^{14}$$

Solving these two equations simultaneously gives

$$HCN^{14} = 1.003\ A_{27} - .203\ A_{28}$$

and

$$HCN^{15} = 1.003\ A_{28} - 0.015\ A_{27}$$

The nitrogen source tracing for NH_3 is very similar. A typical mass spectrum for natural abundance NH_3 gives normalized peak areas of 100 for mass 17 and 66.7 for mass 16. The mass 18 peak was negligible. Again the normalized peak areas for $N^{15}H_3$ would be shifted by 1 mass unit. For an arbitrary mixture of $N^{14}H_3$ and $N^{15}H_3$ the peak areas for mass 18 and mass 17 would be given by

$$A_{18} = N^{15}H_3$$

and

$$A_{17} = N^{14}H_3 + .667N^{15}H_3$$

solving these equations for $N^{15}H_3$ and $N^{14}H_3$ in terms of measured mass peak areas gives

$$N^{15}H_3 = A_{18}$$

and

$$N^{14}H_3 = A_{17} - .667\ A_{18}$$

For both HCN and NH_3 nitrogen tracing, the effect of natural abundance N^{15} was neglected. However, the error introduced was less than 1% for all cases.

Probability Analysis

Probability analysis was used to predict diatomic nitrogen isotope distributions by using measured isotope distributions for the reactants involved in a given mechanism. For example, with the $N + NO \rightarrow N_2$ mechanism, the probability of the three isotopes of N_2 were predicted by

$$P(N^{14}N^{14}) = P(N^{14}O) \times P(N^{14})$$

$$P(N^{15}N^{15}) = P(N^{15}O) \times P(N^{15})$$

and

$$P(N^{14}N^{15}) = P(N^{15}O) \times P(N^{14}) + P(N^{14}O) \times P(N^{15})$$

In the calculations, N atoms were assumed to be derived from HCN or NH_3. Thus the isotope distributions measured for NO and HCN (NH_3) yielded the probability values needed for this analysis.

For the non-NO mechanism, NH and NH_2 were both assumed to be derivatives of HCN or NH_3. The predicted N_2 isotope distribution for this mechanism was given by,

$$P(N^{14}N^{14}) = P(N^{14}H) \times P(N^{14}H_2)$$

$$P(N^{15}N^{15}) = P(N^{15}H) \times P(N^{15}H_2)$$

and

$$P(N^{14}N^{15}) = P(N^{14}H) \times P(N^{15}H_2) + P(N^{15}H) \times P(N^{14}H_2)$$

Vita

The author was born on July 20, 1956 in Moulton, Alabama. In June of 1974 he graduated from Lawrence County High School. He attended Auburn University in Auburn, Alabama, and received a B.S. degree in Mechanical Engineering in March, 1979. After working for Auburn University for approximately one year he entered the Graduate school there and received an M.S. degree in Mechanical Engineering in December 1982.

The author came to Louisiana State University on an Alumni Federation Fellowship to pursue his Ph.D degree in August 1982. He married Patti Dianne Reaves on June 9, 1984.

DOCTORAL EXAMINATION AND DISSERTATION REPORT

Candidate: Thomas Emmett Burch

Major Field: Mechanical Engineering

Title of Dissertation: Formation and Destruction of Nitric Oxide in Fuel Rich Combustion: Reburning

Approved:

Major Professor and Chairman

Dean of the Graduate School

EXAMINING COMMITTEE:

Date of Examination:

April 20, 1990